Identification and characterization of Dop1p as an essential component of the Neo1p-Ysl2p-Arl1p membrane remodeling complex

Von der Fakultät Energie-, Verfahrens- und und Biotechnik der Universität Stuttgart zur Erlangung der Würde eines Doktors der Naturwissenschaften (Dr. rer. nat.) genehmigte Abhandlung

Vorgelegt von Dipl.-Bioch.
Sónia Cristina de Oliveira Barbosa
geboren in Paris (Frankreich)

Hauptberichter: Prof. Dr. Dieter H. Wolf
Mitberichter: Privatdozentin Dr. Birgit Singer-Krüger

Tag der mündlichen Prüfung: 14.01.2011

Institut für Biochemie der Universität Stuttgart
2011

Hiermit versichere ich, dass ich die Arbeit selbst verfasst und dabei keine enderen als die angegebenen Quellen und Hilfsmittel verwendet habe.
Stuttgart, den 23.06.2010

Sónia Cristina de Oliveira Barbosa

Table of contents

Abbreviation

aa	amino acids
ALP	alcaline phosphatase
Amp	ampicilin
AP	clathrin heterotetrameric adaptor protein
APLT	aminophospholipid translocase
APS	ammonium persulfate
Arf	ADP-ribosylation factor
Arl	Arf-like
ATP	adenosine 5`-triphosphate
BAR	Bin/Amphiphysin/Rvs
BSA	bovine serum albumine
CCV	clathrin-coated vesicle
CLAP	chymostatin, leupeptin, antipain, pepstatin
CPY	carboxypeptidase Y
Cy3	indocarbocyanine
kDa	kilo Dalton
DMSO	dimethylsulfoxide
DNA	desoxyribonucleic acid
DTT	D,L Dithiothreitol
EE	early endosome
EDTA	ethylenediamine tetraacetic acid
ENTH	epsin N-terminal homology domain
ER	endoplasmic reticulum
ERAD	ER-associated degradation
5-FOA	5-fluoro orotic acid
FYVE	(Fab1, YOTB, Vac1, and early endosomal antigen 1) domain
GAP	GTPase activating protein
GEF	guanine nucleotide exchange factor
GGA	Golgi-associated, γ-adaptin homologous, Arf-interacting protein
GFP	green fluorescent protein
HA	hemagglutinin
IF	indirect immunofluorescence
IgG	immunoglobulin G
IP	immunoprecipitation
LE	late endosome
M	molar
mM	millimolar
MVB	multivesicular body
NBD	7-nitrobenz-2-oxa-1,3-diazol-4-yl
NEB	New England Biolabs
NEM	N-ethtylmaleimide
NP40	nonidet P-40

OD_{600}	optical density at 600 nm
ORF	open reading frame
PA	phosphatidic acid
PBS	phosphate saline buffer
PC	phosphatidylcholine
PCR	polymerase chain reaction
PE	phosphatidylethanolamine
PEG	Polyethylene glycol
PGK	phosphoglycerokinase
PI	phosphoinositide
PI3P	phosphatidylinositol-3-phosphate
PI4P	phosphatidylinositol-4-phosphate
$PI(4,5)P_2$	phosphatidylinositol-4,5-bisphosphate
PLT	phospholipid translocase
PMSF	phenylmethylsulfonyl fluoride
PS	phosphatidylserine
PtdIns	phosphatidylinositol
rpm	rotations per minute
SD	synthetic growth medium
SDS	sodium dodecyl sulfate
SDS-PAGE	sodium dodecyl sulfate-polyacrylamide gel
SNARE	soluble N-ethylmaleimide-sensitive factor attachment protein receptor
TAP	tandem affinity purification
TCA	trichloracetic acid
TEMED	tetramethylethylenediamine
TGN	*trans*-Golgi network
v/v	volume per volume
w/v	weight per volume
YPD	yeast complete medium

Abstract

Vesicular trafficking requires molecular mechanisms that drive membrane-enclosed organelles to bud vesicles and fuse with incoming ones. Understanding how these highly-curved transport structures are generated has been challenging. The best understood mechanisms for the generation of vesicles in the secretory and endocytic pathways involve the assembly of cytosolic coat proteins. However some other proteins have been implicated in the generation of the high curvature needed to form a vesicle. Prime candidates are the phospholipid translocases from the P_4-ATPase subfamily, which are thought to pump phospholipids from the exocytosolic leaflet of a membrane to its cytosolic leaflet thereby deforming membranes.

In the group of B. Singer-Krüger, the yeast P_4-ATPase Neo1p was identified as being an interaction partner of Ysl2p, a protein that has sequence similarity to large Arf GEFs from the BIG and GBF family, and to be genetically linked to the small Arf-like GTPase Arl1p. A recent study demonstrated that a network formed by these proteins (the Neo1p-Ysl2p-Arl1p network), helps recruiting the GGAs clathrin adaptors to the TGN/endosomal system.

Recently, members of the conserved Cdc50 family were identified as being transport chaperones for some of the P_4-ATPases. Therefore, initially in this PhD thesis I studied the putative connection of Neo1p with this protein family. However, while all the other yeast P_4-ATPases seem to require a specific member of the Cdc50 family for their export from the ER, this does not seem to be the case for Neo1p. This result led to the search for a novel protein required for Neo1p function.

Herein, Dop1p, an essential yeast protein of about 195 kDa and highly conserved among eukaryotes, was identified as being a binding partner of Neo1p and Ysl2p. Studies using *neo1*, *dop1*, Δ*ysl2* mutants, revealed that the respective proteins, Neo1p, Dop1p and Ysl2p, are interdependent thereby suggesting that they might exist in a complex. Significantly, in a temperature-sensitive *dop1-3* mutant both Neo1p and Ysl2p were found to be specifically destabilised. Similarly, a comparable loss of Ysl2p and Dop1p was also found in *neo1-69* cells while in Δ*ysl2* cells a remarkable reduction of both Neo1p and Dop1p was observed. Consistent with this reciprocal dependency effect, *NEO1* is a suppressor of *dop1-3* and Δ*ysl2* mutants and *DOP1* a suppressor of *neo1-69* and Δ*ysl2* mutants. The relationship between Dop1p and Neo1p is further

strengthened by the observation that the *neo1-69* and *dop1-3* mutants display several similar phenotypic defects and that similarly to Neo1p, Dop1p also localises to the endosomes. Interestingly, although Ysl2p interacts with Dop1p, the Neo1p-Dop1p interaction is independent of Ysl2p and Dop1p is still localised to the TGN/endosomes in the absence of Ysl2p.

In order to get some insights in the features of the large protein Dop1, the conserved N-terminal region, the C-terminal region containing leucine zipper-like repeats, and the less conserved internal segment were separately expressed as GFP-fusions and their subcellular localisations and molecular interactions were analysed. These analyses revealed that the different regions of Dop1p had distinct localisation patterns and binding affinities to Neo1p and Ysl2p. The internal region of Dop1p seems to be particularly important for the endosomal membrane association of the protein. Additionally, the presence of leucine zipper-like repeats at the C-terminus of Dop1p suggested that this protein could form dimers or oligomers and indeed Dop1p is able to self-interact.

In addition, a conserved PPSY motif in the C-terminus of Neo1p was identified. This led to the examination of Neo1p ubiquitination. The introduction of point mutations in this motif resulted in an improved cell growth at high temperatures. However, whether this motif is related to Neo1p ubiquitination awaits further investigations.

In summary, this work identified Dop1p as a novel component of the Neo1p-Ysl2p-Arl1p complex. Moreover, the analysis of the distinct regions of Dop1p shed some light in their putative role within this protein.

Zusammenfassung

Der vesikuläre Transport bedarf molekularer Mechanismen, durch welche membranumschlossene Organellen Vesikel abknospen sowie mit hinzukommenden Vesikeln fusionieren. Eine große Herausforderung besteht darin zu erkennen wie diese stark gekrümmten Transportstrukturen erzeugt werden. Der am besten verstandene Mechanismus zur Erzeugung von Vesikeln im sekretorischen und endocytischen Vesikelweg umfasst die Assemblierung von zytosolischen Hüllenproteinen. Es wurden jedoch auch andere, für die Erzeugung der starken Krümmung verantwortlichen, Proteine identifiziert. Erste Kandidaten sind Phospholipid-Translokasen aus der Subfamilie der P_4-ATPasen, welche Phospholipide aus der exozytosolischen in die zytosolische Schicht der Membran überführen sollen, um dadurch zu einer Deformation der Membran zu führen.

In der Gruppe von PD Dr. B. Singer-Krüger wurde Neo1p, eine P_4-ATPase aus der Hefe, identifiziert als Interaktionspartner von Ysl2p, einem Protein mit Sequenzänlichkeit mit großen Arf GEFs der BIG und GBF Familie sowie genetischer Interaktion mit der kleinen Arf-ähnlichen GTPase Arl1p. Eine kürzlich durchgeführte Studie hat gezeigt, dass ein Netzwerk dieser Proteine (das Neo1p-Ysl2p-Arl1p-Netzwerk) bei der Rekrutierung der GGA Clathrin-Adaptoren zum TGN/endosomalen System mitwirkt.

Mitglieder der konservierten Cdc50 Familie wurden kürzlich als Transport-Chaperone für manche P_4-ATPasen identifiziert. Aufgrund dessen habe ich in dieser Doktorarbeit zunächst die mögliche Verknüpfung von Neo1p mit dieser Proteinfamilie untersucht. Während, alle anderen vier P_4-ATPasen der Hefe ein spezifisches Mitglied der Cdc50 Familie benötigen um aus dem ER transportiert zu werden, scheint diese Bedingung nicht auf Neo1p zuzutreffen. Dieses Ergebnis führte zu der Suche nach neuen Proteinen, die für die Neo1p-Funktion benötigt werden.

Daraufhin wurde Dop1p, ein essentielles Hefeprotein von ca. 195 kDa, das stark konserviert ist unter Eukaryoten, als Bindungspartner von Neo1p und Ysl2p identifiziert. Untersuchungen der *neo1*, *dop1*, Δ*ysl2* Mutanten zeigt en, dass die betreffenden Proteine Neo1p, Dop1p and Ysl2p gegenseitig abhängig sind, wodurch sich die Möglichkeit ergibt, dass diese Proteine in einem Komplex vorliegen. Bezeichnenderweise, in der temperatur-sensitiven *dop1-3* Mutante wurden sowohl Neo1p als auch Ysl2p gezielt destabilisiert. Ein vergleichbarer Verlust von Ysl2p und

Dop1p wurde auch in *neo1-69* Zellen verzeichnet, während in Δ*ysl2* Zellen eine beträchtliche Reduktion sowohl von Neo1p als auch von Dop1p beobachtet werden konnte. Im Einklang mit dieser reziproken Abhängigkeit ist *NEO1* ein Supressor der *dop1-3* und Δ*ysl2* Mutanten sowie *DOP1* ein Supressor der *neo1-69* und Δ*ysl2* Mutanten. Die Wechselwirkung zwischen Dop1p und Neo1p ist ausserdem verstärkt durch die Beobachtung, dass die *neo1-69* und *dop1-3* Mutanten einige ähnliche phänotypische Defekte aufweisen und ausserdem Dop1p, ähnlich wie Neo1p, an Endosomen lokalisiert. Interessanterweise, obwohl Ysl2p mit Dop1p interagiert, ist die Neo1p-Dop1p-Interaktion unabhängig von Ysl2p und ausserdem lokalisiert Dop1p am TGN/Endosomen auch in der Abwesenheit von Ysl2p.

Um einige Einblicke in die Besonderheiten des großen Proteins Dop1p zu bekommen, wurde die C-terminale Region mit den konservierten Leucin-Zippern-Motiv sowie das weniger konservierte interne Segment separat als GFP-Fusionen exprimiert und daraufhin deren subzelluläre Lokalisierung und die molekularen Interaktionen untersucht. Diese Analysen zeigten, dass die verschiedenen Regionen von Dop1p unterschiedliche Lokalisierungsmuster aufweisen und verschiedene Affinitäten für Neo1p und Ysl2p aufweisen. Die interne Region von Dop1p scheint insbesondere für die endosomale Lokalisierung des Proteins von Bedetung zu sein. Zusätzlich könnte die Anwesenheit der Leucin-Zipper am C-Terminus ein Indiz dafür sein, dass das Protein Dimere oder Oligomere bildet. Und in der Tat, Dop1p ist in der Lage mit sich selbst zu interagieren.

Des Weiteren wurde ein konserviertes PPSY-Motiv am C-Terminus von Neo1p identifiziert. Dies führte zu der Untersuchung der Ubiquitinierung von Neo1p. Punktmutationen in dieser Region führten zu einem verbesserten Wachstum bei höheren Temperaturen. Ob dieses Motiv mit einer Ubiquitinierung von Neo1p zusammenhängt muss noch weiter untersucht werden.

Zusammenfassend wurde in dieser Arbeit Dop1p al seine neue Komponente des Neo1p-Ysl2p-Arl1p-Komplexes identifiziert. Des Weiteren hat die Analyse der unterschiedlichen Regionen von Dop1p etwas Licht gebracht in deren mögliche Rollen innerhalb dieses Proteins.

1 Introduction

1.1 The secretory and endocytic pathways are interconnected at the TGN/endosomes

Eukaryotic cells contain a diverse range of organelles, many of which are connected to each other by pathways of membrane trafficking. The plasma membrane, a boundary between the extracellular milieu and the cellular constituents of the cells is continuously remodelled in response to extracellular and intracellular signals, a process that highly dependents on the secretory and endocytic trafficking pathways. Transport along these pathways occurs by the transfer of secretory or endocytic cargo between different membrane-enclosed organelles.

The secretory system is composed of a succession of endomembrane compartments that includes the endoplasmatic reticulum (ER), Golgi cisternae, the trans-Golgi network (TGN), several types of secretory vesicles and the plasma membrane. Newly synthesised proteins either destined to be secreted to the extracellular space or residents of the secretory and endocytic system (see below) are synthesised in the ER and transported through the Golgi to their final destination.

The endocytic system comprises three main compartments that have distinct roles in the sorting, processing and degradation of internalised cargo. These compartments include the early endosomes (EE), the multivesicular bodies (MVB) or late endosomes (LE) and the vacuole/ lysosomes, which are connected with each other and the plasma membrane by diverse pathways.

In the secretory system, the TGN has a central role as a site for protein sorting (Griffiths and Simons 1986; Rodriguez-Boulan and Musch 2005). The transport of newly synthesized proteins from the ER to Golgi cisternae occurs with no deviation (figure 1.1, arrow 1). However, once at the TGN proteins can be directed to numerous possible destinations, the extracellular space and the plasma membrane (figure 1.1, arrow 2), the early endosomes (figure 1.1, arrow 3), the late endosomes (figure 1.1, arrow 4) and the vacuole (figure 1.1, arrow 5). Furthermore, the TGN functions as an acceptor compartment for the endosomal trafficking and hence constitutes the interface between the secretory and endocytic systems (Sandvig and van Deurs 2002). This bidirectional traffic between the TGN and the endocytic system (figure 1.1, arrows 3-4

and 7-8) is essential for the proper sorting of proteins to the vacuole which require association with a receptor. For instance, the soluble vacuolar hydrolases carboxypeptidase Y (CPY) is transported from the TGN to the endosomes in a receptor-mediated process after its association with Vps10p (Marcusson *et al.* 1994). Once in the endocytic compartment, CPY dissociates from Vps10p and the later is recycled back to the TGN in order to bind more CPY (figure 1.1, arrow 8) (Cooper and Stevens 1996). A different pathway from the TGN to the vacuole, but bypassing the endosomes is described for the internal membrane protein ALP (Alkaline Phosphatase) (figure 1.1, arrow 5) (Cowles *et al.* 1997a).

Endocytosis, a process by which plasma membrane proteins, lipids and extracellular macromolecules are internalised, starts with the invagination of the plasma membrane and the pinching off of the vesicle. The vesicles formed at the plasma membrane fuse with the early endosomes (figure 1.1, arrow 9). Thereafter, the cargo contained in these vesicles are either recycled back to the plasma membrane (figure 1.1, arrow 10), sorted to the TGN (figure 1.1, arrow 7) or transported to the vacuole to be degraded through a process of maturation of the early endosomes to the late endosomes and/or MVB (figure 1.1, large dashed lines) (for review, see Pelham 2002). In *S. cerevisiae*, the first evidence for the existence fluid-phase endocytosis was obtained using the fluid-phase marker Lucifer yellow (Riezman 1985). Subsequently, receptor-mediated endocytosis was described for the pheromone α-factor (Chvatchko *et al.* 1986 and Jenness *et al.* 1986) . These two pathways are time-, temperature- and energy-dependent and seem to depend from the same endocytic machinery (Vida and Emr 1995 and Raths *et al.* 1993). In the endocytic pathway, the early endosomes are the station of sorting decision, where proteins destined to be recycled are diverted away from the bulk flow of proteins destined for the vacuole (reviewed by Shaw *et al.* 2001). While in mammalian cells the recycling to the plasma membrane from the endosomes has been well described (figure 1.1, arrow 10). In *S. cerevisiae* this route was only identified for Gap1p, the general amino acid permease in this organism, and Pma1-7p, a mutant from the plasma membrane ATPase (Luo and Chang 2000; Gao and Kaiser 2006; Seaman 2008). The other few yeast proteins known to be recycled to the plasma membrane, the a-factor receptor Ste3p, the v-SNARE Snc1p and the chitin synthase Chs3p seem first to be retrieved to the Golgi (figure 1.1, arrow 7) and from there re-directed to the plasma membrane (figure 1.1, arrow 2) (Chen and Davis 2000; Lewis *et al.* 2000; Ziman *et al.* 1996; Holthuis *et al.* 1998).

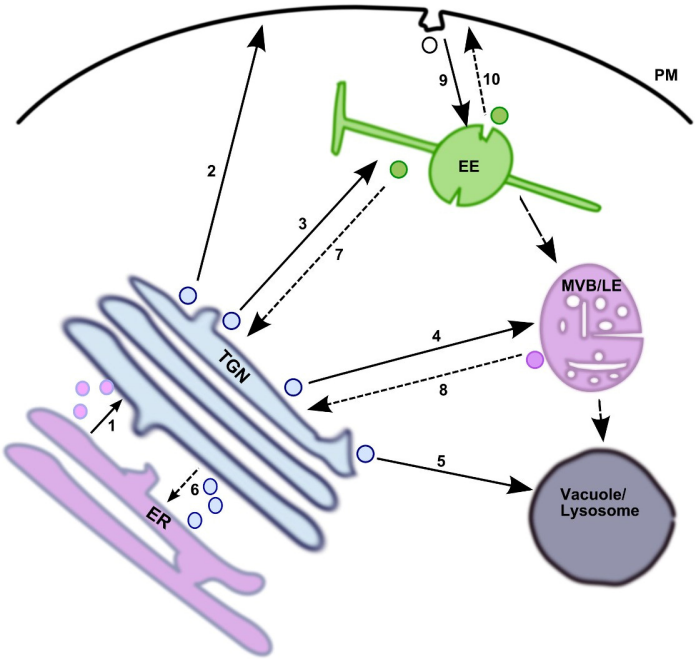

Figure 1.1: The biosynthetic and endocytic transport pathways in *S. cerevisiae*. Newly synthesised proteins destined to be secreted or to reside within the biosynthetic and endocytic pathway are synthesised in the ER and from there sorted to the Golgi compartment. Once at the Golgi compartment, proteins can be transported to the different compartments in the cell by several different routes. They can be recycled back to the ER (arrow 6) or be sorted at the TGN to the plasma membrane or extracellular milieu (arrow 2), to the early endosomes (EE) (arrow 3), to the late endosomes (MVB/LE) (arrow 4) and to the vacuole (arrow 5). Proteins residents at the TGN and necessary for transporting cargo to their final destinations are recycled back to the TGN (arrow 7 and 8). Proteins, membrane lipids and fluid from the extracellular milieu are endocytised at the plasma membrane and the corresponding vesicles fuse with the early endosomes (arrow 9). At the early endosomes, proteins can be sorted either to the TGN (arrow 7), recycle back to the plasma membrane (arrow 10) or follow the maturation to late endosomes in order to be delivered to the vacuole.

1.2 Vesicular transport

The communication between the different organelles is mediated by vesicular carriers formed in the donor organelles that move toward and fuse with the correct acceptor organelle. The steps of vesicle formation (budding), positioning in the right acceptor compartment (tethering) and vesicle fusion require proper machinery to allow the accurate functioning of membrane trafficking.

1.2.1 Vesicle formation

Vesicle formation is mediated by cytoplasmic coat proteins that are recruited onto the specific donor membrane (Schekman and Orci 1996). Coat proteins have several main functions: the cargo recognition and concentration as well as membrane deformation to generate a free vesicle (Kirchhausen et al. 1997; Bonifacino and Lippincott-Schwartz 2003). Three major types of vesicle coats have been implicated in

diverse transport steps: COP-I, COP-II and clathrin (Pearse 1975; Waters et al. 1991; Barlowe et al. 1994).

The COP-II coat which is composed of two two subcomplexes, Sec23p-Sec24p and Sec13-Sec31p, and the Ras-like GTPase Sar1p (d'Enfert *et al.* 1991), is known to mediate the exit of vesicles from the ER to the Golgi (Barlowe et al. 1994). While the COP-I coat which consist of a heptameric protein complex that is recruited by the activated form of Arf is involved in the intra-Golgi transport and retrograde transport from the Golgi to the ER (figure 1.2) (Letourneur et al. 1994).

Clathrin-coated vesicles (CCVs) are involved in the transport between organelles such as the TGN, endosomes and plasma membrane (figure 1.2). The main proteins of these coated vesicles are the clathrin-heavy chain (Chc1p) and the clathrin-light chain (Clc1p). They associate to form a triskelion of three clathrin heavy and light chains that after oligomerisation form a lattice made-up of pentagons and hexagons which surrounds the vesicle (Kirchhausen 2000; Wilbur et al. 2005). The binding of clathrin to membranes is mediated by clathrin adaptors that can bind directly to both clathrin and the lipid and/or protein components of the membranes (Kirchhausen 2000; Owen et al. 2004). In addition, clathrin adaptors participate in the incorporation of cargo molecules and in the recruitment of accessory factors which regulate and participate in CCV formation (Heilker et al. 1999; Slepnev and De Camilli 2000).

One of the main classes of adaptors that cooperate with clathrin are the heterotetrameric adaptor protein (AP) complexes which are composed of four subunits (reviewed by Kirchhausen 1999; Boehm and Bonifacino 2001; Robinson and Bonifacino 2001). In yeast there are three AP complexes: AP-1, AP-2 and AP-3 (reviewed by Boehm and Bonifacino 2001). AP-1 is the only AP complex that seems to physically interact with clathrin (Yeung *et al.* 1999; Yeung and Payne 2001) and is implicated in the transport between the TGN and the endocytic intermediates, as well as in the retrograde transport from early endosomes to the TGN (Stepp *et al.* 1995; Valdivia *et al.* 2002) (figure 1.2). The function of AP-2 in yeast is yet unknown (reviewed by Boehm and Bonifacino 2002). However, a recent study has identified yeast AP-2 as a specific endocytic adaptor for the K28 killer toxin receptor (Carroll *et al.* 2009), involving AP-2 in endocytosis from the plasma membrane (figure 1.2). The yeast AP-3 is implicated in the sorting of the alkaline phosphatase (ALP) and the vacuolar t-SNARE Vam3p from the TGN to the vacuole bypassing the endosomes (figure 1.2) (Piper *et al.* 1997; Stepp *et al.* 1997; Cowles *et al.* 1997b). The monomeric

GGAs (Golgi-localised, γ-ear-containing, ADP-ribosilation factor-binding proteins) represent another family of clathrin adaptors. They consist of four distinct segments: a VHS domain that binds an acidic di-leucine sorting signal; a GAT domain which binds Arf:GTP; a hinge region which recruits clathrin; and a GAE domain which exhibits sequence similarity to the ear region of gamma adaptin and recruits a number of accessory proteins (Pelham 2004). In yeast deletion of the two GGA genes, *GGA1* and *GGA2*, leads to trafficking defects between the TGN and the endosomes (figure 1.2) (Black and Pelham 2000; Dell'Angelica *et al.* 2000; Hirst *et al.* 2000; Costaguta *et al.* 2001; Zhdankina *et al.* 2001). However, it is not clear whether GGAs and AP-1 function together in the packaging of cargo molecules into CCVs at the TGN (Doray *et al.* 2002) or if they act in distinct pathways from the TGN to the endosomes (Costaguta *et al.* 2001; Abazeed and Fuller 2008). Similarly to COP-I recruitment, the recruitment of clathrin adaptors to the membrane is mediated by the GTP bound form of Arfs (Bonifacino and Lippincott-Schwartz 2003; Wang *et al.* 2003).

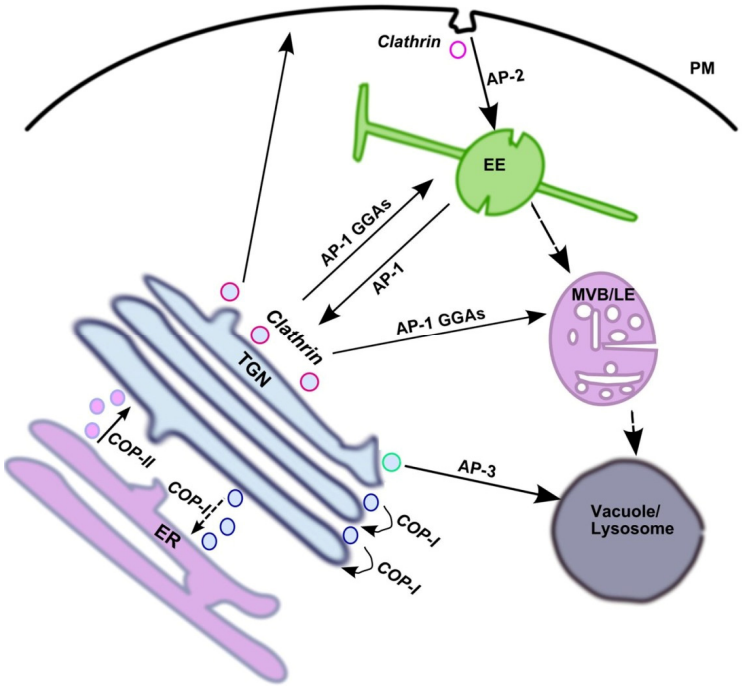

Figure 1.2: Proposed roles for the different coat components and clathrin adaptors in the different transport pathways. COP-I and COP-II mediate the retrograde and anterograde transport from the ER to the Golgi, respectively. Clathrin mediates the sorting from the TGN as well as endocytosis from the plasma membrane. The clathrin adaptor AP-2 mediates the recruitment of clathrin at the plasma membrane, AP-1 at the TGN and endosomes and GGAs at the TGN. AP-3 recruits Vps41p and mediates the traffic of vesicles from the TGN to the vacuole by bypassing the endosomes in a clathrin -independent pathway.

Arfs GTPases are a subfamily of the highly conserved Ras superfamily of small GTPases which regulate vesicular traffic and organelle structure by recruiting coat

proteins and modulating the actin cytoskeleton (reviewed by Gillingham and Munro 2007). The Arf family comprises Sar1p, Arfs and a number of Arf-like GTPases (Arl) (Pasqualato *et al.* 2002; Kahn *et al.* 2006). Most of the Arf GTPases have a myristoylated N-terminal helix that seems to be important for their membrane association (Amor *et al.* 1994), and they cycle between a GTP-bound active state and a GDP-bound inactive state (reviewed by D'Souza-Schorey and Chavrier 2006; Gillingham and Munro 2007). The activation of the Arfs from the GDP to the GTP form induces a conformational change which involves the switch 1 and switch 2 regions of the proteins as well as an intermediary region only present in the Arf family, the interswitch. The sliding of the interswitch region displaces the N-terminal amphipathic helix from the hydrophobic pocket and promotes the insertion of this helix into the adjacent lipid bilayer (figure 1.3) (Goldberg 1998; Pasqualato *et al.* 2002). Recently, the McMahon lab showed that the insertion of the N-terminal amphipathic helix of Arfs into the membrane generates a high positive membrane curvature, thereby initiating membrane budding (Lundmark *et al.* 2008) an effect which was previously observed for the non-myristoylated N-terminal helix of Sar1p (Lee *et al.* 2005). The activation of Arfs and exchange of GDP for the tri-phosphate nucleotide is mediated by guanine nucleotide exchange factors (GEFs) and the hydrolysis of bound GTP is mediated by GTPases-activating proteins (GAPs). Since membrane recruitment of Arfs is tightly coupled to their active GTP-bound state, GEFs are thought not only to control the activity of the Arfs but also to define their distribution (Donaldson and Jackson 2000; Jackson and Casanova 2000).

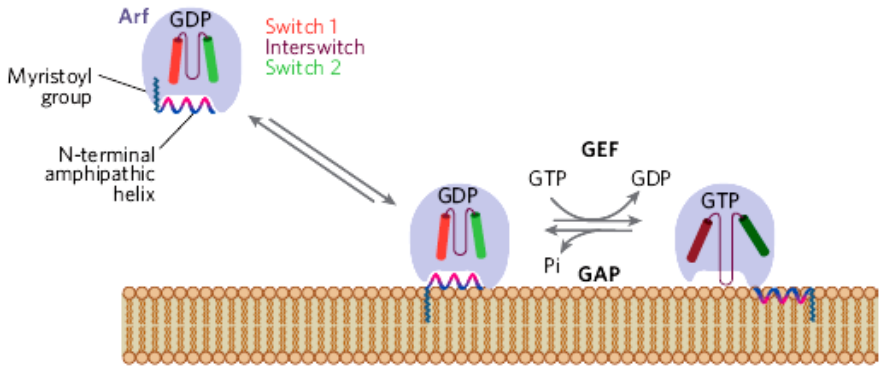

Figure 1.3: Schematic representation of the mechanism of Arf GTPase activation and recruitment to membranes. In the cytoplasm the N-terminal amphipathic helix of Arf-GDP is inserted into a hydrophobic pocket. When close to the membrane the N-terminal myristoyl group is able to bind the lipid bylayer in a reversible manner. At the membrane, the Arf GTPase is activated by a GEF that exchanges GDP to GTP. The nucleotide exchange in the Arf induces a conformational change in the switch 1 and 2 and in the interswitch loop, the later slides and displaces the N-terminal helix out of the pocket and the Arf-GTP binds then tightly to the membrane through the hydrophobic residues of the N-terminal helix. (adapted from Behnia and Munro 2005).

1.2.2 Vesicle targeting and fusion

After vesicles have budded off the donor membrane they must be targeted to the appropriate acceptor compartment.

The recognition of the targeted membrane by the vesicle is referred to as the tethering stage, a stage in which specificity is conferred to the fusion reaction. The tethering stage involves recruitment of tethering factors by Rab/Ypt GTPases (for review, see Stenmark 2009). Tethering factors are assumed to allow the long distance contacts between the vesicle and the target compartment. Two types of tethering factors have been described: proteins containing extensive coiled-coil domains and large multisubunit complexes. In *S. cerevisiae*, Uso1p, Imh1p are examples of coiled-coil tethers while the COG (conserved oligomeric Golgi) complex, GRAP (Golgi-associated retrograde protein) complex and TRAPP I and II (transport protein particle) complexes are examples of multisubunit tethering complexes (reviewed by Whyte and Munro 2002).

Once the vesicle and the acceptor membrane are in close proximity, their fusion is initiated by the aid of SNAREs. SNAREs can be divided into two categories: v-SNAREs, which are incorporated into the membranes of transport vesicles during budding, and t-SNAREs, which are located at the membranes of the target compartments. v- and t-SNAREs recognize each other and assemble into biochemically stable *trans*-SNARE complexes, which bring the vesicle close to the target membrane and mediate vesicle fusion (Sollner *et al.* 1993). t-SNAREs are frequently used as markers to distinguish the distinct organelles. As examples, the yeast t-SNAREs Tlg1p, Pep12p and Vamp3p are used as markers of the early-endosome, late-endosomes and vacuole, respectively (Becherer *et al.* 1996; Darsow *et al.* 1998; Holthuis *et al.* 1998).

1.2.3 The role of phosphoinositides as regulators of vesicular transport

Phosphoinositides (PIPs) are phosphorilylated derivates of phosphatidylinositol (PtdIns) in which a phosphate group is attached to the 3, 4, or 5 position of the inositol ring. They are constitutively present in the cells and each of the distinct phosphoinositide is found in only one or a small set of organelles, thus representing key membrane-localised signals in the regulation of processes such as membrane traffic and cytoskeleton remodelling (Sechi and Wehland 2000; Roth 2004). For instance, $PI(4,5)P_2$

localises mainly at the plasma membrane, PI4P at the Golgi, PI3P on the endosomes and PI(3,5)P_2 on the MVB and vacuole (reviewed by Roth 2004).

In membrane traffic, the phosphoinositides have an important role in establishing membrane identity since they are recognised by peripheral-membrane proteins that contain specific motifs which bind to a particular form of phosphoinositide (reviewed by Behnia and Munro 2005). Hence, their strict distribution has to be spatially and temporally ensured by organelle specific phosphoinositide phosphatases and kinases (for review, see De Matteis and Godi 2004). Motifs that bind phosphoinositides are: the pleckstrin homology (PH) domain; the FYVE domain; the ENTH (epsin1 NH_2-terminal homology)/ANTH domains and the Phagocyte oxidase (PX) domains (for review, see Roth 2004). The PH domain and the ENTH/ANTH domains have specificity for PI(4,5)P2 (Harlan *et al.* 1994; Itoh *et al.* 2001) and indeed proteins bearing one of these domains are often targeted to the plasma membrane. This is the case of the phosphoinositide-specific phospholipase Cδ1 which contains a PH domain used as a probe for PI(4,5)P_2 (Musacchio *et al.* 1993; Lemmon *et al.* 1995), of yeast Ent1p and Ent2p which are implicated in endocytosis at the plasma membrane and contain ENTH domains (Wendland *et al.* 1999). The FYVE domain and PX domains recognise PI3P in endosomal membranes (Yu and Lemmon 2001; Stenmark *et al.* 2002). Vps27p, a yeast class E vps protein, bears a FYVE domain and is recruited to the endosomal membranes (Stahelin *et al.* 2002). The yeast sorting nexin orthologues and components of the retromer complex, Vps5p and Vps17p, contain PX domains and are thought to restrict retromer complex assembly to membranes containing PI3P and relevant cargo (Burda *et al.* 2002).

1.3 Cellular mechanisms of membrane remodelling and membrane curvature generation

Most membrane-bound organelles have characteristic shapes that are elaborate, dynamic and often contain regions of distinct morphologies (Zimmerberg and Kozlov 2006; Voeltz and Prinz 2007; Shibata *et al.* 2009). Organelles such as the lysosome or peroxisomes are relatively spherical, but the Golgi complex and the ER contain regions that form intricate networks of interconnected cisternae, tubules and fenestrations (Zimmerberg and Kozlov 2006; Voeltz and Prinz 2007). Others like the mitochondria and the multivesicular bodies, have an outer limiting membrane and complex networks of internal membranes (Voeltz and Prinz 2007). Moreover, the intracellular transport intermediates have a broad range of shapes from small spheres and narrow tubes to tubular-saccular carriers (Rothman and Wieland 1996; Polishchuk *et al.* 2000; Bonifacino and Lippincott-Schwartz 2003; Luini *et al.* 2005). All cellular membranes are highly dynamic, changing their shape continuously. Therefore, the question of how organelle shape and membrane curvature are generated has been of interest for physicists, mathematicians and cell biologists. While the answer to this question is still unclear, it is now recognised that the generation of membrane curvature and membrane shapes results from an interplay between membrane proteins, lipids and physical forces applied to the membrane surface (McMahon and Gallop 2005; Zimmerberg and Kozlov 2006; Shibata *et al.* 2009).

Lipid bilayers tend to be flat, since generation of curvature requires energy. The energy cost for bending a bilayer can be determined from the elastic model of lipid membranes (Helfrich 1973). From this model, the energy to bend a membrane is much larger than the thermal energy, meaning that membrane bending cannot be generated simply by thermal fluctuations. Thus, the generation of high membrane curvature requires molecular mechanisms that generate and stabilise these energetically unfavourable states (Shibata *et al.* 2009).

One of the best studied mechanisms of membrane curvature is the formation of a budding vesicle. The term “positive” curvature is commonly used to define regions of membrane that curve inwards, *i.e* towards the cytoplasm while the term “negative” curvature refers to the formation of a concave surface or budding out of the cell. The types of curvature involved through the process of vesicle budding are illustrated in the figure 1.4 (McMahon and Gallop 2005).

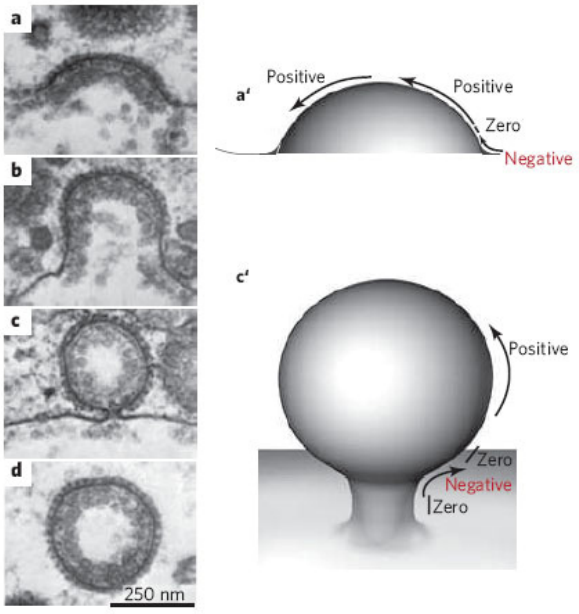

Figure 1.4: **Clathrin-coated vesicle budding and dynamic of membrane curvature.** (a-d) The different stages of a budding vesicle. (a') The curvature of the initial stage of a budding vesicle is mainly positive (convex surface). (c') The curvature of a late-stage budding vesicle is more complex. (adapted from McMahon and Gallop 2005).

There are several mechanisms that can generate positive or negative membrane curvature. An earlier experiment using red blood cells demonstrated that the insertion of a small fraction of exogenous lyso-phosphatidylcholine or of chlorpromazine to the plasma membrane was accompanied by drastic changes in membrane shape which were explained by the famous bilayer-couple model (Sheetz and Singer 1974). This model predicts that an increase in the surface area of one of the monolayers of a lipid bilayer induces various perturbations and increases the spontaneous curvature of the bilayer. This proved to be true for experiments involving liposomes, in which insertion of some lipids deformed liposomes into tubules (Farge and Devaux 1992; Stowell *et al.* 1999). The *in vitro* lipid asymmetry generated by insertion of external lipids to an existing lipid bilayer may *in vivo* be accomplished by the so called "flippases" (Farge *et al.* 1999). "Flippases" catalyse the unidirectional transport of one specific phospholipid or phospholipids from one leaflet of the lipid bilayer to another by use of ATP (adenosine triphosphate). Moreover, proteins themselves can account for the difference in the surface area of two monolayers in a lipid bilayer. This is the case of membrane bending by hydrophobic insertion. Here, proteins insert hydrophobic domains, such as the hydrophobic surface of an amphipathic helix, into the surface of a membrane monolayer (see figure 1.3 section 1.2.1). This generates a perturbation of the packing of the lipids head groups and allows positive membrane curvature. Examples include the N-terminal helix of epsin (Ford *et al.* 2002), the amphipathic N-terminal helices of the BAR

domain-containing proteins amphiphysin (Gallop *et al.* 2006) and endophilin (Masuda *et al.* 2006) and the amphipathic helices of the Arf-GTPases ARF1 (Lundmark *et al.* 2008) and Sar1p (Lee *et al.* 2005).

Another way to produce membrane curvature is to apply intrinsic forces on the membrane, in a process termed the scaffold mechanism. In this mechanism, proteins recruited from the cytoplasm can function as scaffolds by presenting the intrinsic curvature of the protein to the lipid bilayer (Farsad and De Camilli 2003; Zimmerberg and Kozlov 2006). The most prominent examples of proteins that use the scaffold mechanism to produce membrane curvature are the N-BAR and F-BAR domain containing proteins which produce positive membrane curvatures (Farsad *et al.* 2001; Peter *et al.* 2004; Richnau *et al.* 2004; Weissenhorn 2005; Henne *et al.* 2007), the I-BAR domain containing proteins that produce negative membrane curvature (Saarikangas *et al.* 2009) and coat components such as clathrin, COP-I and COP-II that polymerise into curved structures, even though they do not have direct membrane association (Nossal 2001; Antonny *et al.* 2003). A more indirect way to produce membrane curvature and deformation is used by cytoskeletal elements. Cytoskeletal assembly and disassembly influences membrane shape changes by affecting membrane tension (reviewed by Farsad and De Camilli 2003; McMahon and Gallop 2005). A well documented example is the role of actin polymerisation in the endocytic invagination events at the plasma membrane (Merrifield *et al.* 2005; Yarar *et al.* 2005).

Although most of the mechanisms described here have been shown to be able to generate deformations of lipid bilayers *in vitro* independently of one another, *in vivo* they seem to act together to remodel membranes.

1.4 P_4-ATPases: their role in maintaining lipid asymmetry and in vesicle-mediated transport

1.4.1 Transbilayer lipid asymmetry in biological membranes

In eukaryotic cells the plasma membrane is composed of different lipid species which are asymmetrically distributed across the bilayer. The extracellular leaflet is mainly composed of sphingolipids, glycolipids and the glycerolphospholipid phosphatidylcholine (PC), while the intracellular leaflet contains mainly the aminophospholipids phosphatidylserine (PS) and phophatidylethanolamine (PE),

phosphoinositides (PI) and phosphatidic acid (PA) (Op den Kamp 1979; Zachowski 1993; reviewed by Daleke 2007). Similarly, the subcellular organelles from the late-secretory and the endocytic pathways have each a characteristic lipid composition as well as membrane asymmetry, while in the ER all lipids are symmetrically distribuited between the two leaflets (for review, see van Meer *et al.* 2008). Along the secretory pathway sterols and sphingolipids are gradually concentrated. Their highest levels are at the plasma membrane where they confer the necessary compactness and thickness for its barrier function (Holthuis *et al.* 2001).

The maintenance of the lipid asymmetry is important particularly with respect to the restriction of PS and PE to the cytosolic leaflet. For instance, the interactions between PS and skeletal proteins like spectrin improve the mechanical stability of the membranes of red blood cells (Manno *et al.* 2002). Moreover, the enrichment of aminophospholipids, in the cytosolic leaflet of the vesicles, organelles and plasma membrane may help these surfaces to be in a fusion-competent state necessary for vesicular trafficking (Kinnunen and Holopainen 2000; Chernomordik and Kozlov 2008). In addition, exposure of PS on the cell surface of apoptotic cells, due to a global loss of the lipid asymmetry, acts as a signal for recognition by macrophages and phagocytes which bear PS receptors (Fadok *et al.* 1992; Savill *et al.* 1993; Fadok *et al.* 2000). On the other hand, the transient exposure of PS and PE at the cell surface may be necessary for a variety of cellular responses (for review see Balasubramanian and Schroit 2003). As examples, the transient exposure of PE on the cell surface seems to be necessary for cytokinesis (Emoto and Umeda 2000), while the transient exposure of PS in the time course of blood coagulation is important for the formation of the procoagulant surface (Solum 1999). Thus, cells have to possess mechanisms to control such stages of transient exposure of PS and PE, and the rapid reposition of the lipid asymmetry.

The idea of a catalysed transbilayer movement of phospholipids (or flip-flop) in biological membranes arose from several observations: first, in protein-free liposomes the flip-flop of phospholipids is very slow, with half-times ranging from hours to days (Kornberg and McConnell 1971); second, the *de novo* synthesis of the majority of phospholipids takes place on the cytosolic side of the ER (Bell *et al.* 1981) and hence there is a need of a rapid redistribution of phospholipids to maintain the bilayer balance; and last but not least, the rapid phospholipid flip-flop observed in ER membranes is sensitive to proteases (Bishop and Bell 1985; Buton *et al.* 1996). In fact, at least three

classes of proteins seem to be involved in the translocation of phospholipids across membranes (Pomorski *et al.* 2004). The "flippases" or aminophospholipid translocases (APLTs) which catalyse the inward transbilayer transport of phospholipids, *i.e* from the extracytoplasmic leaflet to the cytoplasmic leaflet of the bilayer, with the use of ATP. The "floppases", which catalyse the outward transbilayer transport of phospholipids in an ATP-dependent manner. And the "scramblases" which catalyse the non-specific and bidirectional transbilayer transport of phospholipids in a calcium-dependent manner (figure 1.5).

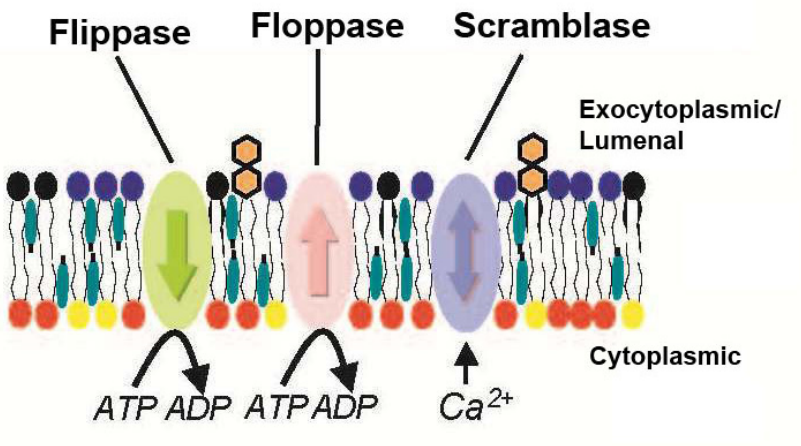

Figure 1.5: Proteins thought to mediate the transbilayer movement of phospholipids and to regulate membrane lipid asymmetry. ATP-dependent flippases catalyse the translocation of phosphatidylethanolamine (PE) and phosphatidylserine (PS) from the extracitoplasmic or lumenal leaflet to the cytosolic leaflet. The ATP-dependent floppases catalyse the reverse movement but with no known apparent headgroup specificity. These both activities seem to be responsible for the lipid asymmetry in the membranes. Scramblases are activated by the Ca^{2+} influx and they enable the flip-flop of phospholipids according to their concentration gradient to produce symmetry in the membrane. (adapted from Pomorski *et al.* 2004)

1.4.2 P_4-ATPases are prime candidates for being aminophospholipid translocases

The first evidence for an ATP-dependent inward transport of phospholipids (or flippase activity) came from the studies made by Seigneuret and Devaux. They found that in human erythrocytes the spin-labelled analogues of aminophospholipids (PS and PE) were rapidly translocated to the cytosolic leaflet, while a PC analogue remained in the outer leaflet of the plasma membrane (Seigneuret and Devaux 1984). The biochemical characterisation of this APLT activity showed that it requires Mg^{2+} and ATP and that it was sensitive to the sulfhrydryl group reagent N-ethylmaleimide and to vanadate (Seigneuret and Devaux 1984; Daleke and Huestis 1985; Zachowski *et al.*

1986). These biochemical characteristics have therefore served as selection criteria for the identification of the responsible enzyme. Hence, the discovery of an APLT activity in bovine chromafin granules led to the purification and cloning of the respective enzyme, ATPase II, now called ATP8A1 (Moriyama and Nelson 1988; Tang *et al.* 1996). Sequence alignment identified a member of an unrecognised subfamily of P-type ATPases, Drs2p from *S. cerevisiae*, as the closest homologue of ATP8A1 (Tang et al. 1996). Later an increased number of homologues were identified in the *S. cerevisiae* genome and classified as the P4 subfamily with possible APLT activity (Catty et al. 1997; Axelsen and Palmgren 1998). The P_4-ATPase family members are predicted to contain 10 transmembrane segments with the N- and C-termini facing the cytosol. They differ from the cation-transporting P-type ATPases since they lack negatively charged amino acids within the transmembrane segments critically involved in cation transport (Catty et al. 1997). Nowadays, over 100 members of the P_4-ATPase subfamily have been identified, all of which are exclusively found in eukaryotic organisms (Halleck et al. 1999; Paulusma and Oude Elferink 2005). Among them, 5 members can be found in *S. cerevisiae*, 12 in *Arabidopsis thaliana* and 14 in mammalians (Catty *et al.* 1997; Gomes *et al.* 2000; Paulusma and Oude Elferink 2005).

The implication of the P_4-ATPases in the inward transbilayer movement of phospholipids across the bilayer was further strengthened by several functional studies using yeast cells lacking different members of this subfamily. In *S. cerevisiae*, the P_4-ATPases Drs2p, Dnf1p, Dnf2p, Dnf3p and Neo1p are distinctly distributed throughout the late-secretory and endocytic pathways. Dnf1p and Dnf2p localise mainly to the plasma membrane, Dnf3p to the late Golgi, Drs2p to the late Golgi and Neo1p to the late Golgi and to the endosomes (Chen *et al.* 1999; Hua *et al.* 2002; Pomorski *et al.* 2003; Wicky *et al.* 2004). For instance, removal of the yeast plasma membrane-associated, Dnf1p and Dnf2p, abolishes the energy-dependent inward translocation of fluorescent 7-nitrobenz-2-oxa-1,3-diazol-4-yl (NBD)-labeled PE, PC and PS and causes aberrant exposure of endogenous aminophospholipids at the cell surface (Pomorski *et al.* 2003). In addition, the translocation of NBD-PS in purified trans-Golgi membranes from a yeast strain lacking all the *DNF* genes and containing a temperature-sensitive *drs2* allele, instead of the wild-type *DRS2*, becomes defective when this mutant is shifted to non-permissive temperature (Natarajan *et al.* 2004). This later discovery provided compelling evidence that Drs2p is directly coupled to an APLT activity at the trans-Golgi. This was subsequently reinforced by the finding that Drs2p together with

Dnf3p are required to translocate phospholipids and to maintain lipid asymmetry in post-Golgi secretory vesicles (Alder-Baerens *et al.* 2006). Finally, Zhou and Graham recently succeeded to directly demonstrate NBD-PS flippase activity with purified Drs2p reconstituted into proteoliposomes (Zhou and Graham 2009). This flippase activity was shown to be Mg^{2+}-ATP dependent and orthovanadate-sensitive which is consistent with the properties of the purified mammalian ATP8A1 and demonstrates that Drs2p is a "flippase" (Zhou and Graham 2009). The P_4-ATPase Neo1p is essential for yeast cells viability and therefore similar functional studies were not yet possible. However, since Neo1p is also a P_4-ATPases it may also have a "flippase" activity.

In other organisms, several members of the P_4-ATPase subfamily have also been implicated in the translocation of aminophospholipids. For instance, the heterologous co-expression of the P_4-ATPase ATPase3 (ALA3) from *A. thaliana* with one of its β-subunit (see below) in yeast cells lacking Drs2p, Dnf1p and Dnf2p resulted in the restitution of the transbilayer movement of the phospholipids analogues NBD-PS, NBD-PE and NBD-PC (Poulsen *et al.* 2008a). The same experiment carried out with ALA2, another *A. thaliana* P_4-ATPase, restored the transbilayer movement of the phospholipid analogue NBD-PS (Lopez-Marques *et al.* 2010). This indicates that plant P_4-ATPases also have PLT activity. Moreover, a similar experiment performed with the recently identified murine P_4-ATPase, specifically expressed in testis, FetA, also resulted in the restoration of the translocation of the NBD analogues of PC and PE in this yeast mutant strain which suggests that FetA has PLT activity (Xu *et al.* 2009). The mammalian P_4-ATPase, ATP8B1, whose mutations have been implicated in a severe liver disease (Intrahepatic Cholestasis), also seems to be a flippase for PS. The co-expression of ATP8B1 with one of the CDC50 proteins (see below) in a cell line defective for the non-endocytic uptake of NBD-PS resulted in an enhanced NBD-PS internalisation (Paulusma *et al.* 2008). In addition, a recent study identified the P_4-ATPase TAT-1 from *Caenorhabditis elegans* as being necessary for the maintainance of the PS asymmetry at the plasma membrane of this animal (Darland-Ransom *et al.* 2008). Thus, all these evidences suggest that P_4-ATPase actively transport phospholipids.

1.4.3 The Cdc50 family members are β-subunits of the P_4-ATPases

Although it seems most evident that the inward transport of phospholipids is catalysed by the P_4-ATPases, another yeast protein, Lem3p/Ros3p, has also been implicated in this type of transport across the plasma membrane (Kato *et al.* 2002). This finding has for a while put in question the direct role of P_4-ATPases as APLTs. Lem3p/Ros3p belongs to the well conserved CDC50 family, which is composed of 3 members in yeast (Cdc50p, Lem3p and Crf1p) (Kato *et al.* 2002), 5 in *A. thaliana* (ALIS1-5) (Poulsen *et al.* 2008a) and 3 in mammalians (CDC50A, CDC50B, CDC50C) (Katoh and Katoh 2004). These proteins contain two transmembrane segments and an extracellular glycosylated loop (Kato *et al.* 2002), but lack any similarity to known transporters. Instead, they were found to form heteromeric complexes with P_4-ATPases and to be required for their stability and export from the ER (Saito *et al.* 2004; Chen *et al.* 2006; Furuta *et al.* 2007; Paulusma *et al.* 2008). For instance, in yeast, Lem3p is required for the transport of Dnf1p and Dnf2p to the plasma membrane, Cdc50p is required for the Golgi localisation of Drs2p and Crf1p for transporting Dnf3p to the Golgi (Saito *et al.* 2004; Furuta *et al.* 2007). Thus, rather than directly transporting phospholipids, this family of proteins seems to function as chaperones involved in the proper localisation of the P_4-ATPases pumps.

Recently, it was suggested that the Cdc50 family members may help to determine the substrate specificity of the P_4-ATPases complexes once they reached their destination (Poulsen *et al.* 2008b; Puts and Holthuis 2009). This suggestion was based on the observation that the yeast trans-Golgi P_4-ATPases, Drs2p and Dnf3p, which have different translocation preferences (Alder-Baerens *et al.* 2006), interact with different subunits, Cdc50p and Crf1p, respectively; while the P_4-ATPases Dnf1p and Dnf2p which have the same substrate specificity (Pomorski *et al.* 2003), both interact with Lem3p. However, a recent study demonstrated that the substrate specificity and localisation of the plant P_4-ATPases, ALA2 and ALA3, is determined by the catalytic subunit and not by the CDC50 homologue with which they form a complex to exit the ER (Lopez-Marques *et al.* 2010). Whereas another work demonstrated that the separation of Drs2p from its binding partner Cdc50p affected the ability of Drs2p to form a phosphoenzyme intermediate, suggesting that Cdc50p is implicated in the reaction cycle of Drs2p (Lenoir *et al.* 2009). Thus, at present, the role of CDC50 proteins in the P_4-ATPases catalysed lipid transport awaits further elucidation.

Although most P-type ATPases only need a single α-subunit polipeptide to carry out ATP hydrolysis and ion pumping, the Na^+/K^+-ATPase requires two subunits for its full functionality. The β- subunit of the Na^+/K^+ ATPase is mainly involved in the proper folding and trafficking of the catalytic α-subunit (Geering 2001), while the γ-subunit has a role in fine tuning the activity of this pump but is not essential for its functionality (Geering 2008). Interestingly, the Cdc50 family members are structurally similar to the fusion between the β- and γ-subunits of the Na^+/K^+ ATPase, in terms of polypeptide lengths and membrane segment topology (Poulsen *et al.* 2008b). Thus, the Cdc50p family members migh also be involved in the proper folding and trafficking of the P_4-ATPases and hence represent their β-subunits. However, it is also possible that these proteins might have a more direct role in the P_4-ATPase-catalysed lipid transport which is still undisclosed.

1.4.4 Role of P_4-ATPases in vesicle-mediated transport

Based on the bilayer couple model of Sheetz and Singer (see section 1.3), P_4-ATPases have been proposed to bend membranes by coupling ATP to the unidirectional translocation of phospholipids across the bilayer. This activity would create an imbalance in phospholipid number between the two leaflets and cause bending of the membrane in the direction of lipid translocation (Graham 2004; Pomorski *et al.* 2004). Indeed, it has been shown that the addition of phospholipids in the exocytoplasmic leaflet of the plasma membrane and their subsequent translocation to the cytosolic leaflet accelerates endocytosis in erythroleukemia cells (Farge *et al.* 1999).

The first indication that P_4-ATPases might be part of the general trafficking machinery came from the finding that yeast *DRS2* exhibited genetic interactions with *ARF1* and *CHC1* (clathrin heavy chain) (Chen *et al.* 1999). A later study found that inactivation of the temperature sensitive allele *drs2-ts* blocked the formation of a specific clathrin-dependent class of post-Golgi vesicle, the "higher density" class, which contains exocytic cargo (Gall *et al.* 2002). These findings led to propose that the generation of lipid asymmetry could be intimately connected to coat assembly during membrane budding. This proposal was further strengthened with the discovery that Drs2p physically interacts with Gea2p, a Sec7 domain containing Arf GEF from the well conserved GBF subfamily, and that this interaction is necessary for the fenestration and tubulation events along the secretory pathway (Chantalat *et al.* 2004). On the other

hand, a recent study demonstrates that Drs2p is involved in the formation of vesicle in the AP-1 (clathrin adaptor) pathway, and indeed it physically interacts with AP-1, but is not necessary to recruit ARF, AP-1 or clathrin to membranes (Liu *et al.* 2008). Instead, Drs2p seems to be necessary for the budding of AP-1/clathrin-coated vesicles, since in the absence of this protein the recruitment of ARF, AP-1 and clathrin is not sufficient to allow the budding of this type of vesicles (Liu *et al.* 2008). Overall, the authors suggest that Drs2p catalyses the ATP-dependent transbilayer movement of lipids that conveys the membrane curvature required to facilitate vesicle budding. Additionally, Drs2p and its binding partner Cdc50p have for a while been implicated in several trafficking pathways. In agreement with the aforementioned role of Drs2p in the formation of AP-1/CCV, Drs2p was shown to be, similarly to AP-1, necessary for the retrograde transport of Chs3p (Chitin synthase III) from the early endosomes to the TGN (Liu *et al.* 2008). Moreover, Drs2p is transported from the TGN to the endosomes in an AP-1-dependent manner in which its own flippase activity seems to be necessary (Liu *et al.* 2008). In absence of Drs2p flippase activity or AP-1 function, Drs2p is incorporated in exocytic vesicles where it reaches the plasma membrane and is consequently internalised via the NPFXD/Sla1p and Ub-dependent endocytic pathways (Liu *et al.* 2007; Liu *et al.* 2008). Additionally, both Drs2p and Cdc50p seem to be involved in the Rcy1 retrieval pathway from the endosomes to the TGN (Furuta *et al.* 2007). Rcy1p is an effector of the Ypt31p/32p RabGTPases which is involved in the recycling out of the early endosomes (Wiederkehr *et al.* 2000; Chen *et al.* 2005). Both Cdc50p and Drs2p physically and genetically interact with Rcy1p (Furuta *et al.* 2007). Significantly, the Δ*ryc1* mutant is cold sensitive like the Δ*cdc50* or Δ*drs2* mutants and the deletion of *RYC1* in a *Δcdc50* background did not exacerbate the cold sensitivity of the Δ*cdc50* mutant (Furuta *et al.* 2007). Consistently, the recycling of the v-SNARE Snc1p is impaired in the *cdc50ts* and Δ*drs2* mutants, a defect also observed in the Δ*rcy1* mutant (Hua *et al.* 2002; Furuta *et al.* 2007). Furthermore, Cdc50p seems to depend on the Rcy1p pathway to be retrieved from the endosomes to the TGN (Furuta *et al.* 2007). Altogether, these data suggest that the Cdc50p-Drs2p complex might be involved in the exocytic, AP-1 and Rcy1p pathways.

Interestingly, another yeast P_4-ATPase, Neo1p, was identified in the laboratory of Birgit Singer-Krüger in a high-copy number suppression screen for the temperature sensitivity of *Δysl2* cells (Wicky *et al.* 2004). *YSL2* encodes a well conserved protein

related to the Arf GEFs from the BIG/GBF subfamilies which localises to the TGN and endosomes (Jochum *et al.* 2002; Efe *et al.* 2005; Gillingham *et al.* 2006). Similarly to Ysl2p, Neo1p was also found to localise to the late Golgi and endosomes. Furthermore, Ysl2p and Neo1p physically interact and their functions seem to be tightly connected to the Arf-like GTPase Arl1p (Jochum *et al.* 2002; Wicky *et al.* 2004). In particularly, the disruption of *ARL1* in a Δ*ysl2* background results in synthetic lethality while overexpression of *ARL1* suppresses the defects of the Δ*ysl2* mutant in growth, endocytosis and vacuole biogenesis (Jochum *et al.* 2002). Ysl2p and Arl1p were also found to physically interact via the N-terminal region of Ysl2p, which contains a region with homology to the Sec7 domain of ArfGEFs (Jochum *et al.* 2002). However, at present it is unknown whether Ysl2p can mediate the nucleotide exchange on Arl1p. Additionally, a genetic interaction was also found between *NEO1* and *ARL1* in which the growth defect of the conditional *neo1-69* mutant allele could be rescued by deletion of *ARL1* (Wicky et al. 2004). In fact, in this mutant, the subcellular distributions of both Ysl2p and Arl1p seem affected; as if these proteins accumulated excessively on punctuate membrane structures (Wicky *et al.* 2004). This observation led to the hypothesis that in this mutant Neo1-69p, Ysl2p and Arl1p would produce a detrimental interaction which resulted in growth defect. This suggestion led to the identification of *GGA2*, whose deletion also improved the growth of the *neo1-69* mutant (Singer-Krüger *et al.* 2008). Further studies demonstrated that the cooperation between Neo1p, Ysl2p, and Arl1p allows the proper recruitment of the monomeric Gga clathrin adaptors via direct interaction with Ysl2p (Singer-Krüger *et al.* 2008). In particular, deletion of *ARL1* or *YSL2* resulted in a decreased association of Gga2p with membranes, suggesting that Arl1p might cooperate with Arf1p to recruit Gga proteins to the Golgi (Singer-Krüger *et al.* 2008). The connection of Neo1p and its associated network with GGAs is consistent with the previous observation that *neo1-69* and *neo1-37* alleles have a delayed transport and processing of CPY a defect also observed for the double mutant Δ*gga1*Δ*gga2* (Mullins and Bonifacino 2001; Wicky *et al.* 2004). However, while the connection of Neo1p to GGAs seems evident, it is yet not clear in which pathways Neo1p and GGAs are involved.

In addition, a previous distinct study implicated Neo1p in the retrograde transport from the Golgi to the ER (Hua and Graham 2003). Genetic interactions were observed in *neo1-ts* COPI (*sec21-1*, *ret1-1*) double mutants which either were inviable or very

slow growing. Moreover, like in the COPI mutants, the Rer1-GFP Golgi localised protein was mislocalised to the vacuole in several *neo1-ts* mutants after shift to non-permissive temperature (Hua and Graham 2003; Wicky *et al.* 2004). Thus, Neo1p might also play a role in the early secretory pathway. In any case, the aforementioned evidences and the fact that several conditional *neo1-ts* alleles lead to defects in protein transport and accumulation of abnormal membrane structures (Hua and Graham 2003; Wicky *et al.* 2004), strongly suggest that Neo1p is involved in vesicle transport.

Several other P_4-ATPases seem to be implicated in vesicular trafficking. For instance, the yeast plasma membrane P_4-ATPases, Dnf1p and Dnf2p, have been suggested to play a role in endocytosis, as double mutants lacking these proteins are unable to internalize the FM4-64 endocytic dye at 15ºC (Pomorski *et al.* 2003). In plants, mutations in the Golgi localised P_4-ATPase ALA3, leads to defects in slime vesicle production (a type of secretory vesicles) at the peripheral columella cells of the root tip (Poulsen *et al.* 2008a). Moreover the P_4-ATPase TAT-1 from *C. elegans* has been recently implicated in the early stages of the endocytic pathway in the intestine of this organism (Ruaud *et al.* 2009).

Taken together, these data strongly suggest that P_4-ATPases are components of the vesicular trafficking machinery and they may directly contribute to the initial step of budding of vesicles by performing the ATP-dependent translocation of phospholipids.

1.5 Scope of this work

The major goal of this project was to identify new proteins necessary for the functionality of the endosomal P_4-ATPase Neo1p.

As previously mentioned in the section 1.4.3, the proteins from the CDC50 family are β-subunits for a large number of P_4-ATPases and are required for the ER exit of the catalytic α-subunit. Interestingly, the identification of *NEO1* in a high copy number suppression screen for the cold sensitivity of Δ*cdc50* cells was crucial for these findings (Saito *et al.* 2004). Therefore, I analysed whether Neo1p physically associates with Cdc50p and requires it to exit the ER. However, since no association between these two proteins could be found I explored other possibilities.

Neo1p was previously identified in the group of B. Singer-Krüger as being a binding partner of Ysl2p, a protein related to the large Arf GEFs of the GBF and BIG subfamilies (see section 1.4.4). Similarly to *NEO1* another essential gene, *DOP1,* was

identified as being a high copy suppressor of the growth defect of Δ*ysl2* mutant (Efe *et al.* 2005). In the present work I identified Dop1p as being a binding partner of Neo1p and Ysl2p. After concluding that Dop1p is part of a complex containing Neo1p and Ysl2p, I analysed this protein in more detail. To that end, several localisation studies for Dop1p were performed. Additionally, I also expressed 3 different portions of this large protein and analysed their localisation and binding affinities to Neo1p and Ysl2p. Moreover, I explored the phenotypic similarities between the previously characterised temperature sensitive mutants of *NEO1*, *neo1-37* and *neo1-69* (Wicky *et al.* 2004), and the uncharacterised temperature sensitive mutant, *dop1-3*, kindly provided by Richard Kahn (Atlanta, USA).

Furthermore, in a previous study the tagging or truncation of the C-terminus of Neo1p was shown to result in a non-functional protein retained within the ER (Wicky *et al.* 2004). Here, I identified a conserved PPSY motif within the C-terminus of Neo1p which I further analysed by introducing point mutations.

2 Materials and Methods

2.1 Materials

2.1.1 *Saccharomyces cerevisiae* strains

Yeast strain	Genotype	Source
RH1201	*MAT***a**/α *his4/his4 ura3/ura3 leu2/leu2 lys2/lys2 bar1-1/bar1-1*	H. Riezman, Switzerland
BS25	*MAT***a** *his4 ura3 leu2 lys2 bar1-1Δypt51*	Singer-Krüger *et al.* 1994
BS64	*MAT***a** *his4 ura3 leu2 lys2 bar1-1*	Singer-Krüger *et al.* 1994
BS188	*MAT*α *his4 ura3 leu2 lys2 bar1-1*	B. Singer-Krüger
BS694	*MAT***a** *his4 ura3 leu2 lys2 bar1-1 ysl2::kan^r*	Jochum *et al.* 2002
BS845	*MAT***a** *his4 ura3 leu2 lys2 bar1-1 neo1::kan^r* + pRS316-NEO1	Wicky *et al.* 2004
BS862	*MAT***a** *his4 ura3 leu2 lys2 bar1-1 neo1::kan^r* + pRS315-3-HA-*NEO1*	Wicky *et al.* 2004
BS915	*MAT***a** *his4 ura3 leu2 lys2 bar1-1 neo1::kan^r* + pRS315-neo1-37	Wicky *et al.* 2004
BS917	*MAT***a** *his4 ura3 leu2 lys2 bar1-1 neo1::kan^r* + pRS315-neo1-36	Wicky *et al.* 2004
BS957	*MAT***a** *his4 ura3 leu2 lys2 vps27*	B. Singer-Krüger
BS1121	*MAT*α *his4 ura3 leu2 lys2 bar1-1 YSL2::3-HA-HIS5 (S. pombe)*	Wicky *et al.* 2004
BS1361	*MAT*α *his4 ura3 leu2 lys2 bar1-1 dop1::kan^r* + pRS315-*dop1-3*	B. Singer-Krüger
BS1488	*MAT***a** *his4 ura3 leu2 lys2 bar1-1 3-HA ::NEO1*	B. Singer-Krüger
BS1806	*MAT***a**/α *his4/his4 ura3/ura3 leu2/leu2 lys2/lys2 bar1-1/bar1-1 dop1::kan^r/ dop1::kan^r* + pRS315-*dop1-3*	B. Singer-Krüger
CB207	*MAT*a *ura3 leu2 bar1-1 SJL2::3-HA-HIS5* (*S. pombe*) *SLA1::13-Myc-kan^r*	Böttcher, 2006
SB69	*MAT***a** *his4 ura3 leu2 lys2 bar1-1 cdc50::URA3*	this study
SB71	*MAT***a** *his4 ura3 leu2 lys2 bar1-1 cdc50::URA3 3-HA::NEO1*	this study
SB72	*MAT*α *his4 ura3 leu2 lys2 bar1-1 3-HA::NEO1*	this study
SB90	*MAT***a** *his4 ura3 leu2 lys2 bar1-1 CDC50::13myc-Kan^r 3-HA::NEO1*	this study

SB121	*MAT***a** *his4 ura3 leu2 lys2 bar1-1 CDC50::13myc-Kan^r*	this study
SB142	*MATα his4 ura3 leu2 lys2 bar1-1 dop1::kan^r 3-HA::NEO1* + pRS315-*dop1-3*	this study
SB145	BS1488 + pRS316-Myc-Tlg1p	this study
SB149	SB142 + pRS316-Myc-Tlg1p	this study
SB161	*MAT***a** *his4 ura3 leu2 lys2 bar1-1 DOP1::TAP-URA3*	this study
SB179	*MAT***a** *his4 ura3 leu2 lys2 bar1-1 neo1::kan^r* + pRS315-3-HA-*neo1^{Y1142A}*	this study
SB185	*MAT***a** *his4 ura3 leu2 lys2 bar1-1 neo1::kan^r* + pRS315-3-HA-*neo1^{PASA}*	this study
SB201	*MAT***a** *his4 ura3 leu2 lys2 bar1-1 neo1::kan^r* + pRS316-3-HA-*NEO1*	this study
SB205	*MAT***a** *his4 ura3 leu2 lys2 bar1-1 neo1::kan^r DOP1::TAP-URA3 + pRS315-HA-NEO1*	this study
SB216	BS1361+ pRS316-HA-NEO1	this study
SB220	BS188 + pRS316-HA-NEO1	this study
SB228	*MAT***a** *his4 ura3 leu2 lys2 bar1-1 pep4::URA3 3HA::NEO1*	this study
SB232	*MAT***a** *his4 ura3 leu2 lys2 bar1-1 dop1::kan^r pep4::URA3 3HA::NEO1 + pdop1-3*	this study
SB256	*MATα his4 ura3 leu2 lys2 bar1-1 pdr5::kan^r 3HA::NEO1*	this study
SB258	*MATα his4 ura3 leu2 lys2 bar1-1 pdr5::kan^r Dop1::kan^r 3HA::NEO1 + pdop1-3*	this study
SB264	*MAT***a**/α *his4/his4 ura3/ura3 leu2/leu2 lys2/lys2 bar1-1/bar1-1 neo1::kan^r /neo1::kan^r DOP1::TAP-URA3/DOP1::TAP-URA3 +pHA-NEO1*	this study
SB284	*MAT***a** *his4 ura3 leu2 lys2 bar1-1 neo1::kan^r GFP::DOP1*+ pRS316-*NEO1*	this study
SB286	*MAT***a** *his4 ura3 leu2 lys2 bar1-1 neo1::kan^r GFP::DOP1*+ pRS315-*neo1-37*	this study
SB289	*MAT***a** *his4 ura3 leu2 lys2 bar1-1 neo1::kan^r GFP::DOP1*+ pRS315-*neo1-69*	this study
SB296	*MAT***a** *his4 ura3 leu2 lys2 bar1-1 neo1::kan^r ysl2::nat^r DOP1::TAP-URA3 + pRS315-HA-NEO1*	this study
SB306	*MAT***a** *his4 ura3 leu2 lys2 bar1-1 ysl2::kan^r+ pRS315-HA-NEO1*	this study
SB323	*MATα his4 ura3 leu2 lys2 bar1-1 dop1::kan^r 3-HA::NEO1* + pRS315-*DOP1*	this study
SB330	*MATα his4 ura3 leu2 lys2 bar1-1 dop1::kan^r* + pRS315-*DOP1*	this study
SB332	*MATα his4 ura3 leu2 lys2 bar1-1 dop1::kan^r* + pRS315-GFP-*DOP1*	this study

SB335	*MATα his4 ura3 leu2 lys2 bar1-1 dop1::kan^r* + pRS315-GFP-*dop1-3*	this study
SB340	*MAT***a**/α *his4/his4 ura3/ura3 leu2/leu2 lys2/lys2 bar1-1/bar1-1 ysl2*::Kan^r/*ysl2*::Kan^r *3HA ::NEO1 /3HA ::NEO1*	this study
SB356	*MATα his4 ura3 leu2 lys2 bar1-1 dop1::kan^r* + pRS316-*DOP1*	this study
SB375	*MATα his4 ura3 leu2 lys2 bar1-1 dop1::kan^r* + pRS315-P$_{ADH1}$-GFP-DOP1	this study
SB385	SB201 + pRS315-P$_{ADH1}$-GFP-DOP1	this study
SB387	RH1201 + pRS315-P$_{ADH1}$-GFP-DOP1	this study
SB389	BS746 + pRS315-P$_{ADH1}$-GFP-DOP1	this study
SB391	BS64 + pRS315-P$_{ADH1}$-GFP-DOP1	this study
SB393	Vps27 + pRS315-P$_{ADH1}$-GFP-DOP1	this study
SB398	SB201 + pRS315-P$_{ADH1}$-GFP-Cterm	this study
SB401	SB69 + pRS315-P$_{ADH1}$-GFP-DOP1	this study
SB407	SB201 + pRS315-P$_{ADH1}$-GFP-Nterm	this study
SB415	SB201 + pRS315-P$_{ADH1}$-GFP-internal	this study
SB417	BS25 + pRS315-P$_{ADH1}$-GFP-DOP1	this study
SB426	BS1121 + pRS315-P$_{ADH1}$-GFP-DOP1	this study
SB428	BS1121 + pRS315-P$_{ADH1}$-GFP-Cterm	this study
SB430	BS1121 + pRS315-P$_{ADH1}$-GFP-Nterm	this study
SB432	BS1121 + pRS315-P$_{ADH1}$-GFP-internal	this study
SB434	*MAT***a**/α *his4/his4 ura3/ura3 leu2/leu2 lys2/lys2 bar1-1/bar1-1 ysl2*::*Kan^r*/*ysl2*::*Kan^r GFP*::*DOP1*/*GFP*::*DOP1*	this study
SB437	BS64 + pRS315-P$_{ADH1}$-GFP-Dop1ΔCterm	this study

2.1.2 *Escherichia coli* strain

DH5α	F'/endA1 hsdR17(r_{k-}.m_{k+}) supE44 thi-1 recA1 gyrA(Nal_r)	Hanahan 1983

This strain was used for all plasmid amplifications and DNA ligations.

2.1.3 Plasmids

Table 2-1: Plasmids used in ths study

Plasmid name	Characteristics	Source
pRS315-HA-NEO1	*Spe*I/*Sal*I fragment of *3-HA-NEO1*	Wicky *et al.* 2004
pRS316-HA-NEO1	*Spe*I/*Sal*I fragment of *3-HA-NEO1*	this study
pBSKNeo1 (*Hin*dIII/*Sal*I)	*Hin*dIII/*Sal*I fragment of *NEO1*	B. Singer-krüger
pRS315-3-HA-Neo1^{Y1142A}p	*Stu*I/*Sal*I fragment of *NEO1* mutated by overlapping PCR	this study
pRS315-3-HA-Neo1^{PASA}p	*Stu*I/*Sal*I fragment of *NEO1* mutated by overlapping PCR	this study
pRS316-Myc-Tlg1p	*myc-TLG1* in pRS316; *URA3* CEN	J. Holthuis, Utrecht, The Netherlands
pRS426-NEO1	*Spe*I/*Eco*RI fragment of *NEO1*, cloned by *Spe*I/*Sal*I	B. Singer-Krüger
pRS426-ARL1	*Bam*HI/*Xho*I fragment of *ARL1*	Jochum *et al.* 2002
pRS426-DOP1	*Not*I/*Sal*I fragment of *DOP1* (-347 to 5178 bp)	this study
pBS313	*Nhe*I/*Sal*I fragment of *YSL2* in YEp24	Jochum *et al.* 2002
pRS426-DRS2	*Eco*RI fragment of *DRS2*	H. Rudolph, Stuttgart, Germany
pFL-ARF1	*ARF1*, 2μm, URA 3	Cathy Jackson, Bethesda,Md
pRS426-ARL1^{G2A}	*Bam*HI/*Xho*I fragment of *ARL1G2A*	this study
pRS426-ARL1^{Q72L}	*Bam*HI/*Xho*I fragment of *ARL1Q72L*	this study
pRS426-ARL1^{T32N}	*Bam*HI/*Xho*I fragment of *ARL1T32N*	this study
pSB131	~6000 bp of the chromosome IV of containing the *DOP1* ORF and its flanking regions	this study
pRS315-*dop1-3*	*dop1-3* allele (-120 to 5201 bp)	R. Kahn, Boston, MA
pRS315-DOP1	*Not*I/*Sal*I fragment of *DOP1* (-347 to 5178 bp)	this study
pRS316-DOP1	*Not*I/*Sal*I fragment of *DOP1* (-347 to 5178 bp)	this study
pRS315-GFP-DOP1	*DOP1* fused N-terminally to GFP under the control of its own promoter	this study
pRS315-GFP-dop1-3	*dop1-3* allele fused N-terminally to GFP under the control of the *DOP1* promoter	this study
pRS315-P$_{ADH1}$-GFP-DOP1	*DOP1* fragment (4 to 5480 bp) fused N-terminally to GFP and *ADH1* promoter	this study
pRS315-P$_{ADH1}$-GFP-	*DOP1* fragment (4 to 1506 bp) fused N-	this study

Nterm	terminally to GFP and *ADH1* promoter	
pRS315-P$_{ADH1}$-GFP-internal	*DOP1* fragment (1504 to 4399 bp) fused N-terminally to GFP and *ADH1* promoter	this study
pRS315-P$_{ADH1}$-GFP-Cterm	*DOP1* fragment (4397 to 5097 bp) fused N-terminally to GFP and *ADH1* promoter	this study
pRS315-P$_{ADH1}$-GFP-Dop1ΔCterm	*DOP1* fragment (4 to 4399 bp) fused N-terminally to GFP and *ADH1* promoter	this study
pRS315-P$_{ADH1}$-GFP-dop1-3	*dop1-3* allele fused N-terminally to GFP and *ADH1* promoter	this study
pRS426-P$_{ADH1}$-GFP-2xPH(PLCδ)	Two tandem copies of the PH domain of PLCδ fused N-terminally with GFP, expressed under the control of the *ADH1* promoter	B. Singer-Krüger

2.1.4 Kits and enzymes used for molecular biology

Isolation of plasmids DNA from *E. coli* cells, extraction of DNA from agarose gels, purification of PCR products were carried out using the following kits from Qiagen: QIAprep Spin Miniprep Kit, QIAEX II Gel Extraction Kit and QIAquick PCR Purification Kit, respectively.

To directly clone DNA fragments obtained by PCR, the pGEM-Teasy kit from Promega was used.

The DNA polymerases used for amplification of DNA by polymerase chain reaction (PCR) were *Vent* DNA polymerase (NEB), *Taq* DNA polymerase (Fermentas) and Phusion High-Fidelity DNA polymerase (Finnzymes).

Restriction endonucleases used for digesting DNA were provided either by Roche, New England Biolabs (NEB) or Fermentas.

2.1.5 Chemicals

Unless otherwise indicated, the companies Genaxxon, Merck, Roth and Sigma provided the chemicals used in this study.

2.1.6 Media

All media used for cultivation of *S. cereviaiae* and *E. coli* strains were prepared into ddH_2O. Unless otherwise indicated the media was sterilised by autoclaving at 121ºC for 20 min. When solid media was prepared, 2% (w/v) Bacto® agar was added to the composition of the respective liquid media. The mixture was poured into Petri dishes and dried. The addition of antibiotics to the media was carried out when this was not warmer then 60ºC. The antibiotics were previously diluted in 10 ml H_2O and sterilised by filtration.

2.1.6.1 Yeast media

Yeast strains were cultivated depending on their characteristics and on the experimental demand in one of the following media. In complete medium (YPD) which was composed of 1% (w/v) Bacto® yeast extract, 2% (w/v) Bacto® peptone and 2% (w/v) glucose, pH 5.5; or in synthetic medium (SD) which contained 0.67% (w/v) yeast nitrogen base, 2% (w/v) glucose, pH 5.6 further supplemented with the bases adenine (0.3 mM) and uracil (0.2 mM) and with the amino acids tryptophan (0.4 mM), lysine (1 mM), histidine (0.3 mM) and leucine (1.7 mM). In the case of propagation of yeast strains carrying plasmids providing prototrophy to one or more amino acid or base, the relevant component was omitted from the SD medium, unless the gene cloned into the plasmid was essential for the cell survival.

The shuffling of URA-containing plasmids from yeast transformants was carried out onto 5-FOA plates. 5-FOA plates were composed of 0.67% (w/v) yeast nitrogen base, 2% (w/v) glucose, 2% (w/v) of Bacto® agar, 1mg/ml fluoro-orotic acid (5-FOA), supplemented with the bases adenine (0.3 mM) and uracil (0.2 mM) and with the amino acids tryptophan (0.4 mM), lysine (1 mM), histidine (0.3 mM) and leucine (1.7 mM). In the presence of a plasmid providing prototrophy for another component, this component was not added. This medium was sterilized by filtration.

To induce sporulation, diploid cells were first incubated in presporulation plates and then transferred to sporulation plates. The presporulation plates were composed of 0.8% (w/v) Bacto® yeast extract, 0.3% (w/v) Bacto® peptone, 10% (w/v) glucose and 2% (w/v) Bacto® Agar. The sporulation plates consisted of 1% (w/v) potassium acetate, 0.1% (w/v), Bacto® yeast extract, 0.05% (w/v) glucose, 2% (w/v) Bacto® Agar, 0.075 mM adenine, 0.1 mM tryptophan, 0.25 mM lysine, 0.075 mM histidine, 0.42 mM leucine and 0.05 mM uracil.

The selection of yeast cells transformed with a resistance gene marker for a given antibiotic was carried onto YPD plates containing the respective antibiotic (Geneticin Sulphate (G418) 300 μg/ml or Nouseothricin 100 μg/ml).

2.1.6.2 *E. coli* media

E. coli cells were cultivated in LB (Luria-Bertani) media composed of 0.5% (w/v) yeast extract, 1% (w/v) Bacto® trypton and 0.5% (w/v) NaCl, pH 7.5. For *E. coli* cells carrying a plasmid with the Amp^r gene, a final concentration of 100 μg/ml of ampicillin was added.

2.2 Methods

2.2.1 *S. cerevisiae* and *E. coli* growth

2.2.1.1 Yeast cell cultures

Cells were streaked out from 30% glycerol stock cultures kept at -80ºC onto solid media and let grown for two to three days either at 30ºC or 25ºC.

For liquid cultures, one colony or two of cells were taken from a Petri dish containing the appropriated solid media for the growth of the cells (see section 2.1.6.1) and inoculated into 5 ml of the respective liquid media and let grown for 2 days at 30ºC or 3 days at 25ºC, shaking at 250 rpm. Then, a certain amount of these dense cultures was taken and inoculated into a higher volume of fresh media and the cells were allow to grow for about 16 hours at either 30ºC or 25ºC shaking at 160 rpm.

For assays involving temperature sensitive mutants the cells were grown at 25ºC until an early logarithmic phase (approximately 0.2 OD_{600nm}) and then shifted to 37ºC for 2 to 3 hours. In the case of preparing cells for immunofluorescence or fluorescence microscopy the cells were grown at 25ºC until early logarithmic phase (approximately 0.2 OD_{600nm}). Unless otherwise indicated for performing immunoprecipitation experiments the cells were grown in 600 ml of either YDP or SD medium (see section 2.1.6.1) at 30 ºC until late logarithmic phase (approximately 0.8 OD_{600nm}).

2.2.1.2 Yeast growth test

Yeast cells were tested for growth either by streaking them onto plates or by making serial dilutions. For the serial dilution technique, a certain amount of cells, similar for the strains to be compared, was resuspended into 200 μl of sterile ddH_2O

and then serially diluted to 1/10, 1/100 and 1/1000. The dilutions were then plated onto plates harbouring the desired characteristics for the test by using a metal stapler.

For testing growth at different temperatures, strains were serial diluted or streaked onto YPD plates and incubated at different temperatures for 2, 3 or 4 days. For testing hypersensitivity to neomycin, the same procedure was adopted, but serial dilution of cells were plated onto YPD plates containing 2 mg/ml of neomycin sulphate and incubated at 25ºC for 2 to 4 days.

2.2.1.3 *E. coli* cell cultures

After transformation of *E. coli* cells, the transformation reaction was plated into LB-Amp plates and the cells were allow to grow overnight at 37ºC. For isolation of plasmid DNA, isolated colonies from LB-Amp plates were inoculated into 5 ml of LB-Amp liquid media and the cells grew overnight at 37ºC shaking at 180 rpm.

2.2.2 Molecular biology methods

2.2.2.1 Generation of DNA constructions

DNA manipulations were performed using standard techniques (Maniatis *et al.* 1989). PCR-amplified DNA fragments subcloned into vectors were sequenced (using the service of Eurofins MWG Operon, Germany) to confirm the presence of the introduced mutations and to exclude the presence of PCR errors. The conditions used in all the reactions such as ligation of DNA fragments, digestion of DNA with restriction endonucleases and PCR were the ones suggested by their respective supplier.

For all the steps that involved amplification of plasmid DNA, *E. coli* DH5α highly competent cells were prepared as described by Inoue *et al.* 1990 and transformed using the heat shock method.

2.2.2.1.1 Mutagenesis of the PPSY motif present in the C-terminal tail of Neo1p

To mutagenise the conserved PPSY motif in the C-terminal tail of Neo1p, two DNA fragments were amplified separately by PCR, and then fused with a second round of PCR. The resulting DNA fragment was introduced into pRS315-HA-NEO1, by substitution of the original *Stu*I/ *Sal*I fragment of *NEO1* generating either pRS315-HA-

NEO1^{Y1142A} or pRS315-HA-NEO1$^{P1140A-Y1142A}$. The primary DNA fragments were amplified from pBSKNeo1 (*Hin*dIII/ *Sal*I) using specific oligonucleotides. In the case of pRS315-HA-NEO1^{Y1142A}, the oligonucleotides StuINeo1fw and Neo1y/arev were used to generate one of the fragments and the oligonucleotides NEO1^{Y1142A} and *3'SalINeo1* to generate the other. To create pRS315-HA-NEO1$^{P1140A-Y1142A}$ one of the fragments was amplified using the oligonucleotides StuINeo1fw and Neo1revp/ay/a and the other using the oligonucleotides Neo1fwp/ay/a and 3'SalINeo1. Finally, the fusion of the two PCR products of each of the constructions was achieved after amplification with the primers StuINeo1fw and 3'SalINeo1. The primers used to generate these two plasmids are listed below.

Primer	**Sequence**	**Source**
NEO1^{Y1142A}	GCTACATCCTCCAAGCGCTGCAAAAGTGCAAGA	this study
Neo1y/arev	GCGCTTGGAGGATGTAGCCTT	this study
Neo1revp/ay/a	AGCGCTAGCAGGATGTAGCCTTCTATA	this study
Neo1fwp/ay/a	CTACATCCTGCTAGCGCTGCAAAAGTGCAA	this study
StuINeo1fw		B. Singer-Krüger
3'SalINeo1		B. Singer-Krüger

2.2.2.1.2 Cloning the *DOP1* gene

To isolate the *DOP1* gene, a suppressor screen was performed and a plasmid containing the complete ORF of *DOP1* and its flanking regions was acquired. The strain BS1361 (*dop1-3* mutant) was transformed with an Ycp50-based genomic library of *S. cerevisiae* and the transformants were selected on SD-URA plates at 25ºC. Later, the obtained transformants were replica plated onto YPD plates and placed at 37ºC. The colonies able to grow at 37ºC were selected, their plasmids were extracted and analysed for the presence of *DOP1*. The isolated plasmid clone #4 (pSB131) was used to subclone *DOP1*. First, two PCRs were performed using pSB131 as a template. The 5' region of *DOP1* and the promoter (-347 to 577 bp) were amplified using the oligonucleotides Dop1prfwSacINot and Dop1Nrev and the 3' region and the terminator (3358 to 5178 bp) using the oligonucleotides Dop1SpeIBamHI and Dop13'SalIrev. The fragment containing the 3' region was cloned into pRS426 using the restriction endonucleases *Sal*I and *Bam*HI. Subsequently, the 5' region fragment was inserted into

the resulting plasmid by cutting with the endonucleases *Not*I and *Bam*HI. Finally, the internal region of *DOP1* (354 to 3549 bp) was subcloned, after being released from pSB131 with the endonucleases *Spe*I and *Bam*HI, into the plasmid obtained in the previous step. The *DOP1* gene was introduced into the vectors pRS315 and pRS316 using *Not*I/ *Sal*I. The primers used to generate the PCR fragments are listed below.

Primer	Sequence	Source
Dop1prfwSacINotI	ACTAGAGCTCGCGGCCGCTTCTGACTGTGCAAAAG	this study
Dop1Nrev	CATCATCCAAGTTCTCCTGC	this study
Dop1SpeIBamHI	ATCAGGATCCGAAGAAACTGTTGGAAACC	this study
Dop13'SalIrev	ATCAGTCGACCACGTTATAATTGATAACC	this study

2.2.2.1.3 Generation of pRS315-P$_{ADH1}$-GFP-DOP1 and pRS315-P$_{ADH1}$-GFP-dop1-3

DOP1 was fused at its 5' coding region with the *GFP* ORF and expressed under the control of the constitutive *ADH1* promoter. A PCR fragment encoding the 5' coding region bearing a *Not*I restriction site at its 5' extremity was amplified from pSB131 with the oligonucleotides Dop1ATGNotIfw and Dop1Nrev (4 to 577 bp). The resulting fragment was digested with the restriction enzymes *Not*I and *Bam*HI and cloned into the plasmid pRS315-*DOP1* by substitution of the previous *Not*I/ *Bam*HI fragment of *DOP1*. Next, to exchange the original terminator of *DOP1* for a longer one, a new terminator was amplified from pSB131 using the oligonucleotides Dop1SpeIBamHIfw and Dop1terrev (3358 to 5480 bp). This PCR product was cloned into the plasmid obtained on the step before by cutting with the restriction enzymes *Nsi*I and *Sal*I. Finally, a fragment that contains the *ADH1* promoter and the *GFP* gene was amplified from the plasmid pYM-N9 (Euroscarf collection) using the oligonucleotides Adhprfw and gfprev. After digestion with *Sac*I and *Not*I this fragment was cloned into the preceding plasmid to create pRS315-P$_{ADH1}$-GFP-DOP1. The oligonucleotides used are listed below.

Primer	Sequence	Source
Dop1ATGNotIfw	CTATGCGGCCGCGTCCTTACCACTAAAGCCCCT	this study
Dop1Nrev	CATCATCCAAGTTCTCCTGC	this study
Dop1SpeIBamHI	ATCAGGATCCGAAGAAACTGTTGGAAACC	this study
Dop1terrev	ACTAGTCGACAGCAGAATGTGTGCCAGATG	this study
ADHprfw	CAAATCGCTCCCCATTTCAC	this study
GFPrev	GCAGGTTAACCTGGCTTATC	this study

The plasmid pRS315-P_{ADH1}-GFPdop1-3 was generated by replacing the *DOP1* *Sma*I/ *Sal*I fragment in pRS315-P_{ADH1}-GFPDOP1 (359- 5480bp) for the *Sma*I/ *Sal*I fragment of the *dop1-3* allele (359- 5197 bp) from pRS315-dop1-3.

2.2.2.1.4 Generation of GFP fused domains of Dop1p

The plasmid pSB131 was used as template for all the DNA amplifications by PCR which involved the *DOP1* gene.

To fuse the C-terminus of Dop1p to GFP, a DNA fragment encoding this region (1466 - 1698 aa) (4397 - 5097 bp) and terminator of Dop1p (5098 - 5480 bp) was amplified using Dop1CtermfwNotI and Dop1terrev as oligonucleotides. Subsequently, the plasmid pRS315-P_{ADH1}-GFP-DOP1 was digested with the endonucleases *Not*I and *Sal*I to discard *DOP1* and the PCR product was introduced into the open plasmid yielding pRS315-P_{ADH1}-GFP-Cterm.

To fuse the N-terminal domain and the internal fragment of Dop1p in frame with GFP, the plasmid pRS315-P_{ADH1}-GFP-DOP1 was digested with the restriction enzymes *Not*I and *Sal*I to discard the *DOP1* gene. Then, the terminator of *DOP1*, amplified with the oligonucleotides TermfwNotINheI and Dop1termrev was cloned directly after the *GFP* ORF by cutting with the same restriction enzymes. The resulting plasmid, pRS315-P_{ADH1}-GFP-NotI-NheI-termDOP1, contains between the *GFP* gene and the terminator of *DOP1* the restrictions sites *Not*I and *Nhe*I which allow further insertions. Hence, the Dopey domain of Dop1p (2 - 502 aa) (4 - 1506 bp), amplified with the oligonucleotides Dop1-ATGNotIfw and Dop1dopeyrevNheI, was subsequently inserted into the plasmid at the restriction sites *Not*I and *Nhe*I yielding to pRS315-P_{ADH1}-GFP-Dopey. The internal part of Dop1p (502 - 1466 aa) (1504 - 4399 bp) was cloned in the

same way into pRS315-P_{ADH1}-GFP-NotI-NheI-termDOP1 to generate pRS315-P_{ADH1}-GFP-internal after being amplified with the oligonucleotides Dop1intfrafwNotI and Dop1intfrarevNheI.

To generate pRS315-P_{ADH1}-GFP-Dop1ΔCterm, two primary DNA fragments were amplified by PCR and then fused by a second PCR. A DNA fragment encoding the region in which a stop codon was placed after the proline 1466 was amplified using the oligonucleotides DOP1-NsiIfw and Dop1intfrarevNheI. The fragment containing the terminator was amplified with the oligonucleotides newDop1terfw and Dop1terrev. These two DNA fragments were fused by PCR, using DOP1-NsiIfw and Dop1termrev as oligonucleotides. The final PCR product was introduced into pRS315-P_{ADH1}-GFP-DOP1 at the sites *Nsi*I and *Sal*I, yelding pRS315-P_{ADH1}-GFPDop1ΔCterm.

The oligonucleotides used are listed below.

Primer	**Sequence**	**Source**
TermfwNotINheI	CTATGCGGCCGCATACAGCTAGCGCATAGCTATGAA TTTTTCT	this study
Dop1terrev	ACTAGTCGACAGCAGAATGTGTGCCAGATG	this study
Dop1ATGNotIfw	CTATGCGGCCGCGTCCTTACCACTAAAGCCCCT	this study
Dop1dopeyrevNheI	ATCAGCTAGCTCAAGGAAGGTGGCGTACGATA	this study
Dop1intfrafwNotI	CTATGCGGCCGCGCCTTTGATATTATTAACTTTACTG	this study
Dop1intfrarevNheI	ATCAGCTAGCTCACGGAGTCACACTTGAACGCT	this study
Dop1CtermfwNotI	CTATGCGGCCGCGCCGACTTTAATCACGTTTAAC	this study
DOP1-NsiIfw	CTTGTTGCCCTTATTTCTGG	this study
newDop1terfw	ACTCCGTGAGCTAGCTGATCATAGCTATGAATTTTTC TTT	this study

2.2.2.2 Generation of strains by homologous recombination

The C-terminal Myc-epitope tag in Cdc50p was introduced as described by Longtine *et al.* 1998. A DNA fragment CDC50-C-Myc was amplified from pFA6a-13Myc-KanMX6 using the oligonucleotides Cdc50-13mycfw and Cdc50-13mycrev. Each of the oligonucleotides has on its 5'end region approximately 45 to 50 bp identical to the chromosomal DNA sequence where homologous recombination will take place. On the 3'end region they contain approximately 20 nucleotides which anneal to the plasmid, at the site of amplification of the cassette. Subsequently, the CDC50-C-Myc

fragment was transformed into BS1488 and RH1201, and positive clones selected for resistance to G418 (geneticin sulphate). Later, the correct integration of the cassette into the chromosome was verified by Western blotting.

The C-terminal TAP-epitope in Dop1p was inserted similarly. A *DOP1*-TAP PCR fragment was amplified from the plasmid pBS1539 (Rigaut *et al.* 1999) with the primers fwdop1TAP and revdop1TAP, and introduced by homologous recombination into the yeast strain RH1201. The positive clones were selected on SD-URA plates and the correct integration of the cassette was assessed by Western blotting.

The N-terminal GFP-epitope tag in *DOP1* was introduced as described by Gauss *et al.* 2005. First, a cassette consisting of a Kan^r marker flanked by two loxP sites with the *GFP* ORF at the 3' end was amplified from the plasmid pOM40 (Euroscarf collection) using the oligonucleotides Dop1-NHAfw and Dop1-NHArev. After transformation into the RH1201 strain, and selection for resistance to G418, the correct insertion of the cassette was confirmed by PCR. Individual clones were subjected to transformation with pSH47, a plasmid containing the Cre recombinase gene under the control of the *GAL1* promoter. The resulting transformants were incubated for 2 hours at 30ºC into galactose-containing medium (YP + 2% galactose + 1% rafinose) for expression of the Cre recombinase gene and consequential excision of the marker from the chromosomal locus due to efficient recombination between the loxP sites. Subsequently, 200 cells were plated onto YPD plates and colonies were subjected to replica plating on YPD plates containing G418 (300 μg/ml). Clones that lost the resistance to G418 were selected and analysed by Western blotting for the expression of GFP-Dop1p and by PCR for the correct excision of the marker. Then the diploid cells were subjected to sporulation and tetrad dissection and the functionality of the tagged protein was assessed in the obtained haploids by growth test at different temperatures.

To delete *CDC50*, a CDC50-URA3 fragment was amplified from pRS426 using the oligonucleotides fwCDC50 and revCDC50. This fragment possesses the *URA3* gene surrounded by 50 bp homologous to the chromosomal DNA sequence where the cassette will be inserted. After transformation into BS862 and homologous recombination, the positive clones were selected on plates for the uracil prototrophy. These clones were then tested by PCR for the correct insertion of the cassette.

YSL2 was deleted using a similar methodology. An YSL2-nat^r fragment was generated by amplification of the Nat^r marker from plasmid pFA6a-natNT2 (Euroscarf collection) using the oligonucleotides dYSL2rev and dYSL2fw. Subsequently, the

YSL2-nat^r specific fragment was transformed into the diploid SB264. After selection of the clones resistant to nouseothricin, the diploid cells were subjected to sporulation and tetrad dissection. The correct insertion of the cassette was verified by the correct segregation of the Nat^r marker and by growth phenotype.

To delete *PDR5*, a fragment was generated by amplification of the kan^r marker from pUG6 plasmid (Euroscarf collection) using the primers deletionpdr5fw and deletionpdr5rev. The PDR5-kan^r specific fragment was subsequently transformed into BS64 and the positive clones selected for resistance to G418. The correct insertion of the cassette was confirmed by PCR. The oligonucleotides used to generate the above integration cassettes are listed below.

Primer	**Sequence**	**Source**
fwCDC50	CAAAGAATAATTGAGTAATCGAACTTGAAGTTCTAT AGAACAGCTTGTATGATTCGGTAATCTCCGAA	this study
revCDC50	TTACTTATAAACACAAATACCTACAGGCACTAAAGT TTGTTTTTTGGCCTAGGGTAATAACTGATATAAT	this study
Cdc50-13mycfw	ACGAGGATTATGAGGATGTACACGCAGAGAATACA ACATTGAGGGAAATTTTACGGATCCCCGGGTTAATT AAC	this study
Cdc50-13mycrev	GCAAACCCTGGGAGTTCTTTGTCGCACTATTTTCCAA GCGTAAAAAGGCATACCATCGATGAATTCGAGCTC	this study
fwdop1TAP	GGGTCAGTTGATTTATATGGTTGTGGTGAAGATCTC AAAAAAGATATTCTGTCATCCATGGAAAAGAGAAG	this study
revdop1TAP	GCAAAACCTTTCACGTTATAATTGATAACCTGTGTCT TTACTCAAAGCGTATAACTACGACTCACTATAGGG	this study
Dop1-NHAfw	AACGGTGAAATAAAAAGCCGACAGAGCAGCTTTTTC TGAGAGGATCGACAAAAAATGTGCAGGTCGACAAC CCTTAAT	this study
Dop1-NHArev	GGAGTCTAGTTGTTTATTATTTGAGTCAATTGTAAGG GGCTTTAGTGGTAAGGAGCGGCCGCATAGGCCACT	this study
deletionpdr5fw	AGACCCTTTTAAGTTTTCGTATCCGCTCGTTCGAAAG ACTTTAGACAAAACAGCTGAAGCTTCGTACGC	Olivier Santt
Deletionpdr5rev	AAAAAGTCCATCTTGGTAAGTTTCTTTTCTTAACCAA ATTCAAAATTCTAGCATAGGCCACTAGTGGATCTG	Olivier Santt
dYSL2fw	CTACTCATCTCGCGATGGAGATTCAATTAAAAGTTT TACAGGTGGTACCCATTGTTGAATTGTCCCCACGC	this study
dYSL2rev	GCTATTCTATTTCTCAGGTTAGAACATGACATATAG CTGATTGCCTCAAAAGTTGTCACTTTAAAATTTGTAT ACAC	this study

2.2.2.3 Mating, sporulation and dissection of *S. cerevisiae* cells

To generate diploid strains, cells of a particular haploid strain of opposite mating type (*MAT***a** or α) were mixed on YPD plates. After an overnight incubation, the mixture was streaked to a selective plate (YPD medium with antibiotic or selective SD medium) or to an YPD plate to obtain single colonies. The bigger colonies were selected and analysed in the light microscope for the diploid cell shape. Such cells were streaked onto presporulation plates (section 2.1.6.1), incubated overnight at 25ºC and transferred to sporulation plates. Cells were kept on sporulation plates at 25ºC for at least 5 days for up to 10 days, until enough spores could be observed. Cells were prepared for tetrad dissection in 100 µl of dissection buffer (1.2 M sorbitol, 50 mM Tris/HCl pH 7.5) containing 3 µl of 5 mg/ml of oxalyticase. Tetrads were separated under the light microscope using a needle for tetrad dissection (Singer Instruments) coupled to a micromanipulator.

2.2.2.4 Transformation of *S. cerevisiae* cells

Transformation of yeast cells was performed according to the lithium acetate method described by Ito *et al.* 1983. Yeast cells were grown overnight until a density of 1 to 2 x 10^7 cells/ml. Fifty ml of culture were collected by centrifugation (4000 rpm) and washed twice with 10 ml of TE buffer (10 mM Tris, 1 mM EDTA, pH 7.5). Thereafter, they were resuspended in 5 ml of 0.1 M of LiOAc and incubated for 1 hour at room temperature. They were then harvested by centrifugation and resuspended in 5 ml of fresh 0.1 M of LiOAc. For the transformation, 300 µl of yeast suspension was incubated with 750 µl of 50% PEG (w/v), 4 µl of 10 mg/ml of Herring Sperm DNA (carrier DNA), and the desired DNA fragment (in case of integration) or plasmid DNA for one hour incubation at room temperature. Next, 100 µl of DMSO were added and the suspension was incubated at 42ºC for 5 min. In the case of transforming a plasmid or an integrative fragment conferring prototrophy for a certain amino acid or base, the suspension was immediately plated onto selective SD plates. For transformations involving DNA cassettes encoding a gene that provides resistance to a certain antibiotic, the complete cell suspension was transferred to a glass tube containing 5 ml of YPD medium and incubated for 3 hours at 30ºC to allow the expression of the

resistance marker. After, the culture was centrifuged to concentrate the cells and plated onto YPD plates containing the corresponding antibiotic for selection.

2.2.3 Protein biochemistry methods

2.2.3.1 Preparation of yeast cell extracts

To prepare yeast cell extracts, 1.7 OD_{600} units of cell were collected by centrifugation at 4000 rpm for 5 min and washed with 1 ml of ice-cold TEPI-buffer (50 mM Tris/HCl pH 7.5; 5 mM EDTA/NaOH pH 8.0). The cell pellet was resuspended in 200 µl TEPI with protease inhibitors (1 x CLAP: pepstatin, antipain, leupeptin, chymostatin each at 5 µg/ml final concentration). Approximately 200 mg of glass beads were added and cells were mechanically lysed by 5 rounds of vortexing during 1 min and cooling on ice for another minute. For analysis of membrane proteins, 200 µl of 2 x Laemmli sample buffer (0.02% [v/v] bromophenolblue; 5 mM EDTA/NaOH pH 8.0; 10% [w/v] glycerol; 4% [w/v] SDS; 100 mM Tris/HCl pH 6.8) containing 8 M urea and 5% β-mercaptoethanol were added to the lysate, the mixture was heated for 10 min at 50ºC and centrifuged for 5 min at 16,000 x g. When soluble proteins were analysed, 200 µl of 2 x Laemmli sample buffer containing 5% β-mercaptoethanol but without urea were added to the lysate, the mixture was then boiled at 95ºC for 5 min and centrifuged for 5 min at 16,000 x g. The cell extracts were transferred to a new Eppendorf tube and keep at -20ºC.

2.2.3.2 Western blotting

2.2.3.2.1 SDS-PAGE

SDS-PAGE (sodium dodecyl sulphate – polyacrylamide gel electrophoresis) is a method used to separate proteins according to their molecular weight (Laemmli 1970).
In this methodology a polyacrylamide gel, of which the degree of reticulation may vary, is combined with the properties of sodium dodecyl sulphate (SDS) to separate proteins. Sodium dodecyl sulphate (SDS) is an anionic detergent which incites the unfolding of proteins, through attachment to their hydrophobic regions. This attachment of the SDS molecules to the polypeptide chain masks the intrinsic charge of the proteins, driving

their migration to the positive electrode uniquely dependent on the size of the polypeptide chain.

The polyacrylamide gels in this work were 1.5 mm thick and consisted of a 4% stacking gel with the loading compartments on the top and a 6%, 7.5% or 10% resolving gel. Resolving and stacking gel were prepared freshly and filled between the glass plates of the pouring system (Biorad, Mini Protean III), the composition of the gels are listed in the table 2-2.

To performe electrophoresis, the polymerised gel between the glass plates was transferred into the Biorad Mini protean III electrophoresis chamber and overlaid with approximately 300 ml SDS running buffer (25 mM Tris; 190 mM glycin; 0.1% [w/v] SDS). The protein samples prepared with Laemmli sample buffer were deposited into the pockets and separated at 23 mA per gel through the stacking gel and 37 mA per gel through the resolving gel.

Table 2-2: Composition of the SDS-polyacrilamide gels

Gel% / Components	6%	7.5%	10%	Stacking gel
ddH_2O	4.4 ml	4 ml	3.3 ml	2.6 ml
1.5 M Tris pH 8.8 + 0.4% (w/v) SDS	2 ml	2 ml	2 ml	-
1.5 M Tris pH 6.8 + 0.4% (w/v) SDS	-	-	-	1 ml
Acrylamide/bisacrylamide solution (37.5 :1)	1.6 ml	2 ml	2.7 ml	0.4 ml
10% (w/v) APS	32 µl	32 µl	32 µl	14 µl
TEMED	3.2 µl	3.2 µl	3.2 µl	5 µl

2.2.3.2.2 Protein transfer to nitrocellulose membranes

Separated proteins were transferred to nitrocellulose membrane by electrophoretic transfer using the Mini-Trans-Blot cell system (Bio-Rad Laboratories). A “sandwich” consisting of two layers of Whatman paper (3 MM), one sponge, two layers of Whatman paper, the SDS-gel, the nitrocellulose membrane and again two layers of

Whatman paper, a sponge, two layers of Whatman paper was placed into the blotting apparatus Min Trans-Blot Cell filled with transfer buffer (150 mM glycine, 20 mM Tris, 20% [v/v] methanol). Proteins were then transferred to the nitrocellulose membrane by applying a current of 200 mA during 3 (6% SDS-gel), 4 (7.5% SDS-gel) or 2 hours (10% SDS-gel). After the transfer, the nitrocellulose membrane was stained for 5 min in Ponceau S solution (5% [v/v] acetic acid; 0.2% [w/v] Ponceau S) and washed with ddH_2O to detect the transferred proteins, dried, and stored at room temperature.

2.2.3.2.3 Immunodetection

The general procedure consisted in blocking the proteins bound to the nitrocellulose membrane in milk buffer [2.5% (w/v) low fat milk powder, 1 x phosphate saline buffer (PBS) (2.7 mM KCl; 137 mM NaCl; 5.6 mM Na_2HPO_4; 1.1 mM NaH_2PO_4; 1.5 mM KH_2PO_4), 0.2% (v/v) Tween 20] for one hour at room temperature, in order to prevent any unspecific binding of the antibody. Then the membrane was incubated with the first antibody diluted in milk buffer for one hour. To remove the unbound antibody the membrane was washed 4 times every 5 min with 10 ml of milk buffer and incubated with the appropriated secondary antibody for another hour. The membrane was washed twice for 5 min with 10 ml of milk buffer and twice for another 5 min with 10 ml of 0.1 M Tris base. The alkaline phosphatase-catalysed colour reaction was carried out in freshly prepared detection reaction buffer (50 mM $MgCl_2$; 100 mM NaCl; 100 mM Tris/HCl pH 9.5; 0.015% [w/v] of BCIP [5-bromo-4-chloro-3-indolyl-phosphate] and 0.03% [w/v] of NBT [nitroblue tetrazolium] [Bio-Rad Laboratories]) until the staining was clearly visible. To stop the colour reaction the membrane was washed with ddH_2O and dried.

Immunodetection for quantitative Western blotting was performed similarly with some minor modifications. After being incubated with the first antibody, the membrane was washed 4 times for 5 min in 1 x phosphate saline buffer (PBS) (2.7 mM KCl; 137 mM NaCl; 5.6 mM Na_2HPO_4; 1.1 mM NaH_2PO_4; 1.5 mM KH_2PO_4) containing 0.2% (v/v) Tween 20 and incubated with the appropriated IRDye infrared secondary antibody in PBS buffer containing Tween (see table 2-5) for one hour. The nitrocellulose membrane was once more washed 4 times for 5 min with the same buffer. To visualise the signal, the nitrocellulose membrane was scanned for the precise wave length (800

nm) on the Odyssey Infrared Imaging System and the signal was quantified using the Odyssey software (LI-COR Biosciences).

To immunodetect ubiquitin, prior to the blocking step, the nitrocellulose membrane was autoclaved at 121ºC for 30 min on a liquid cycle to improve the immunoreactivity of the anti-ubiquitin antibody (Swerdlow *et al.* 1986). For that purpose, the membrane was packed between 12 layers of Whatman paper and submerged into ddH_2O inside of a plastic box, weight down with a 100 ml flask filled with ddH_2O and then autoclaved as described above. Subsequently, the membrane was removed and immediately placed into milk buffer and blocked as previously described. Afterwards the membrane was placed for two hours in milk buffer with anti-ubiquitin antibody (see table 2-3) and treated as above described.

The antibodies used in this study and respective dilution are listed in the tables below.

Table 2-3: Primary antibodies used for immunodetection

Antibody	**Dilution**	**Source**
Mouse monoclonal anti-HA 16B12	1:1500	Covance
Mouse monoclonal anti-c-Myc 9E10	1:500	Calbiochem
Rabbit polyclonal anti-GFP (serum)	1:500	Invitrogen
Rabbit polyclonal anti-TAP	1:500	Open Biosystems
Mouse monoclonal anti-Pma1 40B7 (serum)	1:1000	Abcam
Rabbit polyclonal anti-Ysl2	1:250	Jochum *et al.* 2002
Mouse anti-Ubiquitin P4G7	1:100	Covance
Mouse monoclonal anti-CPY	1:1000	Molecular Probes
Mouse monoclonal anti-PGK	1:1000	Molecular Probes
Rabbit polyclonal anti-Drs2	1:1000	T. Graham, USA
Mouse monoclonal anti-Pep12p	1:500	Molecular Probes
Mouse monoclonal anti-Chc1p ascites fluid	1:500	S. Lemmon, USA

Table 2-4: Secondary antibodies used for immunodetection

Antibody	**Dilution**	**Source**
Goat anti-mouse IgG, alkaline phosphatase-conjugated	1:1000	Kirkegaard & Perry Laboratories
Goat anti-rabbit IgG, alkaline phosphatise-conjugated	1:1000	Kirkegaard & Perry Laboratorie

Table 2-5: Secondary antibodies used for quantitative Western-blotting

Antibody	Dilution	Source
Goat anti-mouse IRDye® 800	1:1000	Rockland
Goat anti-rabbit IRDye® 800	1:1000	Rockland

2.2.3.3 Immunoprecipitation experiments

2.2.3.3.1 Preparation of cell aliquots

Unless otherwise indicated prior to the immunoprecipitation experiment the cells were prepared as follow. Cells were collected by centrifugation at 4000 rpm, washed twice with 100 ml ice cold ddH_2O and once with 40 ml ice cold IP bufferA (115 mM KCl; 5 mM NaCl; 2 mM $MgCl_2$; 1 mM EDTA, pH 8.0; 20 mM HEPES/KOH, pH 7.8). Cells were resuspended in IP buffer to a concentration of 50 OD_{600} units of cells in 300 µl end volume. The cell suspension was distributed in aliquots of 300 µl, frozen in liquid nitrogen and stored at –80ºC.

2.2.3.3.2 General procedure for immunoprecipitation

Clear lysates after extraction of proteins with detergent were incubated for 1 hour at 4ºC in an overhead rotator with the antibody. Thereafter, 60 µl of pre washed ProteinA Sepharose (GE Health Care) 1/3 slurry in IP bufferA (115 mM KCl; 5 mM NaCl; 2 mM $MgCl_2$; 1mM EDTA, pH 8.0; 20 mM HEPES/KOH, pH 7.8) was added to each sample and these were incubated for an additional hour on an overhead rotator at 4ºC. In order to remove the unbounded proteins, the ProteinA Sepharose beads were washed 4 times with IP bufferA containing 1 mM DTT and the corresponding concentration of detergent. The elution of the proteins was performed by adding 60 µl of 1 x Laemmli sample buffer (including 8 M urea in the case of integral membrane proteins) containing 2.5% β-mercaptoethanol and heating at 95ºC for 5 min (or 50ºC for 10 min in the case of integral membrane proteins). The samples were centrifuged at 16,000 x g for 5 min and the supernatants transferred to new Eppendorf tubes. Thirty µl of each sample were analysed by Western-blotting.

The antibodies used in the immunorecipitation experiments are listed in the table below.

Table 2-6: Antibodies used for immunoprecipitations

Antibody	Source
Rat monoclonal anti-HA (3F10)	Roche Applied Science
Rabbit polyclonal anti-GFP (serum)	Invitrogen
Rabbit polyclonal anti-c-Myc, A-14 (Sc-789)	Santa Cruz Biotechnologies, Inc

2.2.3.3.3 Immunoprecipitation of Cdc50p-13-Myc and 3-HA-Neo1p

Two different methods were used to immunoprecipitate 3-HA-Neo1p and Cdc50p-13-Myc to test whether or not these proteins interact.

2.2.3.3.3.1 Immunoprecipitation from total membranes

Cells were grown as described in the section 2.2.1.1. Two hundred OD_{600} units of cells were collected by centrifugation at 4000 rpm for 5 min and washed 3 times with lysis buffer (10 mM Tris/HCl pH 7.5; 0.3 M Sorbitol; 0.1 M NaCl; 5 mM $MgCl_2$). Thereafter, the cells were resuspended in 1 ml of lysis buffer and 20 µl of PIC 50X (5 µ/ml leupeptin; 25 mM 1.10 phenathroline; 25 µg/ml Pepstatin A; 5 mM Pefabloc), 20 µl of Complete 50X (protease inhibitor cocktail, Roche) and 1 µl of 1 M PMSF (phenylmethylsulfonylfluoride) were added. Each sample was divided into two and each of the 500 µl were transferred to 2 ml Eppendorf tube. Approximately 500 mg of glass beads were added and the cells were lysed mechanically by 6 rounds of 30 sec vortexing on a multi-vortex (Disruptor Genie, Bohemia, USA) with one minute incubation on ice in between. The lysates were combined, centrifuged for 5 min at 400 x g to remove unbroken cells and the resulting supernatants were transferred to ultracentrifuge tubes and centrifuged at 100,000 x g for one hour at 4ºC (TLA 120.2 rotor, Beckman Instruments). After the centrifugation, the supernatants were discarded and the pellets were resuspended in 400 µl of IP bufferB (10 mM Tris/HCl pH 7.5; 150 mM NaCl; 2 mM EDTA). Four hundred µl of IP bufferB containing 2% CHAPS were added and the pellets were homogenised using a Dounce homogeniser (1ml). The homogenised suspensions of total membranes were incubated on an overhead rotator for 1 hour at 4ºC to allow further solubilisation of membrane proteins. The insoluble material was removed by centrifugation at 100,000 x g for one hour at 4ºC, and the clear extracts

were incubated with either 5 µl of anti-c-myc antibody or 3 µl anti-HA antibody (table 2-6) and subjected to the procedure described in the section 2.2.3.3.2 with some minor differences. The IP bufferB was used during all the procedure and not the IP bufferA, the washing steps were preformed in absence of DTT and detergent. The proteins were eluted with 80 µl of 1 x Laemmli sample buffer containing 8 M urea and 2.5 % β-mercaptoethanol and heating at 50 ºC for 10 min.

2.2.3.3.3.2 Immunoprecipitation from total cell extracts

To immunoprecipate HA-Neo1p or Cdc50p-Myc, 3 frozen aliquots (per immunoprecipitation sample) were defrosted by incubation at 25ºC and lysed mechanically with glass beads (~480 mg) in the presence of 1 x CLAP (see section 2.2.3.1) by 10 rounds of vortexing for 45 sec and cooling on ice for 1 min in between. Cell lysates were transferred to new Eppendorf tubes and the glass beads washed with 800 µl of IP buffer to collect the remaining lysate. DTT was added to the final concentration of 1 mM and the cell lysates were incubated for 30 min on ice in the presence of 0.01% (w/v) NP40 (final concentration). The cell extracts were centrifuged for 20 min at 13,000 rpm. Resulting supernatants were transferred to ultracentrifuge tubes and centrifuged for 1 hour at 100,000 x g (TLA 120.2 rotor, Beckman Instruments). The 3 clear extracts were combined and incubated with either 5 µl of anti-Myc antibody or 3 µl anti-HA antibody (table 2-6) and subjected to the procedure described in the section 2.2.3.3.2.

2.2.3.3.4 Determination of the extent of protein solubilisation

Thirty µl of supernatant from each sample were kept after the centrifugation at 100,000 x g, and the pellets resuspended in 250 µl of IP buffer without detergent. Samples of both fractions were prepared in sample buffer. Several different volumes from each sample were analysed by Western blotting. The bands from the pellet and supernatant were compared. Those with the same intensity were used to calculate the percentage of protein in each fraction.

2.2.3.3.5 Co-immunoprecipitation experiments using GFP tagged Dop1p, Nterm, internal and Cterm domains of Dop1p

Isolation of the GFP tagged Dop1p and/or domains of Dop1p for testing HA-Neo1p co-immunoprecipitation, was carried out in the same way as described in the section 2.2.3.3.3.2, with some minor differences. Two aliquots of 50 OD_{600} of cells were used per immunoprecipitation sample, after the centrifugation at 100,000 x g the supernatants of the same sample were combined and incubated with the 4 µl of anti-GFP antibody (table 2-6). Five µl of immunoprecipitated was used to analyse the GFP protein and 15 µl to analyse HA-Neo1p.

Immunoprecipitations of GFP tagged Dop1p and/or domains of Dop1p for testing the co-isolation of Ysl2p-HA were identical to the procedure described in the section 2.2.3.3.3.2 with some minor variations. One aliquot of 50 OD_{600} of cells was used per sample, to extract the proteins 0.5% of NP40 at final concentration was used and a total of 20 min of incubation on ice. No centrifugation at 100,000 x g was applied to the supernatants after the centrifugation at 13,000 rpm and those were incubated with 1 µl of anti-GFP antibody (table 2-6). Five µl of immunoprecipitated was used to analyse the GFP protein and 15 µl to analyse Ysl2p-HA.

To immunoprecipitate chromosomal GFP-tagged Dop1p, the procedure applied was the same as for the co-immunoprecipitation with Ysl2p-HA, but instead, 2 µl of anti-GFP antibody (table 2-6) were used to precipitate the protein. Five µl of immunoprecipitated was used to analyse GFP-Dop1p.

2.2.3.3.6 Immunoprecipitation of HA-Neo1p to detect ubiquitination

Cells were grown in 500 ml of YPD at 30 ºC until they reached an OD_{600} between 0.3-0.5 units/ml. Fifty OD_{600} units of cells, for each sample, were collected by centrifugation at 4000 rpm during 5 min. The cells were washed twice with 10 ml of ice cold ddH_2O containing a final concentration of 20 mM NEM (N-ethylmaleimide, used as inhibitor of the deubiquitinases) and 10 mM NaN_3, and once with ice cold IP bufferA (see section 2.2.3.3.2) containing a final concentration of 20 mM NEM. Next, they were resuspended in 200 µl of IP bufferA containing 20 mM NEM and transferred to a 1.5 ml Eppendorf tube. 1 µl of 1000 x CLAP and 0.48 g of glass beads were added and the cells were mechanically lysed by 10 rounds of vortexing for 45 sec and 1 min on ice in between. The lysates were transferred to a new Eppendorf tube and the glass beads were

washed with 800 µl of IP bufferA containing 20 mM NEM, to collect all the remaining lysate. To each lysate, 1 µl of 1 M DTT (1 mM end concentration) and a final concentration of 0.01% NP40 were added to extract the protein. The lysates were incubated on ice for 30 min to allow the extraction of the proteins and centrifuged at 13,000 rpm at 4 ºC for 20 min. Supernatants were collected to a new Eppendorf, incubated with 3 µl of rat anti-HA antibody (table 2-6) and subjected to the procedure described in the section 2.2.3.3.2 with some minor modifications. All the steps were performed in the presence of IP bufferA containing 20 mM NEM. The bounded proteins were eluted by adding 40 µl of 1 x Laemmli sample buffer containing 8 M Urea and 2.5 % β-mercaptoethanol and heated at 50 ºC during 10 min. Twenty µl of each sample were analysed by Western blotting.

2.2.3.4 Co-isolations with Dop1p-TAP

Cells were grown as described in 2.2.1.1. The cell aliquots were prepared as described on the section 2.2.3.3.1. In the case of co-isolations experiments performed in Δ*ysl2* cells the cells were grown at 25 ºC in SD-LEU media.

To isolate Dop1p-TAP complexes the method used was based on that described for isolation of Ysl2-TAP complexes in Wicky *et al.* 2004.

In the case of testing the exact concentration of detergent needed to maintain the integrity of HA-Neo1p for the co-isolation one frozen aliquot (to each condition tested) of the control strain (BS862) and one of the strain containing the epitope tagged Dop1p-TAP and a plasmid holding HA-Neo1p (SB205), were defrost and lysed as described in the section 2.2.3.3.2. One µl of 1 M DTT and the amount of NP40, to obtain a final concentration of 0%, 0.01%, 0.02% and 0.04%, were added. Subsequently, the extraction of the proteins was allowed to proceed during 30 min on ice. The cell extracts were then centrifuged at 13,000 rpm for 20 min at 4ºC and the supernatants transferred to a new Eppendorf tube. Sixty µl of 1/3 slurry of IgG-Sepharose beads (GE Health Care) in IP bufferA (section 2.2.3.3.1) were added to each supernatant and the binding of Dop1p-TAP complexes was achieved by 2 hours incubation at 4 ºC on a overhead rotator. The IgG-Sepharose beads were washed 3 times with IP bufferA containing 1 mM DTT and the respective concentration of NP40 and 2 times with TEV cleavage buffer (10 mM Tris/HCl pH 8.0, 150 mM NaCl, 0.5 mM EDTA/NaOH pH 8.0), also containing 1 mM DTT and the respective concentration of NP40. Proteins bounded to

IgG-Sepharose were subject to TEV protease cleavage. IgG-Sepharose beads were resuspended in 100 µl of TEV cleavage buffer containing 1 mM DTT, NP40 and 3 units of TEV protease. The protease-cleavage reaction was carried out for 2 hours at 16 ºC on a horizontal rotator. Thereafter, the eluates were collected to new Eppendorf tubes and the IgG-Sepharose beads were washed twice with 450 µl of TEV cleavage buffer (containing 1 mM DTT and NP40) to collect the remaining cleaved proteins. The proteins present in the eluates were precipitated in the presence of 5 µg of IgG. To approximately 1 ml of sample an end concentration of 0.015% (w/v) deoxycholic acid was added and the samples were incubated for 10 min at room temperature. Then, TCA was added to 6% (w/v) end concentration and the samples were incubated for 30 min on ice followed by a centrifugation at 13,000 rpm for 20 min at 4ºC. The precipitated proteins were washed with 1 ml of acetone dried and resuspended in 65 µl of 1 x Laemmli sample buffer (containing 8 M urea and 2.5% β-mercaptoethanol) by vortexing 20 min at 37ºC. Samples were heat-denaturated at 50ºC for 10 min, centrifuged 5 min and transferred to a clean Eppendorf tube. Thirty or 20 µl (for detecting HA-Neo1p and DOP1p-TAP, respectively) of each sample were analysed by Western blotting.

To perform the co-isolation of proteins from 100,000 x g supernatants in the presence of 0.01 % NP40, 5 frozen aliquots of cells from each strain were used and later combined. The procedure was the same as described above with some minor modifications. The protease inhibitors added were 20 µl of PIC 50X (5 µ/ml leupeptin; 25 mM 1.10 phenathroline; 25 µg/ml Pepstatin A; 5 mM Pefabloc), 20 µl of Complete 50X (protease inhibitor cocktail, Roche), 1 µl of 1 M PMSF (phenylmethylsulfonylfluoride). Supernatants of solubilised cell extracts obtained after centrifugation at 13,000 rpm were additionally centrifuged for 1 hour at 100,000 x g at 4 ºC (see section 2.2.3.3.3.2). The eluates of each strain obtained after the TEV cleavage were collected to the same tube and the IgG-Sepharose beads were washed twice (successively for the samples from the same strain) with 350 µl of TEV cleavage buffer containing 1 mM DTT and 0.01% NP40. The eluted proteins were precipitated as described above and the proteins denaturated in 70 µl 1 x Laemmli sample buffer containing 8 M urea and 2.5 % β-mercaptoethanol.

Co-isolations of GFP-Dop1p or Ysl2p with Dop1p-TAP were performed as described above with some minor modifications. Cell aliquots were thawed and cells

were lysed with glass beads. Subsequently, proteins were extracted for 20 min in the presence of 0.5% (GFP-Dop1p) or 0.2% (Ysl2p) of NP40 and centrifuged for 20 min at 13,000 rpm. Supernatants were incubated with the IgG-Sepharose beads washed and incubated with the TEV protease as previously described. Eluates containing the protein complexes were collected and the proteins were precipitated with TCA. Protein pellets were resuspendend in 65 µl of 1 x Laemmli sample buffer containing 2.5% β-mercaptoethanol and denatured for 5 min at 95ºC. Thirty µl of each sample were analysed by Western blotting.

2.2.3.5 Pulse-chase analysis

Cells were grown overnight at 25ºC in selective SD medium to early logarithmic phase until they reach an OD_{600} of 0.2 to 0.3 units/ml. 5.6 units of cells (OD_{600}) were collected by centrifugation at 3000 rpm and resuspendend in 2.8 ml of SD medium containing 50 mM potassium phosphate buffer (KP_i) (pH 5.7) and 2 mg/ml of BSA (Bovine Serum Albumin A-7906, Sigma). After 15 min of incubation at 25ºC, 61.6 µl of [^{35}S]-methionines (10 mCi/ml, GE Healthcare, Munich, Germany) were added to the culture and the proteins were labelled for 30 min at 25ºC. At the time point zero, 500 µl of cells were transferred to a precooled Eppendorf tube containing NaN_3 and NaF (10 mM final concentration). To stop the incorporation of [^{35}S]-methionine, unlabelled methionine was added to the culture to a final concentration of 1 mg/ml, and the culture was transferred to 37ºC. Five hundred µl of cells were collected at the time points 30 and 60 min after the chase at 37ºC. Then, 650 µl of SD medium were added to the remaining culture and 750 µl of cells were collected for the time points 120 and 180 min. The cells were centrifuged at 13,000 rpm, washed with 1 ml of 10 mM NaN_3 and resuspended on 100 µl of lysis buffer (50 mM Tris/HCl pH 7.5; 1 mM EDTA/NaOH pH 8.0; 1 x CLAP). Approximately 200 mg of glass beads were added and the cells were lysed by 5 rounds of 1 min vortexing and 1 min cooling on ice. To extract the proteins, 33 µl of solubilisation buffer [4% (w/v) SDS; 600 mM NaCl; 50 mM Tris/HCl pH 7.5; 4 x CLAP] were added to each sample and these were incubated at room temperature for 10 min on an overhead shaker. The extracts were diluted with 1.2 ml of IP buffer [1% (w/v) deoxycholic acid; 1% (w/v) Triton X-100; 150 mM NaCl; 50 mM Tris/HCl pH 7.5; 1 x CLAP] and centrifuged at 13,000 rpm for 30 min at 4ºC. The supernatants were

transferred to fresh Eppendorf tubes and incubated 2 hours at 4ºC with 4 µl of anti-HA antibody (table 2-6). Then, 60 µl of 1/3 slurry of ProteinA-Sepharose (GE Health Care) was added and the binding of the proteins was carry out at 4ºC for 1 hour on an overhead shaker. The ProteinA Sepharose beads were washed 4 times with IP buffer and the proteins were released by heating at 50ºC for 10 min in the presence of 65 µl of 1 x Laemmli sample buffer, containing 8 M urea and 2.5% β-mercaptoethanol. Samples were centrifuged at 16,000 x g for 5 min and the supernatants transferred to new Eppendorfs tubes. Twenty µl of each sample were separated on a 7.5% SDS-gel, this was overlaid with GE Healthcare Phosphor screen and scanned with Strom 860 (GE Healthcare, Uppsala, Sweden).

2.2.4 Cell biology methods

2.2.4.1 Fluorescence microscopy

2.2.4.1.1 Indirect immunofluorescence

Four OD_{600} units of cells were fixed for 4 hours at room temperature with 100 mM potassium phosphate buffer (KP_i, pH 6.5) and 4% formaldehyde. Cells were then harvested by 5 min centrifugation at 2000 rpm, washed 3 times with IF buffer (1.2 M sorbitol, 100 mM KP_i pH 6.5) and resuspended in 1 ml of IF buffer containing 20 mM β-mercaptoethanol. Spheroplasts were prepared by addition of Zymolyase 100T (Seigagaku Kyogo, Japan) at 20 µg/ml final concentration and incubation during 30 min at 30ºC. Spheroplasts were washed twice with 1 ml of IF buffer, resuspendend in 200 to 400 µl of IF buffer and stored at 4ºC for up to 2 days or -20ºC for up to several months.

Fixed cells were labelled on 10-wells immunofluorescence microscope slides (Teflon, ER-240B-CE24, Thermo Scientific). Those were coated with poly-L-lysine by placing 15 µl of a 1 mg/ml poly-L-lysine solution in each well. After 5 min, the solution was removed by aspiration and the wells were allowed to dry. Then, they were washed 5 times with 15 µl ddH_2O and again allowed to dry. Fifteen µl of suspension of fixed cells were placed in each well and allowed to settle for 15 min. The unbounded cells were removed by washing 3 times with 20 µl of PBS-IF buffer (53 mM $NaHPO_4$, 13 mM NaH_2PO_4, 75 mM NaCl). Cells were thereafter pre-incubated with PBT buffer (PBS-IF, 1% (w/v) BSA, 0.1% (w/v) Tween 20) for 30 min, to prevent unspecific binding of the

antibody. PBT was aspirated from the wells and 15 µl of primary antibody diluted in PBT (table 2-7), previously centrifuged for 2 min at 16,000 x g, were added to each well. After one hour incubation, the cells were washed 10 times with PBT and incubated in the dark for one hour with 15 µl of secondary antibody diluted in PBT (table 2-8), also previously centrifuged for 2 min. Cells were washed 6 times with PBT followed by 6 times with PBS-IF and covered with one drop of 99% glycerine for immunofluorescence (Fluka). A coverslip was placed on the slide, sealed using nail polish and the slide was stored at 4ºC in the dark for several days.

The antibodies used and the respective dilution are listed in the table below.

Table 2-7: Primary antibodies used for indirect immunofluorecence

Antibody	Dilution	Source
Mouse monoclonal anti-HA 16B12	1:2000	Covance
Rabbit polyclonal anti-c-Myc, A-14 (Sc-789)	1:300	Santa Cruz Biotechnologies, Inc

Table 2-8: Secondary antibodies used for indirect immunofluorescence

Antibody	Dilution	Source
Cy3-conjugated goat anti-mouse Fab fragment	1:1000	Jackson ImmunoResearch
Alexa488 goat anti-rabbit IgG (H+L)	1:1000	Molecular Probes

2.2.4.1.2 GFP fluorescence

Approximately 4 x 10^7 cells were collect by centrifugation at 4000 rpm washed with ddH_2O and resuspended in 20 µl of IF buffer (see section 2.2.4.1.1). To visualise the cells, 2 µl of the cell suspension in IF buffer was placed on a microscope slide and mixed with 2 µl of 1,6 % low melting agarose dissolved in IF buffer. Cells were observed under the fluorescence microscope using the EGFP filter.

2.2.4.1.3 Alexa598-conjugated alpha-factor uptake and visualisation

Cells were grown to early logarithmic phase (0.5 x 10^7 cells/ ml) for 16 hours at 25 ºC. 4 x10^7 cells were collected by centrifugation at 2,000 rpm for 5 minutes and resuspended in 50 µl of ice cold SD medium. 1 µl of Alexa594α-factor synthesised as

described in Toshima *et al.* 2006 was added and the suspension was incubated for 1 hour on ice to allow the binding of Alexa594α-factor to the plasma membrane of the cells. The cells were washed twice with 800 µl of ice-cold SD medium and resuspended in 100 µl of SD medium. The uptake of Alexa594α-factor was performed at 30ºC during 40 min. Subsequently, the cells were spun down and resuspended in 20 µl of ice-cold IF buffer (see 2.2.4.1.1). To visualize the apha-factor, 2 µl of the suspension was mixed with 2 µl of 1,6% low melting agarose dissolved in IF buffer on a microscope slide and observed under the fluorescence microscope using the Cy3 filter and EGFP filter to perform the double labelling with GFP-Dop1p.

2.2.4.1.4 Nuclei staining with Hoechst 33342

4 x 10^7 cells were collected by 5 minutes centrifugation at 2000 rpm. The cells were washed once with 1 ml of PBS-IF buffer 1X (see section 2.2.4.1.1) and ressuspended in 1 ml of PBS-IF. Three µl of 1 mg/ml of Hoechst 33342 (4.8 µM end concentration) were added and the suspension of cells was incubated for 30 minutes at 30ºC. Subsequently, the cells were spun down, concentrated in 20 µl of IF buffer (see 2.2.4.1.1) and 2 µl of the suspension were mixed with 2 µl of 1,6% low melting agarose dissolved in IF buffer on a microscope slide. To visualize the Hoechst 33342 staining under the fluorescence microscope, the DAPI filter was used and the double labelling with GFP-Cterm was performed by observing the GFP staining with the EGFP filter.

2.2.4.1.5 Actin staining with Rodamine phaloidin

To stain actin, cells were grown to early logarithmic phase (5 x 10^6 cells/ ml) for 16 hours at 25ºC. To 50 ml of culture, formaldehyde was added to a final concentration of 4% and the cells were fixed for 10 min at room temperature. The cells were spun down at 2000 rpm for 5 minutes and fixed for 1 hour in PBS-IF (see section 2.2.4.1.1) containing 4% final concentration of formaldehyde. The fixed cells were washed twice with PBS-1X and resuspended in 500 µl of PBS-1X. To 100 µl of suspension, 10 µl of Rhodamine Phalloidin (6.6 µM in Methanol) were added and the suspension was incubated in the dark for 1 hour. Thereafter, the cells were washed 5 times with 1 ml of PBS-IF 1X and resuspended in a drop of 80 % glycerol. Two µl of the suspension were

mounted on a microscope slide and the cells were observed under the fluorescence microscope using the Cy3 filter.

2.2.4.2 CPY missorting test

Cells were diluted in sterile ddH_2O and plated by the help of a metal stapler onto a plate containing the required media for growth of the respective strain. A nitrocellulose membrane was placed on the top of the agar and the plate was incubated for growth. After 24 to 32 hours (the growth should be in an early phase), the nitrocellulose membrane was removed from the plate and washed with ddH_2O. Next, the membrane was immunodetected (see section 2.2.3.2.3) for the presence of CPY by using an anti-CPY antibody (table 2-3).

3 Results

3.1 The P4-ATPase Neo1p does not interact with Cdc50p

Although P-type ATPases are commonly single α-subunit, some β-subunits were identified to be required for the targeting and function of the P-type ATPases. For instances, the P_{2C}-ATPases (Na^+/K^+-ATPase and H^+/K^+-ATPase) and some of the P_4-ATPases require β-subunits (Saito *et al.* 2004; Durr *et al.* 2009). In *Saccharomyces cerevisiae* the Cdc50 family members Cdc50p, Crf1p and Lem3p were identified as β-subunits of the P_4-ATPases Drs2p, Dnf3p and Dnf1p, Dnf2p, respectively (Saito *et al.* 2004; Furuta *et al.* 2007). In the case of Neo1p, the only essential member of the subfamily of P_4-ATPases, no β-subunits was identified yet. Albeit the genetic interaction between *NEO1* and *CDC50* no physical interaction could be found between them (Saito *et al.* 2004). Herein, the putative interaction between Neo1p and Cdc50p was re-examined using two different immunoprecipitation approaches. One of these approaches is based on the immunoprecipitation used to show the interactions between the Cdc50 family members and the P_4-ATPases Drs2p, Dnf1p, Dnf2p and Dnf3p, the other is based on the immunoprecipitation used to show the interaction between Neo1p and Ysl2p (Saito *et al.* 2004; Wicky *et al.* 2004). To perform these co-immunoprecipitation experiments, a strain containing chromosomally encoded Cdc50p-Myc and HA-Neo1p was generated (SB90) and the strains expressing either Cdc50p-Myc (SB121) or HA-Neo1p (BS1488) were used as negative controls. In the first approach, Cdc50p-Myc or HA-Neo1p were immunoprecipitated from total membranes of the above-mentioned strains after extraction with 1% CHAPS (see section 2.2.3.3.3.1). As observed in the figure 3.1 (A) immunoprecipitation of either Cdc50p-Myc or HA-Neo1p from total membranes could not co-isolate the other protein. In the second approach Cdc50p-Myc or HA-Neo1p were immunoprecipitated from supernatants obtained after a centrifugation at 100,000 g of cell extracts performed in the presence of 0.01% NP40 (see section 2.2.3.3.3.2). Using this extraction condition, approximately 45% of Cdc50p-Myc was soluble while only 29% of HA-Neo1p was retrieved from the membranes. Immunoprecipitation of Cdc50p-Myc in this condition did not co-isolated HA-Neo1p and reciprocally immunoprecipitation of HA-Neo1p did not co-precipitated Cdc50p-Myc (figure 3.1, B).

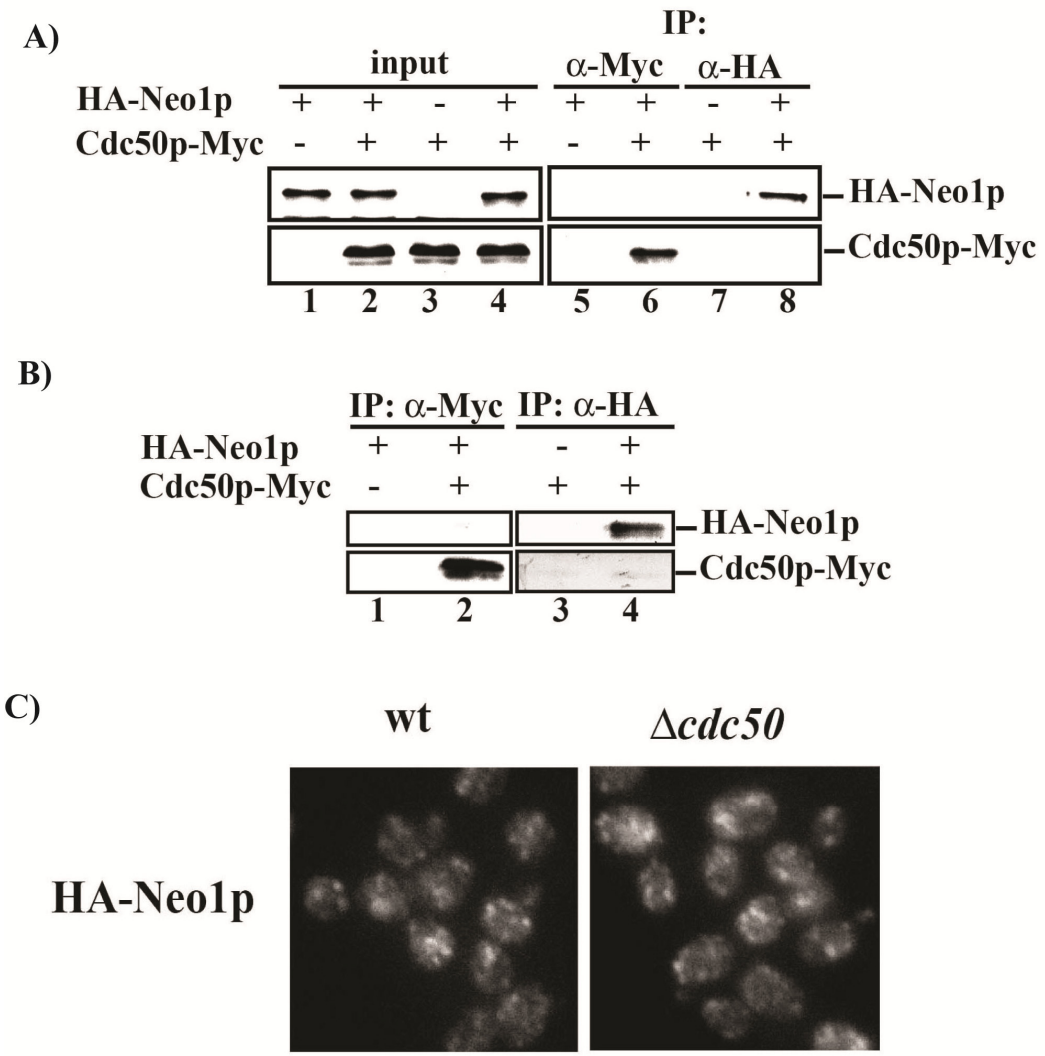

Figure 3.1: Neo1p does not physically interact with Cdc50p neither requires it to exit the ER. (A) Total membrane proteins of 200 OD_{600} units of cells expressing the indicated epitope-tagged proteins (lane1, BS1488; lane 2 and 4, SB90; lane 3, SB121) were subjected to immunoprecipitation after solubilisation in 1% CHAPS (see section 2.2.3.3.3.1). 1% of the solubilised proteins (lanes 1, 2, 3 and 4) and 37.5% of the immunoprecipitated proteins (lanes 5, 6, 7 and 8) were analysed by Western blotting using the α-HA or α-Myc antibodies (table 2-3). B) Total proteins from a 100,000 g supernatant of cell extracts (from 150 OD_{600} of the cells above mentioned) generated in the presence of 0.01% NP40 were subjected to immunoprecipitation (see section 2.2.3.3.3.2). About 50% of the immunoprecipitated proteins (lanes 1, 2, 3 and 4) were analysed by Western blotting. (C) HA-Neo1p immunofluorescence in the presence (BS1488) or absence (SB71) of *CDC50*. Cells were grown at 25ºC, fixed and stained by immunofluorescence with a monoclonal mouse anti-HA (16b12) antibody (table 2-7) as described in the section 2.2.4.1.1. * Cross reaction for the anti-HA antibody.

Since these two approaches did not reveal any physical interaction between Neo1p and Cdc50p, the role of *CDC50* in the transport of HA-Neo1p was further investigated. Therefore, the localization of HA-Neo1p on a strain deleted for *CDC50* was compared with a wild-type strain. As observed in the figure 3.1 (C) in both strains HA-Neo1p staining shows a similar cytoplasmic punctuated pattern characteristic of a Golgi and

endosomal localization. Thus, HA-Neo1p is not retained in the ER compartment when Cdc50p is not present. Together with the previous finding that both proteins are not physically associated, these results strongly indicate that Cdc50p is not a β-subunit of Neo1p neither is responsible for the transport of Neo1p to its final localization.

3.2 Dop1p is physically associated with the Neo1p-Ysl2p-Arl1p network

3.2.1 Dop1p interacts with Neo1p and Ysl2p

A search for elements necessary for the function of Neo1p, revealed Dop1p. Several indications led to the investigation of the relationships between Dop1p and Neo1p. In a genome-wide screen using yeast heterozygous deletion strains to identify targets for therapeutic compounds, *NEO1/Δneo1* and *DOP1/Δdop1* heterozygous strains were identified to be sensitive to the same group of drugs, the tricyclic antidepressants (Lum *et al.* 2004). Among these drugs, the heterozygous deletion strains *NEO1/Δneo1*, *DOP1/Δdop1* and *YNL296w/Δynl296w* were sensitive to the drug chlorpromazine. Interestingly, *YNL296w* ORF overlaps with the *YSL2/MON2* ORF (*YNL297c*), a gene coding for the protein Ysl2p/Mon2p which was previously shown to be physically and functionally linked to Neo1p (Wicky *et al.* 2004). Hence, the deletion of *YNL296w* yields to *YSL2* not being expressed. Furthermore, like *NEO1*, *DOP1* is an essential gene. Thus, the similarity of phenotypes observed for these mutants suggest that their respective proteins might share a similar function. Corroborating this hypothesis, two different strategies have identified Dop1p as a binding partner of Ysl2p/Mon2p (Efe *et al.* 2005; Gillingham *et al.* 2006). Using a genetic approach, *DOP1* was identified as a multicopy suppressor of *Δysl2* cells and co-immunoprecipitation experiments showed that both proteins were physically interacting (Efe *et al.* 2005). Later another group co-purified Dop1p with Ysl2p/Mon2p (Gillingham *et al.* 2006).

Here, the interaction between Dop1p and Ysl2p was re-examined under our experimental conditions and the hypothesis that Dop1p may interact with Neo1p was investigated. To assess the interaction between Dop1p and Ysl2p, Dop1p was chromosomally tagged with a TAP epitope (see section 2.2.2.2) and the Dop1p-TAP assemblies were isolated (see section 2.2.3.4) from total cell lysates after extraction with 0.2% NP40. Isolation of Dop1p-TAP could efficiently co-isolate Ysl2p (figure 3.2, A lane 2). This co-isolation was specific since the same procedure applied to a wild-type

strain (BS64) where no Dop1p-TAP is present did not result in the isolation of Ysl2p (figure 3.2, A lane 1). A similar approach was applied to investigate the physical interaction between Dop1p and Neo1p. Therefore, a strain containing chromosomally encoded Dop1p-TAP in which *HA-NEO1* is expressed from a single copy plasmid as the only copy of *NEO1*, was generated (SB205). As a negative control, an isogenic strain lacking encoded Dop1p-TAP (BS862) was used. Thereafter, Dop1-TAP assemblies were isolated from cell extracts generated in the presence of several concentrations of NP40, 0%, 0.01%, 0.02% and 0.04%. As shown earlier, the critical concentration of 0.01% of NP40 was necessary to observe an interaction between Neo1p and Ysl2p (Wicky *et al.* 2004). Not surprisingly, HA-Neo1p was best co-isolated with Dop1p-TAP from cell extracts obtained in the presence of 0.01% NP40 (figure 3.2, B). To ensure that this co-isolation was specific and not mediated by membranes, prior to the binding of the extracted proteins to the IgG Sepharose beads, the cell extract was centrifuged for 1 hour at 100,000 x g to remove insoluble material (see section 2.2.3.4). Using this conditions 21% of HA-Neo1p and 25% of Dop1p-TAP were efficiently retrieved from the membranes and found in the 100,000 g supernatant (figure 3.2, C). In these conditions, HA-Neo1p could still be efficiently and specifically co-isolated with Dop1p (Figure 3.2, C, lane 4), since after similar treatment of a strain lacking Dop1p-TAP, no signal for HA-Neo1p was observed (figure 3.2, C, lane 3). Moreover, the analysis of several other proteins, Drs2p, Chc1p and Pep12p, revealed no enrichment when in the presence of isolated Dop1p-TAP (figure 3.2, C), once more indicating the specificity of the interaction observed between Dop1p-TAP and HA-Neo1p.

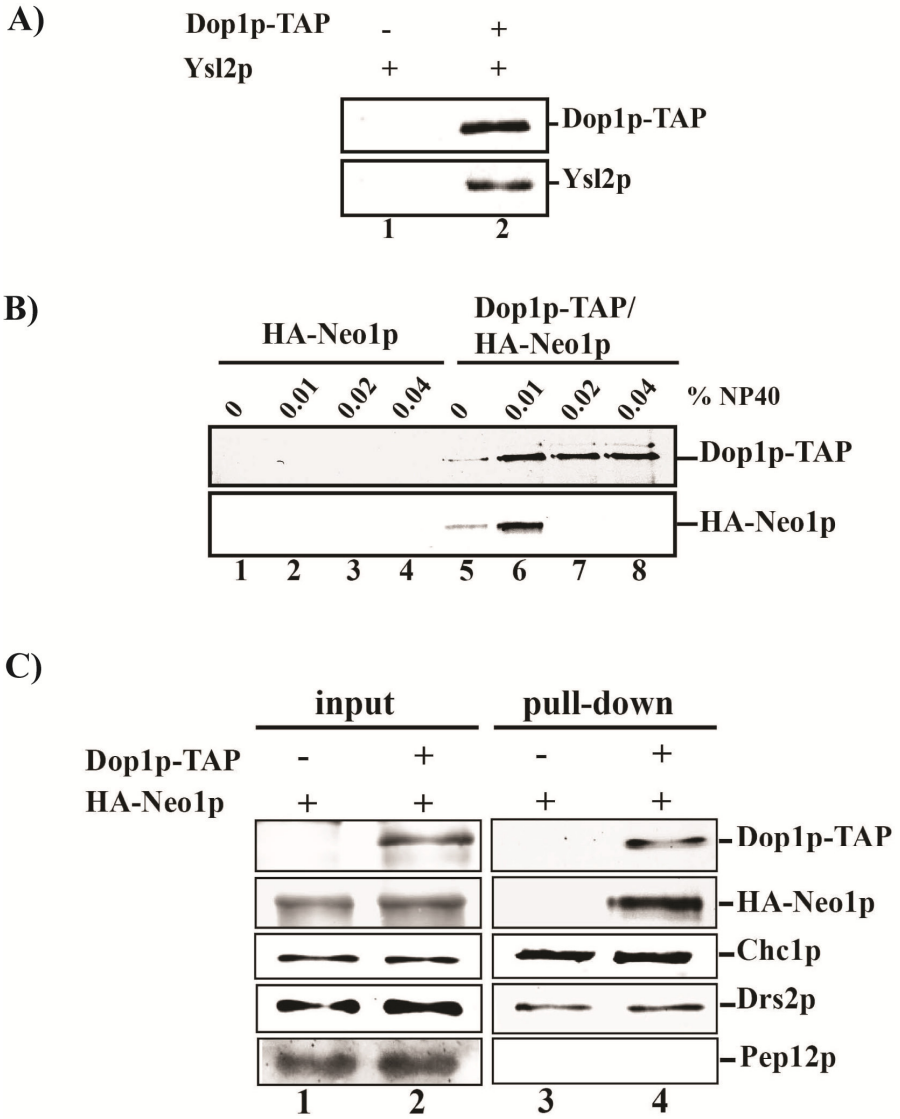

Figure 3.2: Dop1-TAP interacts with HA-Neo1p and Ysl2p. A) Cell extracts from BS64 (lane 1) or SB161 (lane 2) cells were obtained after treatment with 0.2% of NP40 and Dop1p-TAP was isolated on IgG beads and further release with the TEV protease (see section 2.2.3.4). About 40% of the isolated Dop1p-TAP complexes were analysed by Western blotting using α-TAP or α-Ysl2 as primary antibodies (table 2-3). B) BS862 (lanes 1, 2, 3 and 4) or SB205 (lanes 5, 6, 7 and 8) cells, containing the indicated tagged proteins, were lysed and the proteins were extracted in the presence of the indicated concentrations of NP40 and Dop1p-TAP complexes were isolated (see section 2.2.3.4). About 50% of the total isolated Dop1p-TAP complexes were analysed by Western blotting using α-TAP or α-HA as primary antibodies (table 2-3). C) Dop1-TAP assemblies isolated from 100,000 g supernatants of SB205 (lane 4) and BS862 (lane 3) cell extracts prepared in the presence of 0.01% of NP40 (see section 2.2.3.4). About 30% of the isolated proteins were analysed by Western blotting using the respective primary antibodies.

3.2.2 The interaction between Dop1p and Neo1p is independent from Ysl2p

Given the existent physical interaction between Dop1p and Ysl2p and the fact that Ysl2p also interacts with Neo1p, it is possible that the interaction found between Dop1p and Neo1p is mediated by Ysl2p. To test this possibility, the interaction between these proteins was examined in the absence of Ysl2p. Therefore, a strain deleted for *YSL2* and containing Dop1p-TAP and HA-Neo1p was generated (SB296) and used to isolate Dop1p-TAP from total cell lysates obtained after treatment with 0.01% of NP40 or no detergent. Simultaneously, the strain used to show the interaction between Dop1p-TAP and HA-Neo1p (SB205) and a strain lacking *YSL2* and harbouring the plasmid pRS315-HA-NEO1 (SB306) were submitted to the same procedure to serve as positive and negative control, respectively. After isolation of Dop1p-TAP, HA-Neo1p was specifically co-isolated (figure 3.3, A). Significantly, the interaction between Dop1p-TAP and HA-Neo1p was not affected by the absence of Ysl2p (figure 3.3, A). Next, the interaction between Dop1p-TAP and HA-Neo1p in the absence of Ysl2p was analysed from a 100,000 g supernatant to ensure that this interaction was not mediated through membranes. Thus, Dop1p-TAP was isolated from total cell extracts obtained after treatment with 0.01% NP40 and subsequently centrifuged for 1 hour at 100,000 x g. As observed in the Figure 3.3 (B), even in these conditions, isolation of Dop1p-TAP specifically co-isolated HA-Neo1p in the absence of Ysl2p demonstrating that Ysl2p does not mediate the interaction between Dop1-TAP and HA-Neo1p.

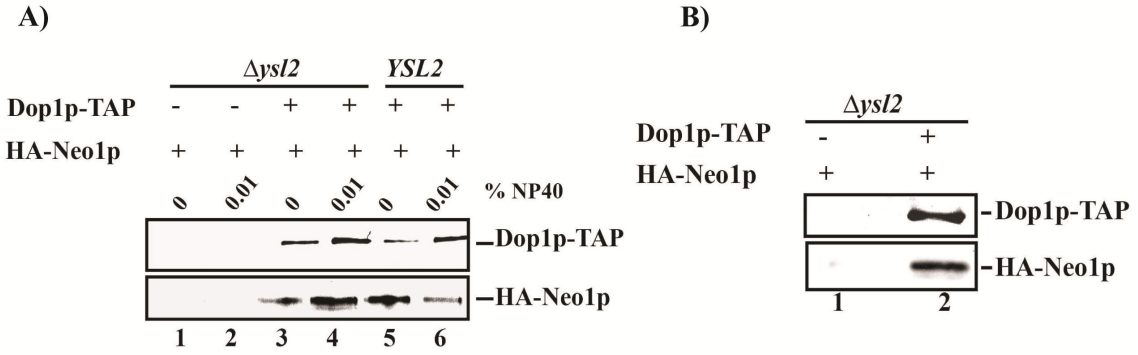

Figure 3.3: The interaction between Dop1p-TAP and HA-Neo1p is independent from Ysl2p. A) Dop1-TAP was isolated from cells carrying the indicated epitope tagged proteins. SB306 (lanes 1 and 2), SB296 (lanes 3 and 4) and SB205 (lanes 5 and 6) cells were lysed and the proteins were extracted in the presence of 0.01% NP40 or not. Dop1-TAP was isolated by affinity on the IgG Sepharose beads and further released using the TEV protease (see section 2.2.3.4). About 50% of the isolated proteins were analysed by Western-blotting using the α-TAP or α-HA antibodies (table 2-3) Cells carrying the indicated epitope tagged proteins SB306 (lane 1) SB296 (lane 2) were lysed and the proteins were extracted with 0.01% NP40. Subsequently, the extract was centrifuged at 100,000 x g to remove insoluble material and Dop1-TAP assemblies were isolated. About 30% of the isolated proteins were analysed by Western blotting using the α-TAP or α-HA antibodies (table 2-3).

3.3 Dop1p, Neo1p and Ysl2p are interdependent

3.3.1 HA-Neo1p and Ysl2p steady state levels are decreased in the temperature sensitive *dop1-3* mutant upon shift to 37 ºC

As previously demonstrated in this study, Dop1p and Neo1p physically interact *in vivo*, thus I further explored new relationships between these two proteins. Given the fact that *DOP1* is an essential gene, disabling its deletion, a mutant allele of *DOP1*, *dop1-3* was used in this study. The *dop1-3* allele has 7 point mutations that result in 7 amino acid changes in Dop1p, two positioned within the conserved N-terminus of Dop1p (L125S; S224L) and five situated in the C-terminus of the protein, a region that contains two to three leucine zipper-like repeats (E1438D; M1494I; Y1515H; C1580Y; E1638K) (figure 3.4, A). First, the steady state levels of HA-Neo1p were monitored in the *dop1-3* mutant. For that purpose, a strain deleted for *DOP1* and expressing HA-Neo1p from the chromosome and the *dop1-3* allele from a single copy plasmid was generated (SB142) and compared to an isogenic strain that expresses *DOP1* (SB323). These strains were grown overnight at permissive temperature and then shifted to 37ºC for up to 3 hours, to inactivate Dop1-3p. Cells were collected at several time points after the shift and HA-Neo1p was analysed by quantitative Western blotting (figure 3.4, B and C). Results showed that while the steady state levels of HA-Neo1p are not affected after the shift to non-permissive temperature in the wild-type strain remaining around the 100 % value, they reduce to about 80% of its initial values in the *dop1-3* mutant. Additionally, the levels of Pma1p, another P-type ATPase, were also monitored to serve as an internal control for the proper function of the secretory pathway. In the case of Pma1p, no significant changes in the steady state levels of the protein, either in the wild-type or in the *dop1-3* cells, were observed along the shift, remaining around the 100% value. Furthermore, Tlg1p, an endosomal protein (data not shown) and Pgk1, a cytosolic protein that served as a loading control, were not affected (figure 3.4, B) demonstrating that HA-Neo1p loss in *dop1-3* cells is a specific effect and is not due to pleiotropic defects exhibited by this mutant (like organelle biogenesis and secretion defects).

Since Ysl2p also interacts with Dop1p, the steady state levels of Ysl2p were also investigated in *dop1-3* mutant. For that purpose, the strains above described were used and treated similarly. As observed in the figure 3.4 (D), the steady state levels of Ysl2p also decreased in *dop1-3* cells upon 2 hours of shift to 37ºC while they remained stable

in the wild-type strain. Together, these results suggest that Neo1p and Ysl2p levels are dependent on Dop1p integrity.

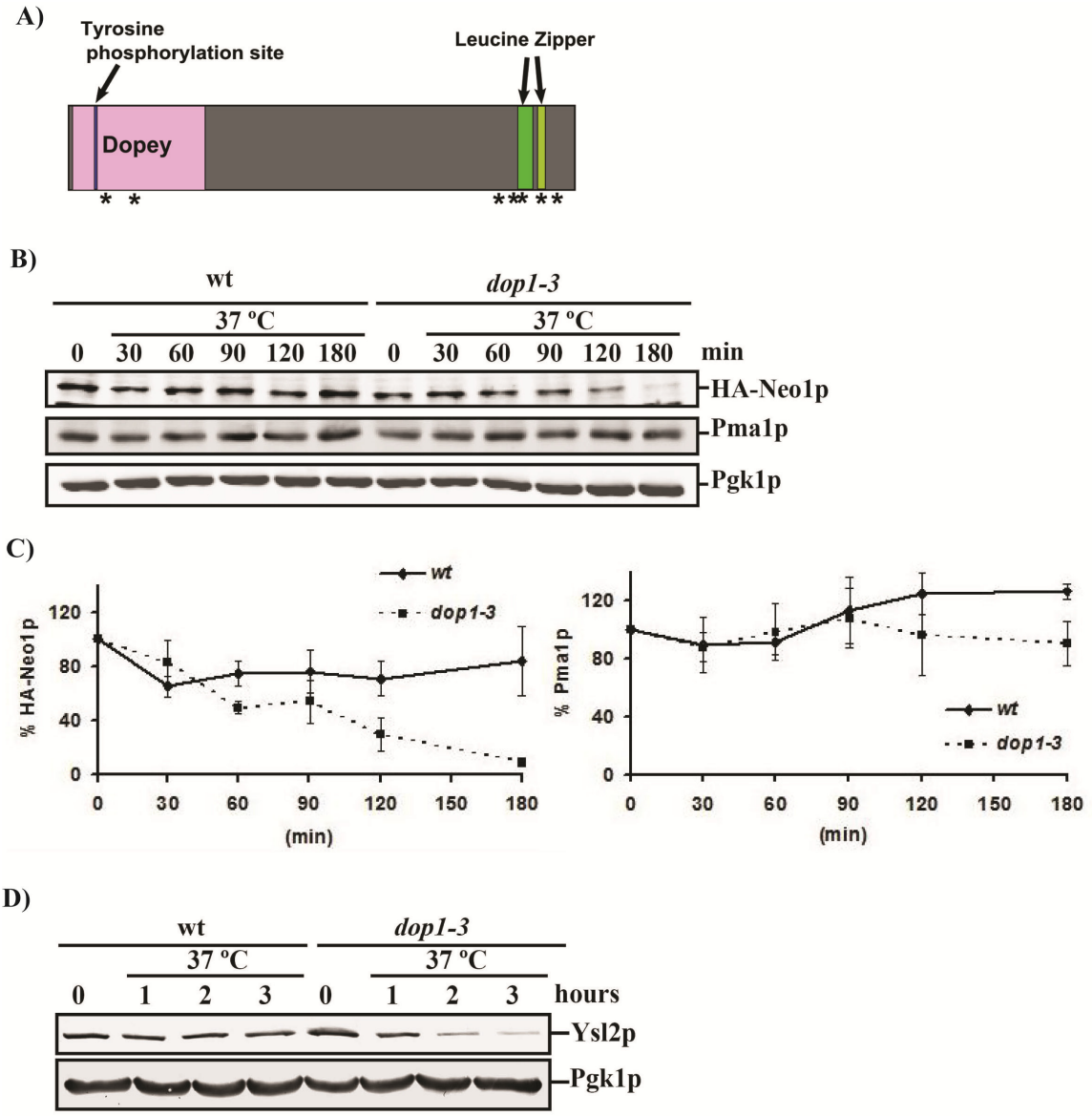

Figure 3.4: HA-Neo1p and Ysl2p steady state levels decrease in the *dop1-3* mutant. A) Diagram showing the various features of Dop1p as described in Pascon and Miller 2000 and the position of the mutation of Dop1-3p (*). B) SB323 (wt) and SB142 (*dop1-3*) cells were grown overnight at 25ºC and shifted for up to 3 hours at 37ºC. 1.7 OD_{600nm} units of cells were collected at the indicated time points and the cell lysates (see section 2.2.3.1) were analysed by Western blotting using the α-HA, α-Pma1 or α-Pgk1 as primary antibodies (table 2-3) and α-mouse IRdye800 (table 2-5) as secondary antibody. C) Signals for HA-Neo1p and Pma1p were scanned using the Odyssey Infrared Imaging System and quantified with the Odyssey software (LI-COR Biosciences). Percentages were calculated from 5 independent experiments. Signal intensity (of HA-Neo1p or Pma1p) from the time point 0 (25ºC) was set to 100% and the percentage of signal for the others time points were calculated based on this one. D) SB323 (wt) and SB142 (*dop1-3*) cells were treated as described in B and the cell lysates (see section 2.2.3.1) were analysed by Western blotting using the α-Ysl2 or α-Pgk1 as primary antibodies (table 2-3).

Given that Ysl2p and Neo1p levels decrease in *dop1-3* cells after shift to 37 ºC, the hypothesis that *YSL2* and *NEO1* genes would be multicopy suppressors of the *dop1-3* mutant was studied. Together, *ARL1*, a gene that is a multicopy suppressor of the *Δysl2* cells phenotypes (Wicky *et al.* 2004) was also tested. The *dop1-3* mutant has no apparent growth defect at 25ºC but does not grow at 37ºC (figure 3.5). Moreover, as already observed for some *neo1* mutants (Hua and Graham 2003), the *dop1-3* mutant does not grow in the presence of neomycin sulphate, an aminoglycosilic antibiotic (figure 3.5). Thus, *Δdop1* homozygous diploid cells expressing the *dop1-3* allele from a single copy plasmid (BS1806) were transformed with an empty 2μ plasmid or a 2μ plasmid containing either *DOP1*, *NEO1*, *DRS2*, *YSL2*, *ARL1* or *ARF1*. After selection of the transformants on the appropriated SD medium, the cells were diluted in series and spotted onto YPD plates or YPD + 2 mg/ml neomycin and incubated at 25ºC or 37ºC. As shown in the figure 3.5, when *DOP1* was expressed from a multicopy plasmid the growth defects of *dop1-3* cells were perfectly suppressed, confirming that the mutations in Dop1-3p are the cause of the growth defects in that strain. Interestingly, *NEO1* overexpression was able to partially suppress the growth defect of the *dop1-3* mutant at 37ºC and to almost completely suppress the neomycin hipersensitivity in that mutant. *ARL1* was able to marginally suppress the hypersensitivity to neomycin of the *dop1-3* mutant but further tests with expression of *arl1* mutants (ARL1G2A, which cannot be myristoylated, ARL1T32N, restricted to the GDP-bound form and ARL1Q72L, restricted to the GTP-bound form) could not reveal any improvement in growth or synthetic growth defect (data not shown). *YSL2* overexpression did not suppress the defects of the *dop1-3* mutant. Importantly, neither *DRS2*, a gene coding for a related P_4-ATPase, nor *ARF1*, a gene coding for a small ARF GTPase from the Golgi were able to rescue the growth defects of the *dop1-3* mutant.

Hence, the suppression of the *dop1-3* cells phenotypes by *NEO1* substantiates the previous results where Neo1p levels were shown to reduce in this mutant and suggests that these two proteins might have a connected role in the cell.

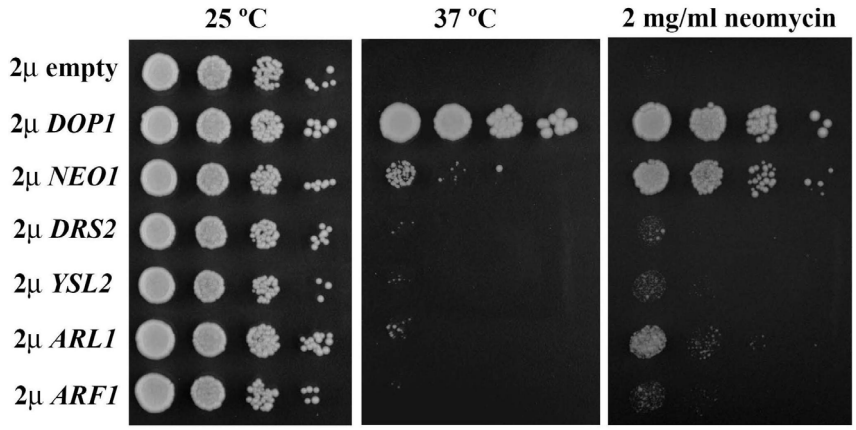

Figure 3.5: *NEO1* is a multicopy suppressor of the growth defects of the *dop1-3* mutant. BS1806 (homozygous *Δdop1* + pRS315-dop1-3) cells were transformed with the indicated plasmids. Similar amounts of the transformants were diluted in series, spotted onto YPD plates or YPD + 2 mg/ml neomycin and incubated at the indicated temperatures or at 25ºC when in the presence of neomycin for up to 3 days.

3.3.2 The steady state levels of GFP-Dop1p are decreased in the temperature sensitive *neo1-69* mutant

Similarly to the loss of Ysl2p observed in the *dop1-3* mutant, a previous study has shown that Ysl2p is also reduced in the *neo1-69* and *neo1-37* mutants (Wicky *et al.* 2004). Thus, the steady-state levels of Dop1p were also investigated in the *neo1* mutants. Therefore, strains encoding GFP-Dop1p and expressing either *NEO1* (SB284), *neo1-37* (SB286) or *neo1-69* (SB289) alleles from a single copy plasmid were generated and the levels of GFP-Dop1p were compared between them. After overnight grow at 25ºC, these strains were shifted to 37ºC for up to 3 hours. Equal amounts of cells were collected at each time point and the cell lysates were analysed by Western blotting for the GFP-Dop1p signal (Figure 3.6, A). As shown, GFP-Dop1p levels are similar between the wild-type (wt) and the *neo1-37* cells whereas in *neo1-69* cells the levels of GFP-Dop1 are dramatically reduced. Since quantification of the signal directly from cell extracts was not possible due to a strong background, GFP-Dop1p was immunoprecipitated, in the presence of 0.5% of NP40, from lysates of 50 OD_{600} units of wild-type (SB284), *neo1-37* (SB286) or *neo1-69* (SB289) cells grown at 25ºC or upon 1 hour of shift to 37ºC. Similar amounts of the immunoprecipitates were analysed for the quantity of GFP-Dop1p by quantitative Western blotting (Figure 3.6, B). At 25ºC, the levels of GFP-Dop1p were similar in both wild-type and *neo1-37* cells, 100% and 109% respectively, while in *neo1-69* cells only 53% of GFP-Dop1p was present. After 1 hour shift to 37ºC it is observed a further reduction of the signal to 30% in *neo1-69* cells

compared to 81% and 73% in wild-type and neo1-37 cells, respectively. In conclusion, these results show that GFP-Dop1p is reduced in the *neo1-69* mutant but not in the *neo1-37* mutant.

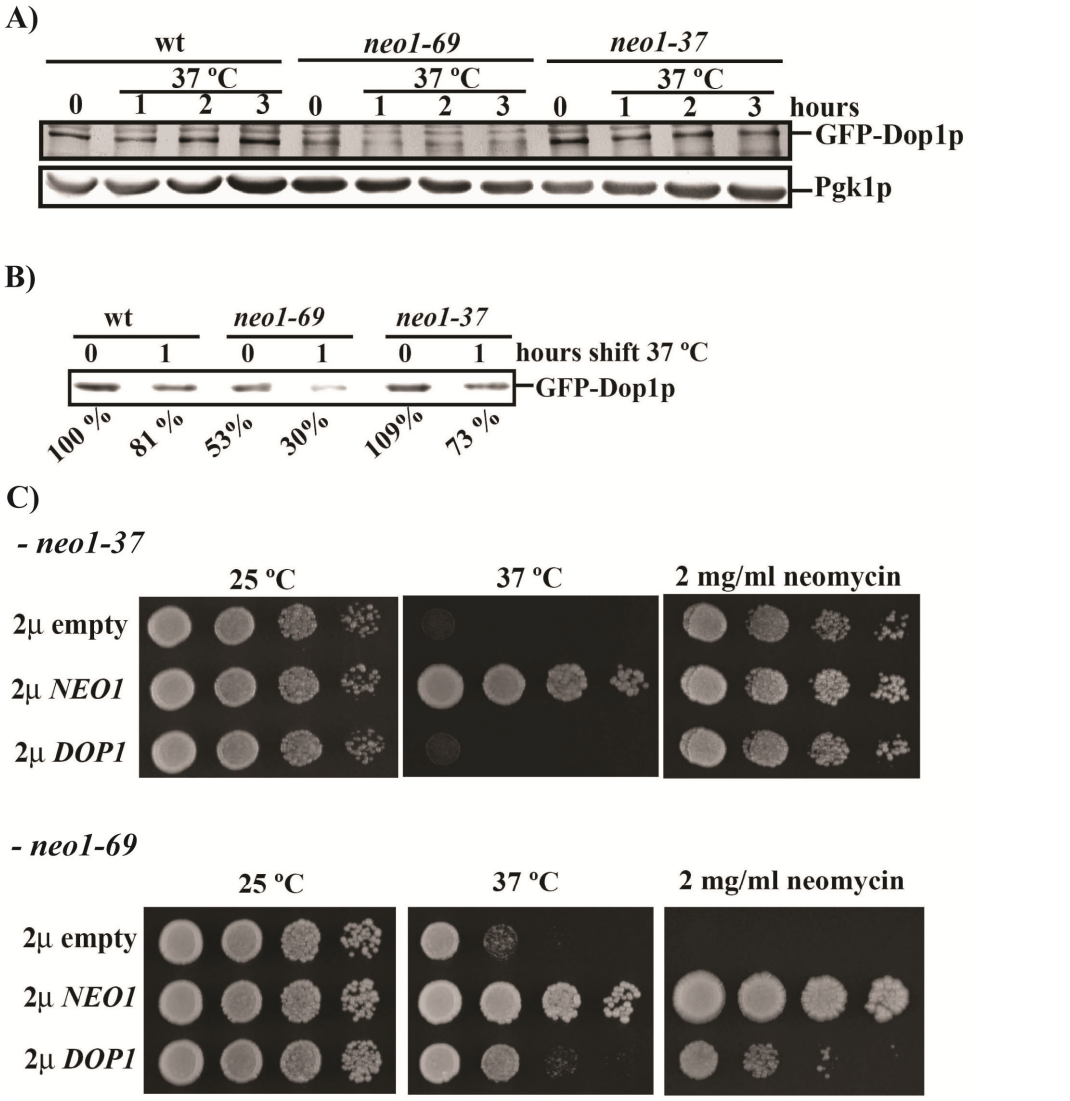

Figure 3.6: GFP-Dop1p steady state levels are decreased in *neo1-69* cells and *DOP1* overexpression suppresses the growth defects of the *neo1-69* cells. A) SB284 (wt), SB286 (*neo1-37*) and SB289 (*neo1-69*) cells were grown at 25ºC and shifted for up to 3 hours at 37ºC. Similar amounts of cells were collected at the indicated time points and the cell lysates were analysed by Western blotting using the α-GFP or α-Pgk1 as primary antibodies (table 2-3) and α-rabbit or α-mouse AP conjugated (table 2-4) as secondary antibodies. B) GFP-Dop1p was immunoprecipitated from total cell lysates treated with 0.5% NP40 from 50 OD_{600} units of SB284 (wt), SB286 (*neo1-37*) and SB289 (*neo1-69*) cells grown at 25ºC or upon 1 hour shift to 37ºC. After immunoblotting, the GFP-Dop1p signal was scanned using the Odyssey Infrared Imaging System and quantified with the Odyssey software (LI-COR Biosciences). The values were calculated from 3 independent experiments. C) Both *neo1-37* (BS915) (upper panel) and *neo1-69* (BS917) (lower panel) cells were transformed with the indicated plasmids. Comparable amounts of cells were diluted in series and spotted onto YPD plates or YPD + 2 mg/ml neomycin and incubated at the indicated temperatures or at 25ºC to test the neomycin hypersensitivity for up to 3 days.

Furthermore, the hypothesis that *DOP1* is a multicopy suppressor of the growth defects of the *neo1-69* mutant was here investigated. Both *neo1-37* and *neo1-69* mutants are temperature sensitive, they grow well at 25ºC but have growth defect at 37ºC (Wicky *et al.* 2004). Additionally, the *neo1-69* but not the *neo1-37* mutant is hypersensitive to neomycin sulphate (B. Singer-krüger, unpublished results). Obviously, overexpression of *NEO1* could suppress the growth defects of both mutants, indicating that they are a consequence of the Neo1p mutations (Figure 3.6, C). Importantly, *DOP1* overexpression was able to partially suppress the growth defect at 37ºC and the neomycin hypersensitivity of the *neo1-69* mutant (Figure 3.6, C), but not the growth defect at 37ºC of *neo1-37* mutant. Hence, these data support the previous results in which Dop1p levels were found to be significantly reduced in the *neo1-69* but not in *neo1-37* mutant.

3.3.3 GFP-Dop1p and HA-Neo1p levels are reduced in *Δysl2* cells, but they can be restored by overexpression of *ARL1*, *DOP1* and *NEO1*

The co-dependency between Dop1p and Neo1p and the dependence of Ysl2p on both Dop1p and Neo1p led to the examination of the levels of both Dop1p and Neo1p in *Δysl2* cells. *Δysl2* cells grow extremely slow at permissive temperature and are temperature sensitive (Jochum *et al.* 2002). However, a normal growth rate in these cells can be restored by overexpression of *ARL1*, *NEO1* or *DOP1* (Jochum *et al.* 2002; Wicky *et al.* 2004; Efe *et al.* 2005). To determine the levels of Neo1p and Dop1p in *Δysl2* cells, two homozygous diploid strains deleted for *YSL2* and expressing either HA-Neo1p (SB340) or GFP-Dop1p (SB434) from the chromosome were generated. Both strains were transformed with multicopy plasmids containing either *ARL1*, *NEO1*, *YSL2* or *DOP1*, known to be capable of suppressing the growth defect of *Δysl2* cells. Simultaneously, they were also transformed with an empty plasmid and with a multicopy plasmid containing *DRS2*. After overnight growth of the transformed SB340 (homozygous *Δysl2 3-HA-NEO1*) and SB434 (homozygous *Δysl2 GFP-DOP1*) cells at 25ºC, comparable amounts of cells were collected from each transformant, cells were lysed and the levels of the proteins were monitored by Western blotting (figure 3.7, A and C). As observed in the figure 3.7 (A), the HA-Neo1p levels were clearly reduced in *Δysl2* cells (containing empty plasmid) and its levels could be restored to the wild-type

levels (*Δysl2* cells containing *YSL2* in a plasmid) by addition of one of the multicopy suppressors of *Δysl2* cells (*ARL1*, *DOP1* or *NEO1*) but not by addition of *DRS2*. Quantification of the signals by quantitative Western blotting showed that HA-Neo1p is reduced in approximately 70% of its wild-type values (100%) in *Δysl2* cells (35%). Interestingly, suppression of *Δysl2* cells by *ARL1*, *DOP1* or *NEO1* was able to completely restore the HA-Neo1p levels to those of the wild-type cells (figure 3.7, B).

As observed in the Figure 3.7 (C), the GFP-Dop1p steady state levels are also substantially reduced in *Δysl2* cells and similarly to the HA-Neo1p case, its levels can be restored to the wild-type levels by addition of *ARL1*, *DOP1* or *NEO1* to *Δysl2* cells. Immunoprecipitation of GFP-Dop1p from each transformant and analysis by quantitative Western blotting (Figure 3.7, D) showed that the steady state levels of GFP-Dop1p are 90 % reduced in *Δysl2* cells (containing a empty plasmid) compared to the wild-type values (*Δysl2* cells containing *YSL2* in a plasmid). Once more, addition of one of the multicopy suppressors of *Δysl2* cells raised the values of GFP-Dop1p near to the wild-type values.

In conclusion, Dop1p, Neo1p and Ysl2p are interdependent. Moreover, suppression of the growth defect of *Δysl2* cells by *ARL1*, *DOP1* or *NEO1* is likely explained by the finding that overexpression of these proteins restores the levels of both Dop1p and Neo1p to the wild-type levels in *Δysl2* cells.

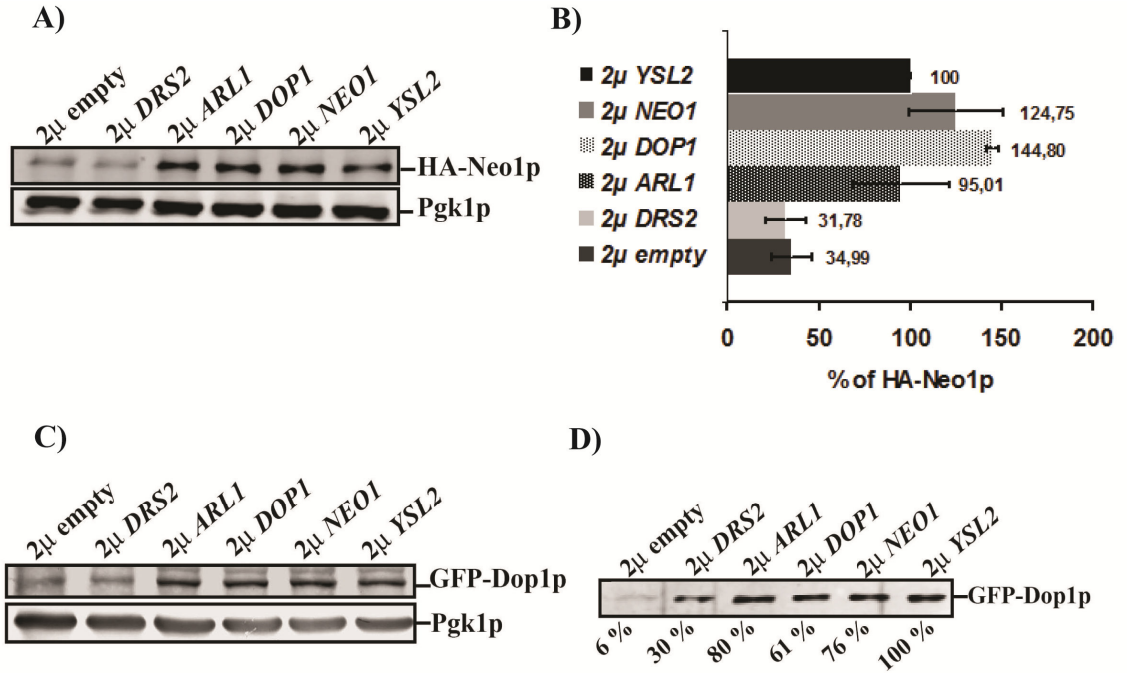

Figure 3.7: HA-Neo1p and GFP-Dop1p steady state levels are reduced in *Δysl2* cells. A) SB340 cells (homozygous *Δysl2 HA-NEO1*) were transformed with the indicated plasmids. After overnight grow at 25ºC similar amounts of cells were collected and an equal volume of cell lysates from each sample were analysed by Western blotting using the α-HA or α-Pgk1 as primary antibodies (table 2-3) and α-mouse IRdye800 (table 2-5) as secondary antibody. B) The HA-Neo1p signals were scanned using the Odyssey Infrared Imaging System and quantified with the Odyssey software (LI-COR Biosciences). Percentages were calculated from 3 independent experiments. The signal intensity of HA-Neo1p in *Δysl2* cells suppressed by overexpression of *YSL2* was set at 100 % and the others values calculated in function of this one. C) SB434 cells (homozygous *Δysl2 GFP-DOP1*) were transformed with the indicated plasmids and the cell lysates were analysed by Western blotting using the α-GFP or α-Pgk1 as primary antibodies (table 2-3) and α-rabbit or α-mouse AP conjugated (table 2-4) as secondary antibodies. D) GFP-Dop1p was immunoprecipitated from total cell lysates treated with 0.5% NP40 from 25 OD_{600} units of SB343 cells transformed with the indicated plasmids. After immunoblot the GFP-Dop1p signal was scanned and quantified as described in B. Percentages were calculated after setting the signal intensity of GFP-Dop1p in *Δysl2* cells suppressed by overexpression of *YSL2* to 100 %.

3.4 Pulse-chase analysis of HA-Neo1p in *dop1-3* cells

To assess whether the decrease of HA-Neo1p steady state levels in *dop1-3* cells was due to a destabilisation of the protein, pulse-chase analysis of HA-Neo1p in *dop1-3* (BS1361) and wild-type (BS188) cells were performed. Wild-type (BS188) and *dop1-3* (BS1361) cells were transformed with a plasmid containing encoded HA-Neo1p (pRS316-HA-NEO1). After overnight grow in SD media the proteins were then pulse-labelled for 30 minutes with radioactive methionine (^{35}S-Met) at permissive temperature, to mark all the newly synthesised proteins. Then, to stop the incorporation, an excess of non-radioactive methionine was added and the cells were chased at non permissive temperature for up to 3 hours. Samples were collected at several time points,

and HA-Neo1p was immunoprecipitated under denaturing conditions. SDS-PAGE was performed with equal amounts of immunoprecipitated samples and the radioactive HA-Neo1p was detected by autoradiography. As observed in the graphic of the figure 3.8, the half life of HA-Neo1p at 37ºC in *dop1-3* cells is of 100 min while in wild-type cells HA-Neo1p has a half life of 193 min. Thus, the half life of HA-Neo1p in *dop1-3* cells is 50% reduced to that of wild-type cells, indicating that HA-Neo1p is destabilised in *dop1-3* cells.

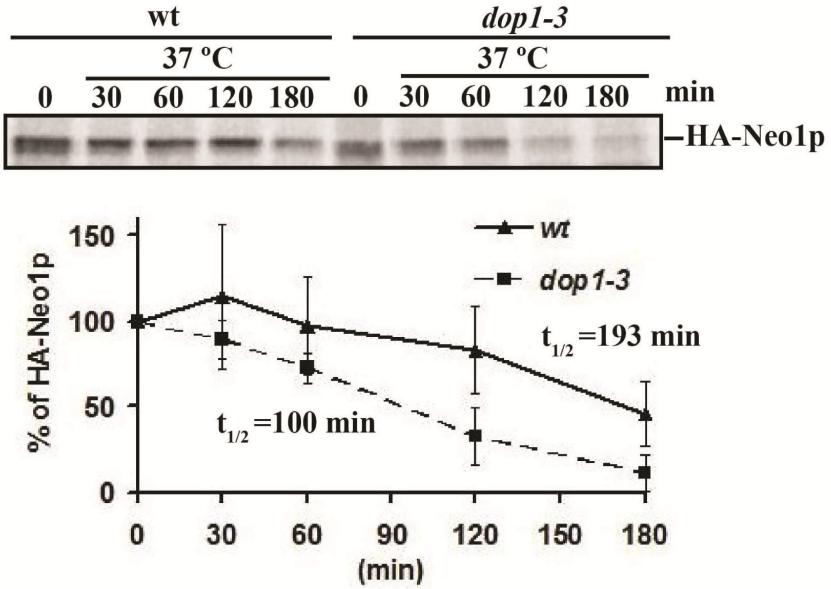

Figure 3.8: HA-Neo1p is destabilised in *dop1-3* cells. Cells SB216 (BS1361 + pRS316-HA-NEO1) and SB220 (BS188 + pRS316-HA-NEO1) were grown overnight at 25ºC and pulse-labelled for 30 minutes with radioactive methionine (^{35}S-Met) at 25ºC. Then, an excess of non-radioactive methionine was added and the cells were chased at 37ºC for up to 3 hours. Samples of 1 OD_{600} cells were taken at the indicated time points and HA-Neo1p was immunoprecipitated under denaturing conditions using rat α-HA antibody (table 2-6). For each time point equal amounts of immunoprecipitated were run in a SDS-PAGE, the radioactive HA-Neo1p was quantified with the phosphoimager (see section 2.2.3.5) and the labelled HA-Neo1p was expressed as percentages of labelled protein at time point 0 (from 5 independent experiments). Bars represent the standard deviation.

3.5 Loss of HA-Neo1p in *dop1-3* cells is due to proteasomal degradation

Previously, two versions of Neo1p, namely Neo1-37p and Neo1p$^{\Delta Ctail}$, were found to be destabilized and retained within the ER compartment (Wicky *et al.* 2004). Hence, to address the question of whether in *dop1-3* cells HA-Neo1p was also retained in the ER, indirect immunofluorescence of HA-Neo1p was performed in wild-type and in *dop1-3* cells. Myc-Tlg1p, a Myc tagged endosomal t-SNARE, was simultaneously immunostained to serve as an internal control. In wild-type cells at permissive temperature, HA-Neo1p had a punctuated pattern throughout the cytoplasm that

persisted after shift for 1 or 2 hours to non-permissive temperature (figure 3.9). In *dop1-3* cells, the HA-Neo1p staining pattern at permissive temperature was similar to the one observed for the wild-type cells, however after shift for 1 or 2 hours at 37ºC the fluorescent signal for HA-Neo1p decreased (figure 3.9). Myc-Tlg1p staining in both strains at permissive and non-permissive temperature was unaffected and perfectly visible in scattered structures throughout the cytoplasm (figure 3.9), indicating that the loss of HA-Neo1p is specific and not due to secondary effects. Thus, these results corroborate the previous results in which the levels of Neo1p diminished in *dop1-3* cells (section 3.3.1). However, they did not reveal the place of HA-Neo1p degradation, maybe because in this mutant HA-Neo1p is rapidly degraded.

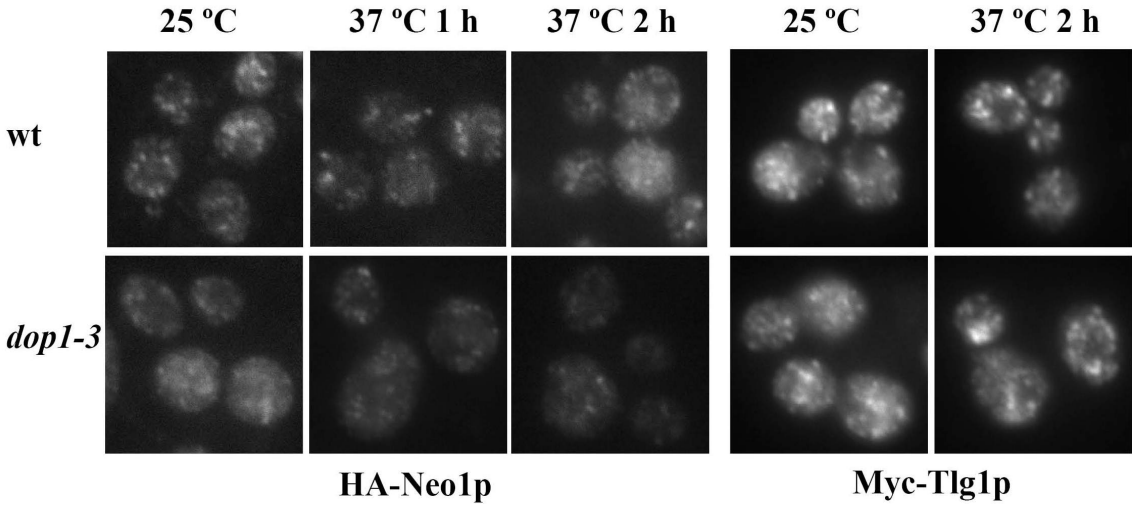

Figure 3.9: In *dop1-3* cells the HA-Neo1p fluorescence is lost, but not the Myc-Tlg1p fluorescence. Wild-type (BS1488) and *dop1-3* (SB142) cells were transformed with pRS316-Myc-Tlg1p (SB145 and SB149, respectively). After overnight growth in SD media cells were shifted to 37ºC for the indicated times. Indirect immunofluorescence of HA-Neo1p and Myc-Tlg1p was performed as described in 2.2.4.1.1.

Integral membrane proteins are intracellularly degraded by two main mechanisms, at the ER by the proteasome or at the vacuole via the multivesicular body pathway. Therefore, in order to determine whether in *dop1-3* cells HA-Neo1p was degraded in the vacuole, a mutant lacking the vacuolar protease Pep4p was used and the localisation of HA-Neo1p assessed in this mutant. A strain expressing HA-Neo1p from the chromosome where *PEP4* was deleted (SB228) was compared to isogenic strain additionally deleted for *DOP1* and expressing the *dop1-3* allele from a single copy plasmid (SB232). After overnight growth at permissive temperature the cells were either immediately fixed or additionally shifted for 2 hours to non-permissive temperature and then fixed. In the strain *Δpep4* at 25ºC or 37ºC, the immunostaining of HA-Neo1p reveals a cytoplasmic punctuated pattern similar to the one observed for the wild-type

strain (*PEP4*) (figure 3.10, A). In *Δpep4 dop1-3* cells at 25ºC, HA-Neo1p staining reveals a similar punctuated pattern, however, after shift at 37ºC for 2 hours the fluorescence of HA-Neo1p decreases (figure 3.10, A). Consistent with these results, the steady state levels of HA-Neo1p in *Δpep4* cells after shift to 37 ºC for up to 3 hours, do not significantly change along the shift while in similarly treated *Δpep4 dop1-3* cells they decrease (figure 3.10, B). Together, these data suggest that HA-Neo1p is not degraded in the vacuole in *dop1-3* cells, since deletion of *PEP4* in this mutant failed to accumulate HA-Neo1p.

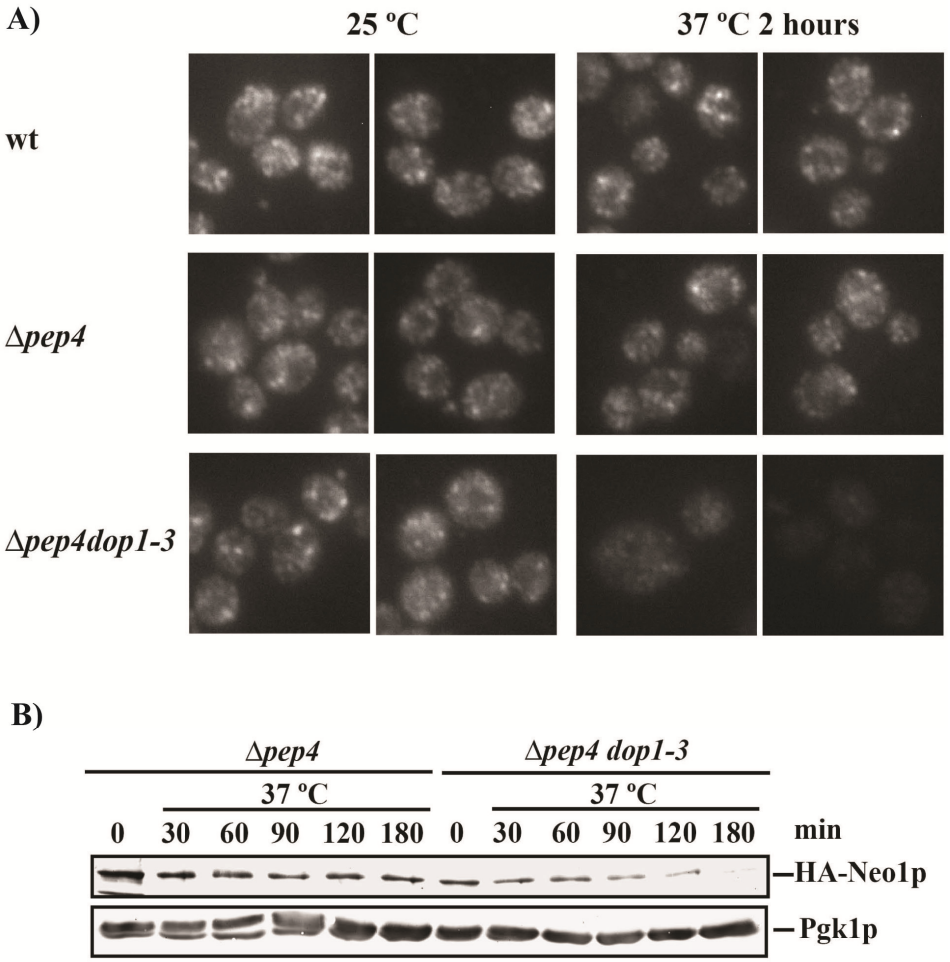

Figure 3.10: HA-Neo1p degradation in *dop1-3* does not require the vacuolar protease Pep4p. A) SB72 (wt), SB228 (*Δpep4*) and SB232 (*Δpep4 dop1-3*) cells were grown overnight at 25ºC and either immediately fixed or shifted for 2 hours at 37ºC and subsequently fixed as described in the section 2.2.4.1.1. After immunostain with the α-HA antibody (table 2-7), they were visualized under the fluorescence microscope. B) SB228 (*Δpep4*) and SB232 (*Δpep4 dop1-3*) cells were grown overnight at 25ºC and shifted for up to 3 hours at 37ºC. 1.7 OD_{600nm} units of cells were collected at the indicated time points and cell extracts analysed by Western blotting using the α-HA or α-Pgk1 as primary antibodies (table 2-3) and α-mouse AP conjugated (table 2-4) as a secondary antibody.

Since, HA-Neo1p in the *dop1-3* mutant is not degraded in the vacuole, the need of the proteasome for the degradation of HA-Neo1p was assessed in this mutant. For that, MG132, a potent inhibitor of the 26S proteasome was added to the cells and the levels of HA-Neo1p were monitored. However, in yeast cells this drug is not maintained inside the cells due to its efflux via Pdr5p, an ABC-tranporter that extrudes lipophilic compounds and is involved in multidrug resistance. Thus, *PDR5* was deleted in both wild-type and *dop1-3* cells, which expressed HA-Neo1p from the chromosome, to ensure an efficient accumulation of the drug inside the cells. First, to ensure that deletion of *PDR5* had no influence on the steady state levels of HA-Neo1p, the strains *Δpdr5* and *Δpdr5 dop1-3*, both expressing HA-Neo1p from the chromosome, were grown and shifted to 37ºC and the levels HA-Neo1p were monitored. As observed in the figure 3.11 (A), the *PDR5* deletion does not influence the steady state levels of HA-Neo1p neither in the wild-type nor in the *dop1-3* cells, since the results obtained in the absence of *PDR5* (figure 3.11, A) confirmed the previously reported when *PDR5* is present (see section 3.3.1). Thus, allowing the use of these strains in this study.

The requirement of the proteasome for the degradation of HA-Neo1p in *dop1-3* cells was assessed by comparing the levels of HA-Neo1p in the *Δpdr5 dop1-3* strain in presence or absence of MG132. Therefore, after overnight grow and before the shift to non-permissive temperature the cells were incubated for 30 min at 25ºC either with 60 μM of MG132 (in DMSO) or with the same volume of DMSO, to allow the drug to enter the cells. Then, they were shifted to 37ºC for 3 hours and both MG132 and DMSO were added every 30 min to ensure a continuous inhibition of the proteasome. As observed in the Western blot shown in the figure 3.11 (B), MG132-treated cells can partially retain HA-Neo1p which was previously lost in *dop1-3* cells. Thus, suggesting that the degradation of HA-Neo1p in *dop1-3* cells is dependent from the proteasome.

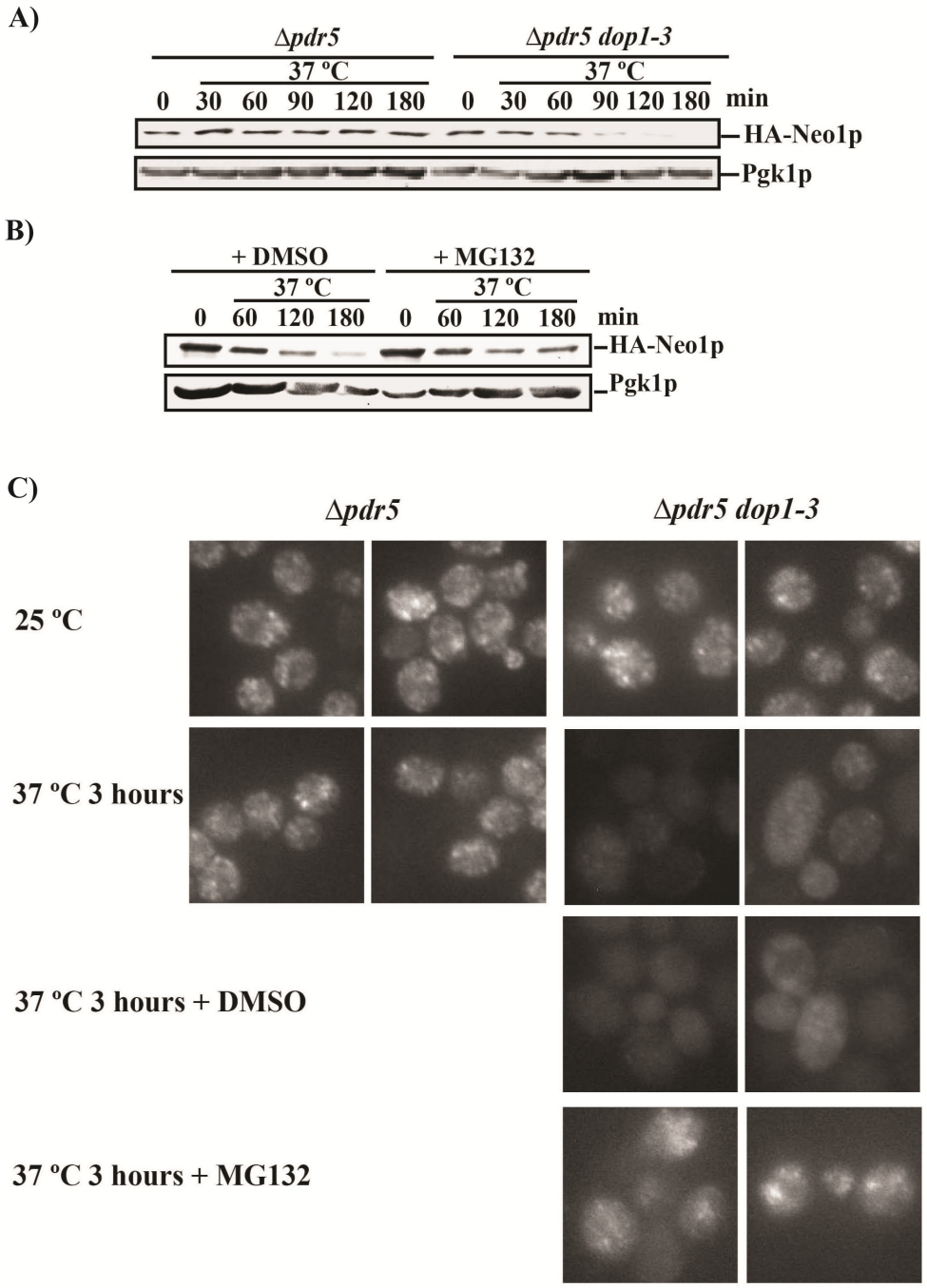

Figure 3.11: HA-Neo1p degradation in *dop1-3* cells is dependent on the proteasome. A) SB256 (*Δpdr5*) and SB258 (*Δpdr5 dop1-3*) cells were grown overnight at 25ºC and further shifted for up to 3 hours at 37 ºC. Similar amounts of cells were collected at the indicated time points and cell lysates were analysed by Western blotting using the α-HA or α-Pgk1 as primary antibodies (table 2-3) and α-mouse AP conjugated (table 2-4) as a secondary antibody. B) SB258 (*Δpdr5 dop1-3*) cells were grown overnight at 25 ºC. Prior to the shift at 37ºC they were incubated for 30 min with either 60 μM of MG132 (in DMSO) or the same volume of DMSO. Cells were shifted to 37ºC (60 μM of MG132 and the corresponding volume of DMSO were added every 30 min) and at each time point the cell extracts were analysed as describe above. C) SB256 (*Δpdr5*) and SB258 (*Δpdr5 dop1-3*) cells were treated as described in B. Cells collected at the indicated conditions were fixed and immunostained using the α-HA antibody as described in 2.2.4.1.1.

In order to assess the place of degradation of HA-Neo1p in *dop1-3* cells, the strain above described was treated similarly and after the 3 hours shift to 37ºC the cells were fixed and immunostained using the α-HA antibody (see section 2.2.4.1.1). Simultaneously, non-treated *Δpdr5* and *Δpdr5 dop1-3* cells expressing HA-Neo1p from the chromosome were also analysed. The scattered pattern obtained for the HA-Neo1p staining in *Δpdr5* cells at 25ºC was unaffected after 3 hours shift to 37ºC, while in *Δpdr5 dop1-3* cells this staining pattern observed at 25ºC was lost after shift to 37ºC (figure 3.11, C). A similar result was obtained in *Δpdr5 dop1-3* cells treated with DMSO and shifted for 3 hours at 37ºC. Conversely, in MG132-treated cells the HA-Neo1p staining was is still visible in some cells after the 3 hours shift at 37 ºC (figure 3.11, C). Together, these support the previous results obtained by Western blot (figure 3.11, B) in which HA-Neo1p was partially retained in MG132-treated cells. However, regarding the place of HA-Neo1p degradation in *dop1-3* cells, the staining of HA-Neo1p in *Δpdr5 dop1-3* cells treated with MG132, did not reveal any clear pattern maybe due to an interference of DMSO with the procedure. Thus, the place of degradation of HA-Neo1p in *dop1-3* cells remains undisclosed.

3.6 Studies on the localisation of Dop1p

3.6.1 Dop1p is localised to the endosomal compartment

Previously Dop1p localisation was restricted to the late Golgi compartment (Gillingham *et al.* 2006). Both Neo1p and Ysl2p localise to the Golgi and endosomal compartments (Jochum *et al.* 2002; Wicky *et al.* 2004; Efe *et al.* 2005). Since, Dop1p interacts with Neo1p and Ysl2p it was examined whether Dop1p also localises to the endosomal compartment. To assess the localisation of Dop1p, the *DOP1* ORF was cloned in a single copy plasmid in frame with the *GFP* ORF under the control of the *ADH1* promoter (pRS315-P_{ADH1}-GFP-DOP1). This plasmid was transformed into SB356, a *Δdop1* strain bearing a URA-based single copy plasmid containing *DOP1* (pRS316-DOP1). After transformation, the transformants were counter-selected onto 5-FOA plates for the pRS316-DOP1 plasmid, leaving pRS315-P_{ADH1}-GFP-DOP1 as the only *DOP1* copy (SB375). Cells expressing Dop1p N-terminally tagged with GFP grew well at all tested temperatures indicating that GFP-Dop1p is functional. The GFP-Dop1p localisation was assessed by fluorescence microscopy. Consistent with the previously

reported localisation data (Gillingham *et al.* 2006), the GFP-Dop1p fluorescence revealed a scattered pattern throughout the cytoplasm, typical of a Golgi and endosomal localisation (figure 3.12, A). To determine whether Dop1p also localises to the endosomes, two independent approaches were used. First, GFP-Dop1p was localised in a class E *vps* mutant, *vps27*, in which the endosomal class E compartment collapses forming an abnormal enlarged structure in the vicinity of the vacuole (Piper *et al.* 1995). In this approach, pRS315-P_{ADH1}-GFP-DOP1 was transformed either in wild-type (BS64) or in *vps27* cells and the GFP-Dop1p localisation was assessed as described above. In wild-type (BS64) transformants, the GFP-Dop1p fluorescence revealed a punctuated pattern similar to the observed in the SB375 cells indicating that in the presence of the endogenous Dop1p, GFP-Dop1p is not mislocalised (figure 3.12, B). In the *vps27* mutant, GFP-Dop1p collapsed into one or few large structures (figure 3.12, B), resembling the previous phenomenon observed for Ysl2p and Neo1p (Jochum *et al.* 2002; Wicky *et al.* 2004). Quantification revealed that 31% of the *vps27* cells (n=238) exhibited large GFP-Dop1p structures reminiscent of the class E compartment opposed to only 1.8% of wild-type cells (n= 433).

Furthermore, GFP-Dop1p was colocalised with the endocytic tracer pheromone α-factor conjugated with the Alexa594 fluorophore (Toshima *et al.* 2006) into *Δypt51 MAT*a cells (BS25). In *Δypt51* cells, due to a defective endocytic delivery to the vacuole, cargo accumulates within the endosomal compartment (Singer-Krüger *et al.* 1995). For the co-localisation studies, *Δypt51* MATa cells (BS25) were transformed with pRS315-P_{ADH1}-GFP-DOP1, grown overnight until they reached early logarithmic phase and incubated on ice for 1 hour with Alexa594-conjugated pheromone α-factor to allow the binding of the pheromone to the plasma membrane of the cells (see section 2.2.4.1.3). Cells were washed to remove the unbounded α-factor and the internalisation was carried by incubation at 30ºC during 40 minutes. Immediately thereafter, the cells were observed under the fluorescence microscope using the Cy3 filter to visualise Alexa594-conjugated pheromone α-factor or the GFP filter to visualise GFP-Dop1p (figure 3.12, C). As observed in the figure 3.12 **(**C) GFP-Dop1p and Alexa594-conjugated pheromone α-factor frequently co-localised, as revealed by an orange/yellow colour in the overlaid image. Together, both results suggest that Dop1p is also localised at the endosomes.

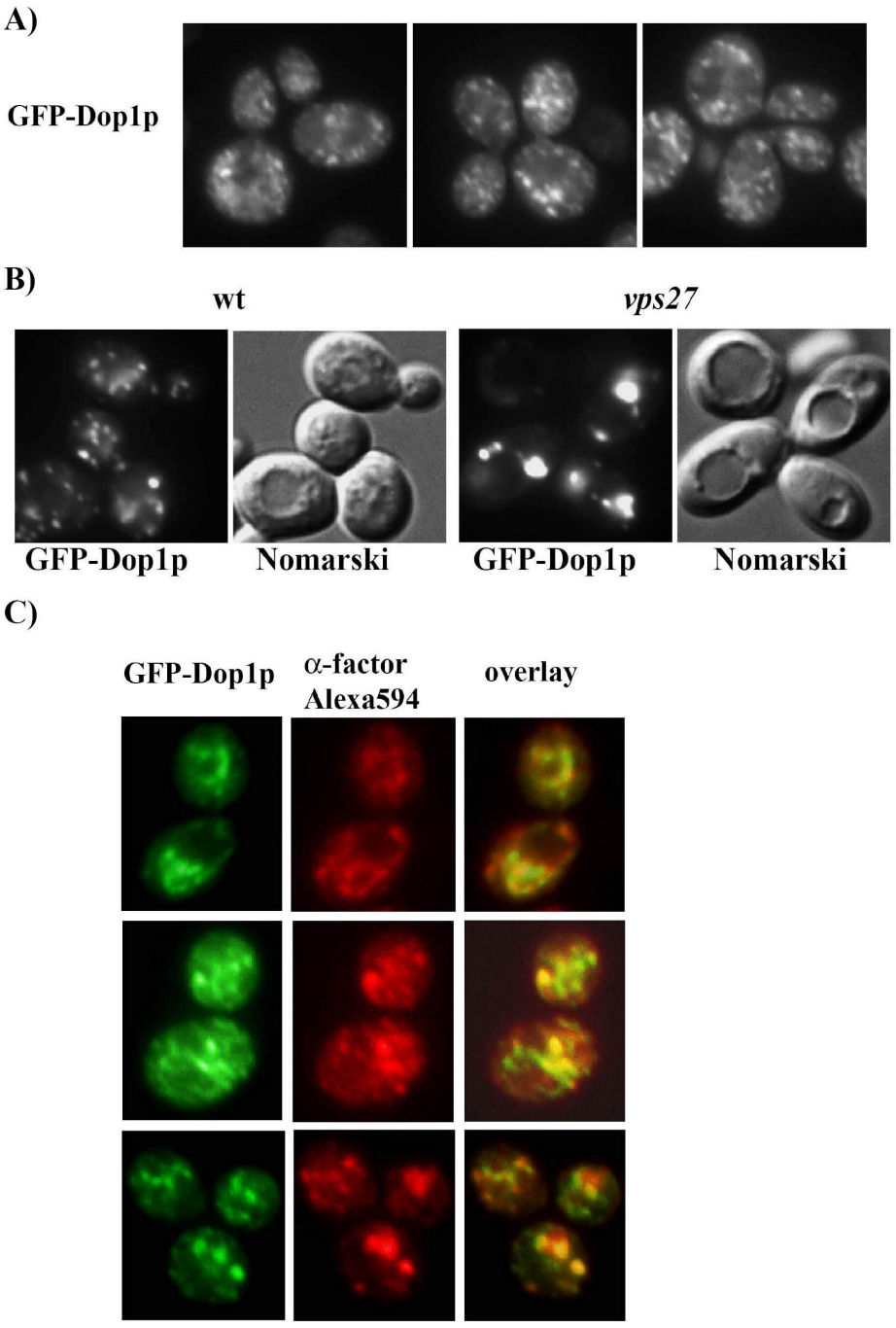

Figure 3.12: Dop1p is localised to the endosomal compartment. A) SB375 cells were grown overnight in SD media at 25ºC. They were collected by centrifugation, resuspended in IF buffer, mounted in a microscope slide with 1.6% of low melting agarose and observed under the fluorescence microscope using the EGFP filter (see section 2.2.4.1.2). B) SB391 (BS64 + pRS315-P_{ADH1}-GFP-DOP1) and SB393 (*vps27* + pRS315-P_{ADH1}-GFP-DOP1) cells were grown overnight in SD media at 25 ºC. Cells were prepared as described above and observed under the fluorescence microscope using the EGFP filter. C) BS25 (*Δypt51*) cells were transformed with pRS315-P_{ADH1}-GFP-DOP1 (SB417), grown overnight in SD media until early logarithmic phase. Cells were collected and incubated with Alexa594-conjugated α-factor for 1 hour in ice. After washing to remove unbounded α-factor, the cells were chased for 40 min at 30 ºC to allow the trafficking of the α-factor until the endosomes (see section 2.2.4.1.3.) Subsequently, cells were immediately placed on a microscope slide as describe above and observed under the microscope using the EGFP filter for visualisation of GFP-Dop1p and the Cy3 filter for visualisation of the Alexa594-conjugated α-factor. The images overlays were performed using the Adobe Photoshop software.

3.6.2 Localisation of Dop1p in the *Δysl2* mutant

The existent physical interaction between Dop1p, Neo1p and Ysl2p and their interdependence strongly hint for an interconnected function of these proteins in the cell. The Neo1p-Ysl2p-Arl1p network has recently been implicated in the recruitment of coat components at the *trans*-Golgi and endosomal compartments (Singer-Krüger *et al.* 2008). In this same study, it is shown that in *Δysl2* cells Gga2p losses its punctuated pattern seen in wild-type cells however, no changes in the levels of protein were observed between the wild-type and the *Δysl2* cells. Moreover, Ysl2p was shown to be implicated in the recruitment of Gga2p to the membranes (Singer-Krüger *et al.* 2008). In a distinct study, Dop1p recruitment to the TGN membranes was proposed to be dependent on Ysl2p (Gillingham *et al.* 2006). Since in the present study, it is shown that the presence of Ysl2p is not necessary for the interaction between Dop1p and Neo1p (section 3.2.2), but rather required to maintain the levels of both proteins (section 3.3.3), the hypothesis that Dop1p may not be mislocalised in *Δysl2* cells was tested. Therefore, wild-type (RH1201) and *Δysl2* (BS746) cells were transformed with pRS315-P_{ADH1}-GFP-DOP1 and the GFP-Dop1p localisation was assessed by fluorescence microscopy. GFP-Dop1p fluorescence in wild-type strain revealed the usual scattered pattern throughout the cytoplasm (figure 3.13, A). In *Δysl2* cells the staining pattern of GFP-Dop1p was also composed of several dotted structures but of considerably weaker intensity (figure 3.13, A), supporting the previous results in which the GFP-Dop1p levels were shown to be reduced in *Δysl2* cells (section 3.3.3).

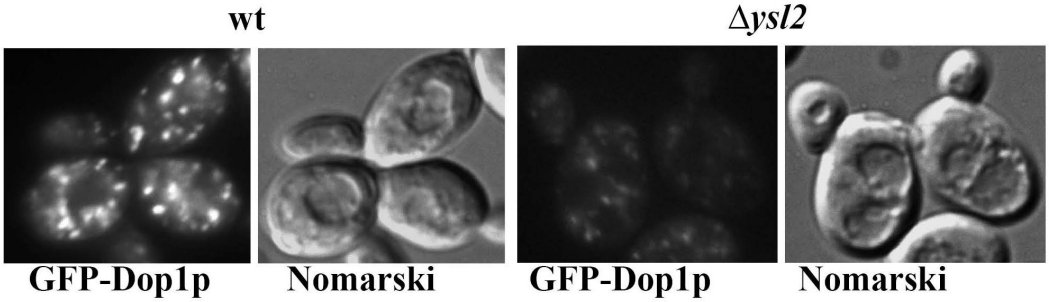

Figure 3.13: GFP-Dop1p localisation is affected by *YSL2* deletion. RH1201 and BS746 cells were transformed with pRS315-P_{ADH1}-GFP-Dop1p (SB387 and SB389, respectively) and grown overnight into SD media. Cells were collected, resuspended in IF buffer, mounted on a microscope slide with 1.6% of low melting agarose and observed under the fluorescence microscope using the EGFP filter.

3.7 Characterisation of Dop1p

3.7.1 Dop1p self-interacts

Protein sequence analysis of several Dop1p orthologues suggested the presence of leucine zipper-like repeats at the C-terminus of these proteins (Pascon and Miller 2000). The leucine zipper motif is a sequence of leucine residues or other accepted hydrophobic amino acid spaced every seven residues along an alpha-helix. According to the zipper model, the leucine side chains are able to interlock with leucine side chains of another polypeptide which contains the same motif (Landschulz *et al.* 1988). Thus, the protein molecules containing this motif might interact to form homo or heterodimers. In the *S. cerevisiae* Dop1p, two to three leucine zippers-like repeats were predicted, one located between the residues 1502 and 1530, another between the residues 1529 and 1550 and the last one between the residues 1568 and 1596 suggesting that this protein might dimerise. As an initial approach to assess this hypothesis, two distinct chromosomally expressed versions of this protein, Dop1p-TAP and GFP-Dop1p, were combined in a same strain (SB303). After isolation of Dop1p-TAP complexes, these were analysed for the presence of GFP-Dop1p. As a negative control a diploid strain containing a single genomic copy of GFP-Dop1p was used (SB262). Isolation of Dop1p-TAP efficiently co-isolated GFP-Dop1p (figure 3.14, lane 4). This co-isolation was specific since no GFP-Dop1p could be detected in the negative control where no Dop1p is isolated via TAP (figure 3.14, lane 3). This result suggests that Dop1p interacts with itself *in vivo*. However, whether this interaction is direct or mediated by other proteins is still a question.

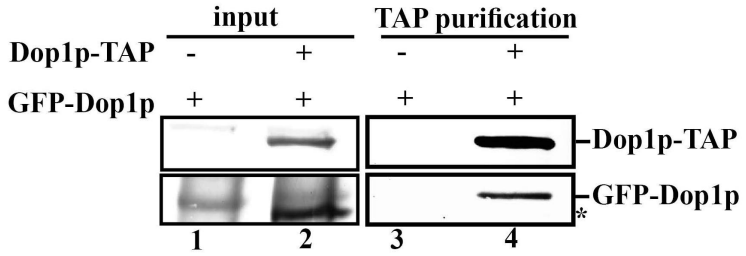

Figure 3.14: Dop1p interacts with itself. Dop1p-TAP complexes were isolated from total cell lysates from 50 $O.D_{600}$ of SB262 (lanes 1 and 3) or SB303 (lanes 2 and 4) cells, treated with 0.5% NP40. After cleavage with the TEV protease the Dop1p-TAP protein assemblies were isolated. About 50% of the isolated proteins (lanes 3 and 4) and 5% of the cell lysate (lanes 1and 2) were analysed by western-blotting using the α-TAP (to detect Dop1-TAP) or α-GFP (to detect GFP-Dop1) antibodies (table 2-3). * Dop1p-TAP detected by the rabbit α-GFP antibody.

3.7.2 Localisation studies for the different GFP-fused regions of Dop1p

In a previous work, the alignment of several protein sequences from the Dop1p orthologues revealed some conserved regions (Pascon and Miller 2000). The members of this family have a conserved N-terminal region (Dopey domain) that contains a putative tyrosine phosphorylation site and at their C-terminus they contain Leucine zippers-like repeats. In Dop1p the conserved N-terminus is located between the residues 16 to 461 and the putative tyrosine phosphorylation site within the residues 93 and 100 of this domain. The three putative Leucine zipper motifs are located at the C-terminus between the residues 1502 and 1596 (figure 3.15, A; and section 3.7.1). The internal region of these proteins has a weak homology between the orthologues. Despite the identification of these regions present in the Dop1p family members, their function remains completely elusive.

Herein to assess the subcellular localisation of the different regions of Dop1p, these were fused to GFP and expressed under the control of the constitutive *ADH1* promoter. In the figure 3.15 (A) the different expressed regions of Dop1p are represented. To analyse whether these regions were functional by themselves, SB356 cells (*Δdop1* + pRS316-DOP1) were transformed with each of the plasmids encoding a different region of Dop1p fused to GFP (pRS315-P_{ADH1}-GFP-N-term, pRS315-P_{ADH1}-GFP-internal and pRS315-P_{ADH1}-GFP-Cterm) and with the plasmid encoding the wild-type Dop1p fused N-terminally with GFP (pRS315-P_{ADH1}-GFP-DOP1) to serve as a control. Then, the SB356 transformants were counterselected onto 5-FOA plates for the loss of the pRS316-*DOP1*. As illustrated in the figure 3.15 (B), none of these Dop1p domains is able to rescue the lethality of *Δdop1* cells, although this lethality is well rescued by the plasmid encoding the wild-type protein fused to GFP. Together, this indicates that none of these domains of Dop1p alone accounts for the Dop1p function.

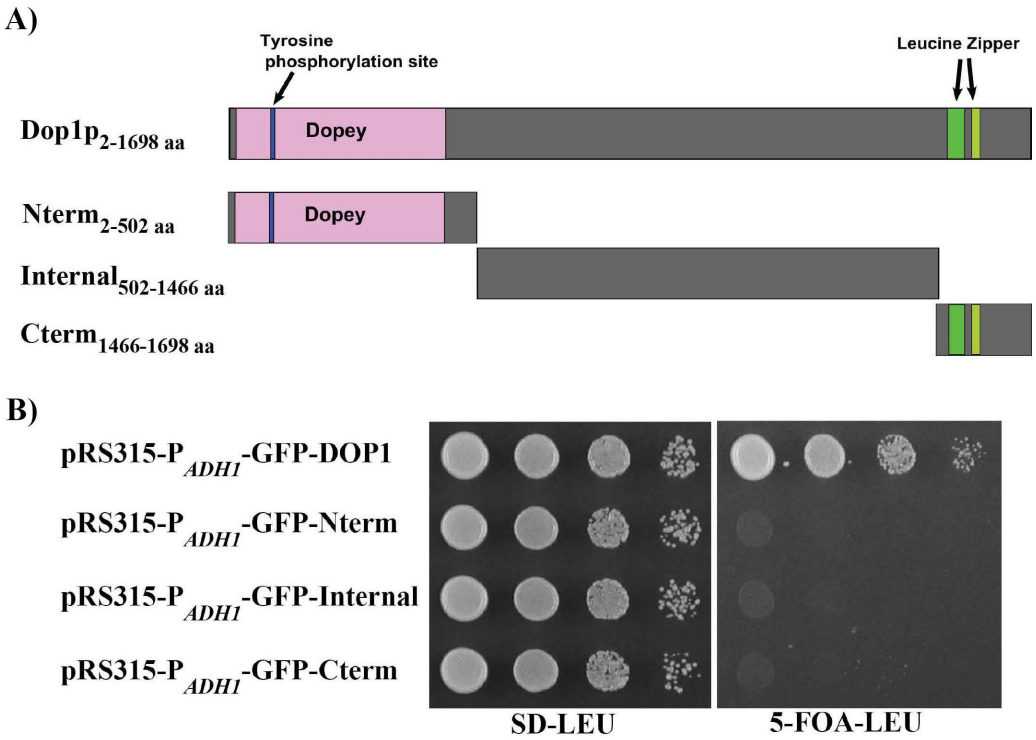

Figure 3.15: The division of Dop1p into three region and demonstration that none of these regions is able to rescue the lethality of *Δdop1* cells. A) Diagram showing the different expressed regions of Dop1p. The location of the identified Dop1p domains is based on the description of Pascon and Miller 2000. B) SB356 (*Δdop1* + pRS316-DOP1) cells were transformed with the indicated plasmids and selected in SD media without leucine. The obtained transformants were then transferred to plates containing 5-FOA and lacking leucine to counterselect for the pRS316-DOP1 plasmid.

The localisation of the three regions of Dop1p was assessed by fluorescence microscopy in transformed SB201 cells. Each of the expressed regions of Dop1p displayed a different subcellular localisation (figure 3.16). As previously observed, the GFP-Dop1p pattern was composed of several cytoplasmic dotted structures. Here, the GFP-Nterm construct showed a diffused pattern with some occasional dotted structures in most of the cells and in some of cells no fluorescence was observed. The internal part of Dop1p showed a scattered pattern in the majority of the cells, similar to that observed for the wild-type protein (77% versus 100% for the wild-type protein) however, in some cells (23% versus 0 % for the wild-type protein) an accumulation of this region in large structures which localised in the vicinity of the vacuole was also observed. Interestingly, the C-terminus of Dop1p had a completely different pattern, the dotted structures observed were concentrated at a particular region of the cell indicating that this domain may localise in a different compartment. Thus, since the different regions of Dop1p have distinct staining patterns they might contribute to different protein-protein interactions and thereby be involved in different functions within the cell.

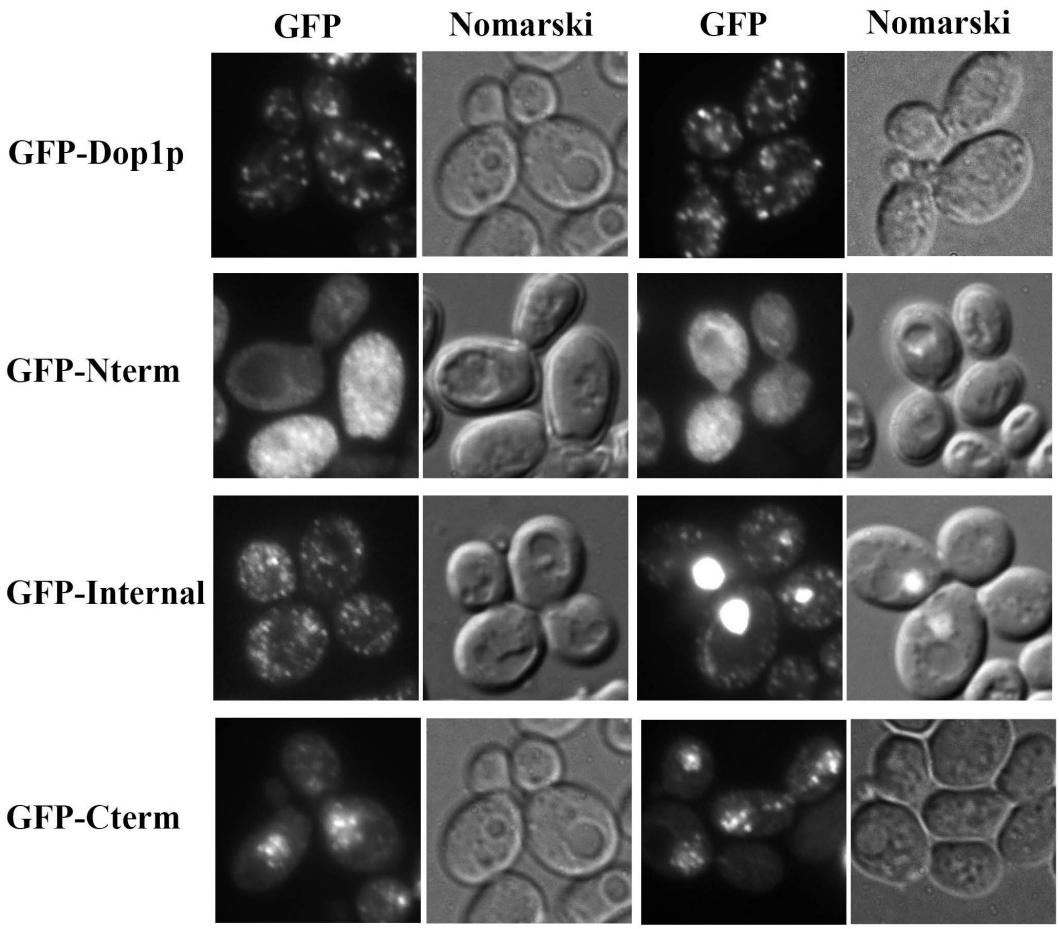

Figure 3.16: Localisation of the different GFP fused regions of Dop1p. SB201 (*Δneo1* + pRS315-NEO1) cells were transformed with the plasmids expressing the indicated constructions (SB385- pRS315-P_{ADH1}-GFP-DOP1; SB407- pRS315-P_{ADH1}-GFP-Dopey; SB415- pRS315-P_{ADH1}-GFP-Internal; SB398- pRS315-P_{ADH1}-GFP-Cterminus) grown overnight in SD media until early logarithmic phase. Cells were collected, resuspended in IF buffer, mounted on a microscope slide with 1.6% of low melting agarose and observed under the fluorescence microscope using the EGFP filter.

The fluorescent pattern observed for the C-terminus of Dop1p is reminiscent of the staining observed for some proteins localised within the nucleus. Thus, cells expressing GFP-Cterm domain were co-stained with the nuclear dye Hoechst 33342, which binds to DNA. After overnight growth the cells expressing GFP-Cterm were collected by centrifugation, resuspended in 1 ml of PBS buffer and incubated with Hoechst 33342 for 30 min at 30 ºC (see section 2.2.4.1.4). Subsequently, they were concentrated by centrifugation, resuspended in IF buffer and observed under the fluorescence microscope using the EGFP filter to visualise the GFP signal and the DAPI filter to visualise the Hoechst 33342 staining. Indeed, the majority of the GFP fluorescent signal observed for the Cterm of Dop1p co-localised with the Hoechst 33342 tracer (figure 3.17). However, occasionally the fluorescent signal for the GFP-Cterm was observed in distinct punctua that was not stained with Hoechst 33342 (figure 3.17).

Thus it is likely that the Cterm of Dop1p goes to the nucleus, but the reason for this nuclear localisation is still not known.

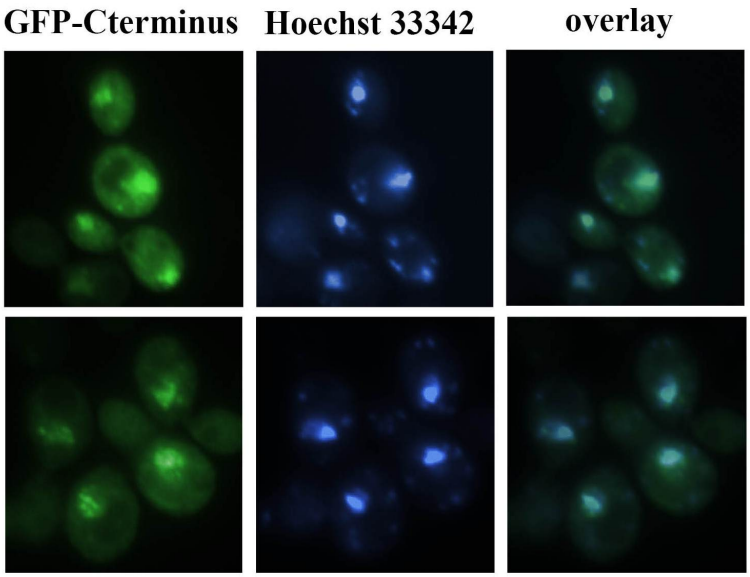

Figure 3.17: Co-staining of the Cterm of Dop1p with the nuclear stain Hoechst 33342. SB201 cells transformed with pRS315-P_{ADH1}-GFP-Cterm (SB398) were grown overnight in SD media. The cells were collected, resuspended in 1 ml of PBS and stained with Hoechst 33342 for 30 min at 30ºC (see section 2.2.4.1.4). Thereafter, the cells were concentrated in IF buffer, mounted on a microscope slide with 1.6% of low melting agarose and observed under the fluorescence microscope using the EGFP filter for visualisation of the GFP-Cterm and the DAPI filter for visualisation of the DNA stained with Hoechst 33342. The images overlays were performed using the Adobe Photoshop software.

Since the Cterm of Dop1p did not localise to the endosomes the requirement of this region for the essential function of Dop1p was addressed. Therefore, this region was removed from the Dop1p sequence (figure 3.18, A). SB356 (*Δdop1* + pRS316-DOP1) cells were transformed with the plasmid pRS315-P_{ADH1}-GFP-Dop1pΔCterm and then counterselect into 5-FOA plates to loose the pRS316-DOP1 plasmid. After streaking these cells onto 5-FOA plates, no growth was observed, indicating that Dop1pΔCterm cannot perform the essential function of Dop1p (data not shown). Thus, the C-terminus of Dop1p is necessary either to allow the correct folding of the protein or to exert an essential function in that protein.

To assess the localisation of GFP-Dop1pΔCterm, the plasmid pRS315-P_{ADH1}-GFP-Dop1pΔCterm was transformed into BS64 cells, grown overnight and the cells visualised under the fluorescence microscope using the GFP filter. SB391 cells (BS64 + pRS315-P_{ADH1}-GFP-DOP1) were treated similarly to serve as an internal control. The GFP-Dop1pΔCterm fluorescence was absent in the majority of the cells, with some cells showing an accumulation of the protein in large aggregates and others showing a

punctuated pattern (figure 3.18, B). Thus, the fact that most cells display no staining indicates that Dop1pΔCterm may not be stable; however the levels of this fusion will need to be considered to verify this hypothesis.

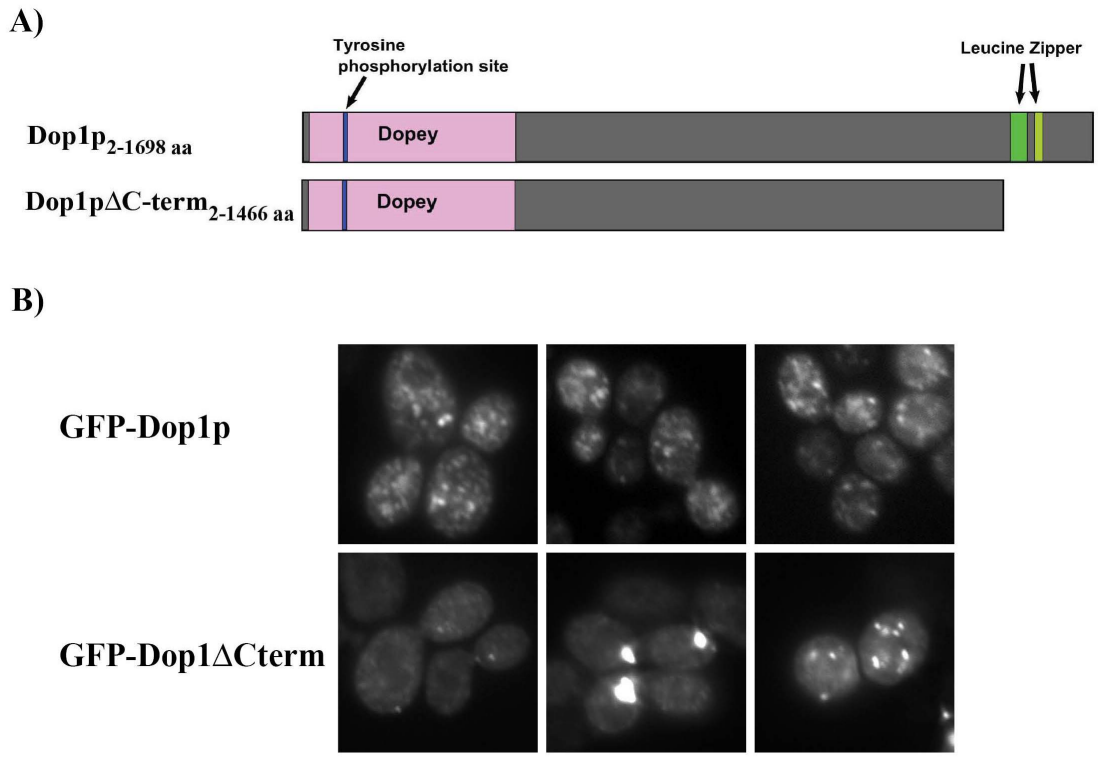

Figure 3.18: Localisation of GFP-Dop1ΔCterm. A) Diagram showing Dop1ΔCterm. The position of the distinct features of Dop1p is based on the description of Pascon and Miller 2000. B) BS64 cells were transformed with the plasmids expressing the indicated constructions (SB391- pRS315-P_{ADH1}-GFP-DOP1 SB437- pRS315-P_{ADH1}-GFP-Dop1ΔCterm) and were grown overnight in selective minimal media until early logarithmic phase. Cells were collected, resuspended in IF buffer, mounted on a microscope slide with 1.6 % of low melting agarose and observed under the fluorescence microscope using the GFP filter.

3.7.3 Interaction of the different GFP-fused regions of Dop1p with Neo1p and Ysl2p

The different localisation patterns obtained for the distinct regions of Dop1p may indicate that this protein may be involved in multiple interactions within the cell. Herein, the physical interactions of these distinct regions of Dop1p with Neo1p and Ysl2p were analysed. First, to determine which of the Dop1p regions mediate the interaction with Neo1p, the three distinct GFP fusions were expressed in a strain harbouring a plasmid encoding HA-Neo1p (SB201). Therefore, SB201 cells were transformed with the plasmids pRS315-P_{ADH1}-GFP-DOP1, pRS315-P_{ADH1}-GFP-Nterm, pRS315-P_{ADH1}-GFP-internal and pRS315-P_{ADH1}-GFP-Cterm and after growth, the expressed GFP-tagged proteins were immunoprecipitated from a 100,000 x g

supernatant of cell extracts prepared with 0.01% NP40 (see section 2.2.3.3.5). All the three Dop1p regions were able to co-immunoprecipitate HA-Neo1p (figure 3.19, A), however only the internal part of Dop1p could co-immunoprecipitate comparable amounts of HA-Neo1p to those obtained after immunoprecipitation of the full-length GFP-Dop1p (figure 3.19, A). However, the internal part of Dop1p seems to have more affinity for low electrophoretic mobility form of HA-Neo1p of yet unknown nature. The Nterm and the Cterm regions of Dop1p could only co-immunoprecipitate a minor fraction of HA-Neo1p (figure 3.19, A). Thus, together, these results suggest that the internal part of Dop1p might be responsible in mediating the interaction between Dop1p and Neo1p while the Nterm and Cterm regions might have a minor role in this interaction.

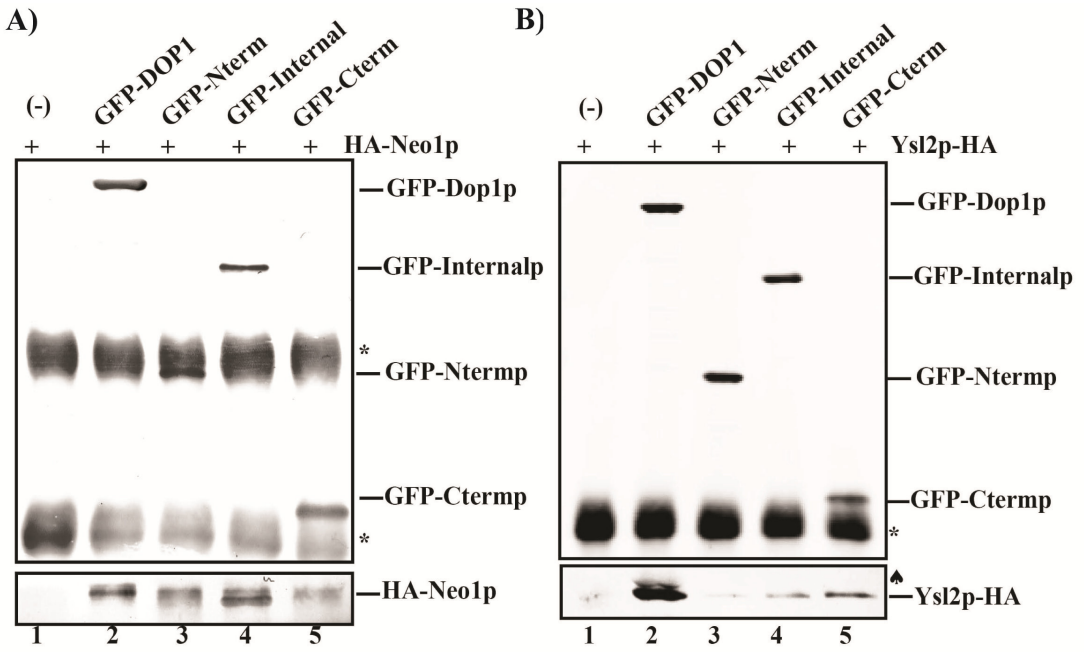

Figure 3.19: Interaction of the Nterm, internal and Cterm of Dop1p with HA-Neo1p and Ysl2p-HA. A) 100,000 x g supernatants from cell extracts of SB201 cells (lane 1) or SB201 cells transformed with the indicated GFP fusions [SB385- pRS315-P_{ADH1}-GFP-DOP1 (lane 2) SB407- pRS315-P_{ADH1}-GFP-Nterm (lane 3); SB415- pRS315-P_{ADH1}-GFP-internal (lane 4); SB398- pRS315-P_{ADH1}-GFP-Cterm (lane 5)], after extraction with 0.01% of NP40 were subjected to immunoprecipitation using the rabbit α-GFP antibody (table 2-6). About 25% of the immunoprecipitated was analysed by Western blotting for the presence of HA-Neo1p and 8% for the presence of the GFP fusion protein. B) Cell lysates of BS1121 alone (lane 1) or transformed with the indicated GFP fusion [SB426- pRS315-P_{ADH1}-GFP-DOP1 (lane 2) SB430- pRS315-P_{ADH1}-GFP-Nterm (lane 3); SB432- pRS315-P_{ADH1}-GFP-internal (lane 4); SB428- pRS315-P_{ADH1}-GFP-Cterm (lane 5)], after solubilisation with 0.5% NP40 were subjected to immunoprecipitation using the rabbit α-GFP antibody (table 2-6). About 25% of the immunoprecipitated was analysed by Western blotting for the presence of Ysl2p-HA and 8% for the GFP fusion protein. * heavy chain of the IgG detected by the α-GFP antibody. ♠ GFP-Dop1p detected by the α-HA antibody.

Similarly, to determine which of the Dop1p regions is involved in the interaction with Ysl2p, the distinct GFP-tagged Dop1p regions were expressed in a strain expressing Ysl2p-HA from the chromosome (BS1121). The expressed GFP-tagged proteins were immunoprecipitated from total cell extracts prepared in the presence of 0.5% NP40 (see section 2.2.3.3.5) and analysed for the co-isolation of Ysl2p-HA. Immunoprecipitation of each of the three Dop1p regions resulted in the co-isolation of Ysl2p-HA however these co-isolations were significantly less efficient than the one obtained with the full-length protein (GFP-Dop1p) (figure 3.19, B). The internal part and the Cterm of Dop1p were more efficient to co-isolated Ysl2p-HA, suggesting that the interaction between Dop1p and Ysl2p may be mediated by these regions of Dop1p (figure 3.19, B).

3.8 Analysis of the temperature sensitive *dop1-3* mutant

3.8.1 *dop1-3* cells display increased levels of CPY in the extracellular space

The interaction of Dop1p with Neo1p and Ysl2p and their interdependence strongly hint for a common function of these proteins. In previous studies it was shown that mutants from the Neo1p-Ysl2p-Arl1p network have defects in the transport of the Golgi modified p2 form of the vacuolar hydrolase carboxypeptidase Y (CPY) to the vacuole leading to its secretion (Jochum *et al.* 2002; Wicky *et al.* 2004). To assess whether the *dop1-3* mutant also has such defects, a quick method for detection of CPY in the extracellular media was applied. For that purpose, BS845 (wt-haploid), BS917 (*neo1-69*- mutant haploid), RH1201 (wt- diploid) and BS1806 (*dop1-3*- diploid) cells were spotted onto a YPD plate, a nitrocellulose membrane was placed over it and the cells were allowed to grow at 25ºC for up to 24-32 hours. The detection of the nitrocellulose membrane with an α-CPY antibody revealed that only the *neo1-69* mutant and the *dop1-3* mutant have increased levels of external CPY as no significant CPY signal was observed for their respective wild-type strains (figure 3.20, A). Thus, it is likely that similar to the mutants of the Neo1p-Ysl2p-Arl1p network, the *dop1-3* mutant also secrets part of p2 form of CPY due to defects in transport between the endosomes and the vacuole.

Since the *dop1-3* mutant was partially suppressed by the overexpression of *NEO1* and marginally suppressed by the overexpression of *ARL1* (see section 3.3.1), it

was tested whether the overexpression of these genes was able to diminish the levels of extracellular CPY in *dop1-3* cells. Therefore, the strain BS1806 (*dop1-3* mutant) was transformed with several multicopy plasmids (see figure 3.20, B) and tested for the presence of extracellular CPY. As observed in the figure 3.20 (B), BS1806 (*dop1-3* mutant) cells transformed with an empty plasmid have increased levels of extracellular CPY comparable to those observed for the non-transformed strain, while in the *dop1-3* cells complemented by *DOP1* this phenotype was rescued. However, when this strain was transformed with a multicopy plasmid encoding either Neo1p or Arl1p, the increased levels of extracellular CPY in the *dop1-3* mutant are maintained, indicating that these genes are not suppressors of the CPY secretion phenotype of the *dop1-3* mutant. This may indicate that Dop1p function is essential for the correct trafficking of CPY to the vacuole.

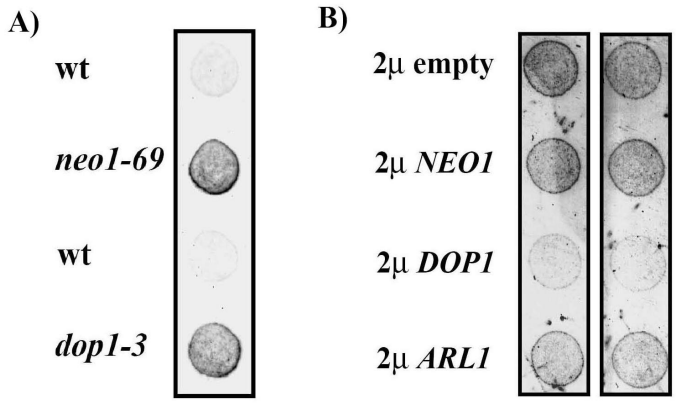

Figure 3.20: *dop1-3* has increased levels of extracellular CPY and this phenotype cannot be rescued by the overexpression of either *NEO1* or *ARL1*. A) BS845 (wt), BS917 (*neo1-69*) and RH1201 (wt), BS1806 (*dop1-3*) were spotted onto YPD plates, a membrane of nitrocellulose was placed on the top of the agar and the plate was incubated at 25ºC for up to 24-32 hours to allow the cells to grow until an early phase. Then the nitrocellulose membrane was washed with water, blocked and immunodetected using the α-CPY antibody (table 2-3). B) BS1806 cells were transformed with the following plasmids: pRS426, pRS426-*NEO1*, pRS426-*DOP1* and pRS426-*ARL1*. The transformants were then spotted onto a SD-URA plate, a membrane of nitrocellulose was placed in the top of the agar and the cells were allowed to grow for 32-40 hours. After growth the nitrocellulose membrane was removed, washed and immunodetected using the α-CPY antibody (table 2-3).

3.8.2 The organisation of the actin cytoskeleton is affected in *dop1-3* and *neo1-69* mutants

Mutations in the DopA gene from *Aspergillus nidulans* led to defects in morphology in this organism. Moreover, the overexpression of the N-terminus of either DopA or Dop1p in *S. cerevisiae* resulted in defects in the polarized growth of the budding yeast (Pascon and Miller 2000). Since the actin cytoskeleton plays a crucial role in polarized growth and morphology, the *dop1-3* mutant was tested for defects in the actin cytoskeleton organisation. To visualise the actin cytoskeleton, the F-actin in wild-type and *dop1-3* cells was stained with the toxin phalloidin conjugated with the fluorophore rhodamine. Wild-type (BS188) and *dop1-3* (BS1361) cells were grown at 25ºC until an early phase of growth in order to have most of the cells with small buds, a phase in which actin cables extent from the bud tip to the mother cell and cortical actin patches are concentrated at the bud tip (a region of active cell growth and endocytosis in this phase). These cells were then fixed with 4% formaldehyde and stained with rhodamine Phalloidin (see section 2.2.4.1.5). As observed in the figure 3.21 (A) upper panels, in the wild-type cells most of the cells show the cortical actin concentrated at the bud tip and cables can be observed in the mother cell. In *dop1-3* cells cortical actin is also concentrated at the bud tip, but instead of actin cables in the mother cell actin patches are observed which indicates an abnormal actin organisation. Quantification revealed that in *dop1-3* cells about 76% of the cells have defective actin organisation versus the 16% observed for the wild-type cells (n=317 and 203, respectively). Furthermore, shift of *dop1-3* cells during one hour to the non-permissive temperature exacerbates this phenotype (figure 3.21, A lower panels) and quantification revealed that 90.4% of the *dop1-3* cells show a defective organisation of the actin cytoskeleton compared to the 27% observed for the wild-type cells (n=301 and 198, respectively).

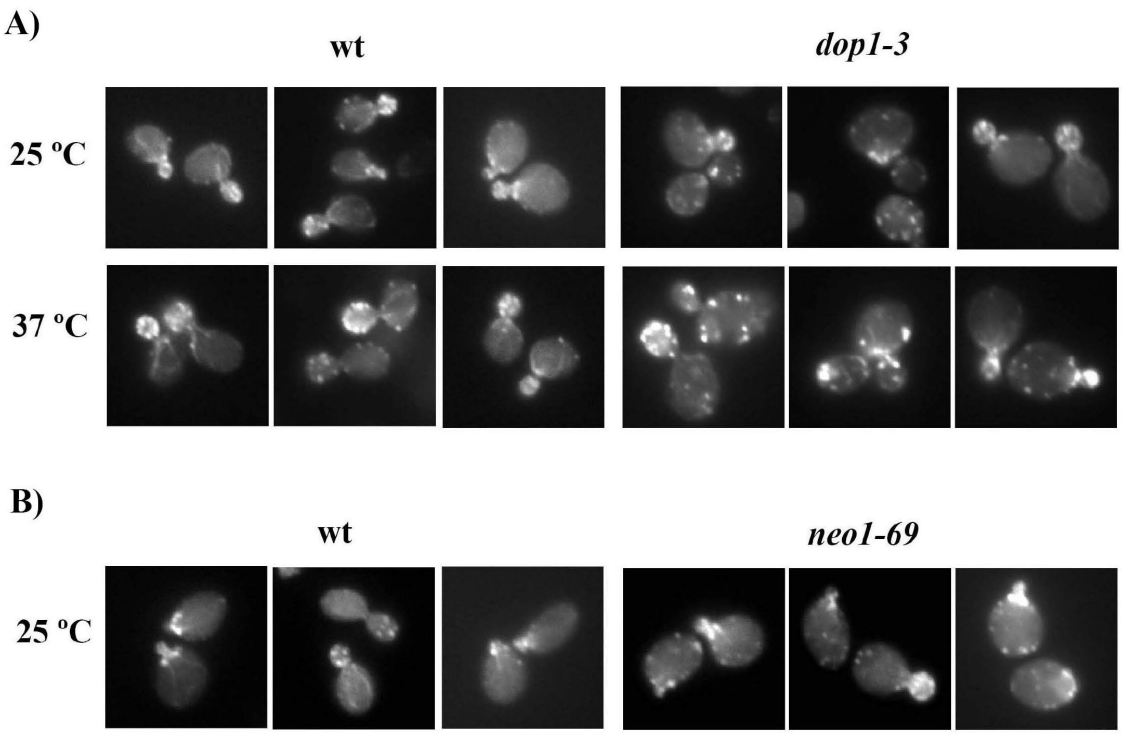

Figure 3.21: Organisation of the actin cytoskeleton in *dop1-3* and *neo1-69* mutants. A) BS188 (wt) and BS1361 (*dop1-3*) cells were grown at 25ºC until early phase of growth, immediately fixed with 4% formaldehyde or additionally sifted for one hour at 37ºC and stained with rhodamine phalloidin (see section 2.2.4.1.5). After, the cells were mounted on a microscope slide with 1.6% agarose and visualised under the fluorescence microscope using the Cy3 filter B) BS845 (wt) and BS917 (*neo1-69*) cells were grown at 25 ºC until early phase of growth, immediately fixed with 4% formaldehyde and stained with rhodamine phalloidin (see section 2.2.4.1.5) and visualised as described above.

In a previous study it was shown that in a *Δysl2* mutant the actin cytoskeleton was adversely affected (Singer-Krüger and Ferro-Novick 1997), this strengthens the notion that Dop1p and Ysl2p may share a common function. Thus, it was also tested if the same defect in the actin organisation was observed in the *neo1-69* mutant. Wild-type (BS845) and *neo1-69* (BS917) cells were prepared as described above and the actin distribution in these cells was assessed. As observed in the figure 3.21 (B), already at permissive temperature the *neo1-69* mutant shows defects in the organisation of the actin cytoskeleton with a majority of mother cells presenting actin patches instead of actin cables. Quantification revealed that in the mutant about 81% of the cells have defects in the organisation of the actin cytoskeleton versus the 6% observed for the wild-type strain (n=196 and 377, respectively). Altogether, these results suggest that Neo1p, Ysl2p and Dop1p are somehow involved in the proper organisation of the actin cytoskeleton. This involvement that may not be direct but rather due to the trafficking defects observed in these mutants.

3.8.3 The cellular distribution of Phosphatidylinositol (4,5)-Bisphosphate is affected in *dop1-3* and *neo1-69* mutants

In the present work it is shown that the *dop1-3* mutant is sensitive to neomycin sulphate (section 3.3.1), a sensitivity shared with the *neo1-69* mutant (B. Singer-Krüger, unpublished results). This sensitivity is allele specific in the case of the *neo1* mutants, since the *neo1-37* mutant allele grows well in the presence of this drug (B. Singer-Krüger, unpublished results). Neomycin is well known for its specificity to binding to phosphoinositol (4,5)-bisphosphate ($PI(4,5)P_2$) (Arbuzova *et al.* 2000). Thus, it was tested whether the *dop1-3* and *neo1-69* mutants had defects in the localization of the GFP-2xPH(PLCδ) FLARE. This FLARE consist in two tandem copies of the PH domain from the PLCδ protein (a pleckstrin homology domain that binds specifically to $PI(4,5)P_2$) tagged to GFP and expressed under the control of the *ADH1* promoter (Stefan *et al.* 2002). Wild-type (SB330), *neo1-37* (BS915), *neo1-69* (BS917) and *dop1-3* (BS1361) cells expressing the GFP-2xPH(PLCδ) FLARE were grown at 25ºC in SD media until early logarithmic phase and visualised under the fluorescence microscope to assess the localization of the FLARE. In wild-type cells, the GFP-2xPH(PLCδ) FLARE was mainly visualised at the plasma membrane and weakly in the cytosol (figure 3.22) as previously described (Stefan *et al.* 2002). The mutant strain *neo1-37* had a similar staining pattern for this FLARE, indicating that the localisation of the phosphoinositide $PI(4,5)P_2$ is not affect in these cells. In *neo1-69* and *dop1-3* cells, however, a more heterogeneous staining pattern was observed. In *neo1-69* cells three populations of cells could be distinguished, a first one in which the FLARE is mainly localised in the cytosol, accounting to 45% of the total observed cells (n= 392). A second population accounting for 40% of the total cells, in which the staining pattern of the FLARE is similar to that observed for the wild-type strain and a third population (15% of total cells) in which the FLARE accumulates in intracellular structures near the plasma membrane in addition to the plasma membrane pattern (figure 3.22). In the case of *dop1-3* cells, 53% of the population of cells displayed a diffuse staining for the FLARE and 47% had a staining pattern similar to that seen for the wild-type strain (n=888) (figure 3.22). Altogether, these results suggest that *neo1-69* and *dop1-3* mutants have an impaired steady-state distribution of the phosphoinositide $PI(4,5)P_2$ but not the *neo1-37* mutant. Consistent with these results, it is possible that the loss of the plasma membrane pool of $PI(4,5)P_2$ may result in the sensitivity of *neo1-69* and *dop1-3* mutants to

neomycin, maybe because the drug can not be sequestered at the plasma membrane and therefore be free and armful for the cell.

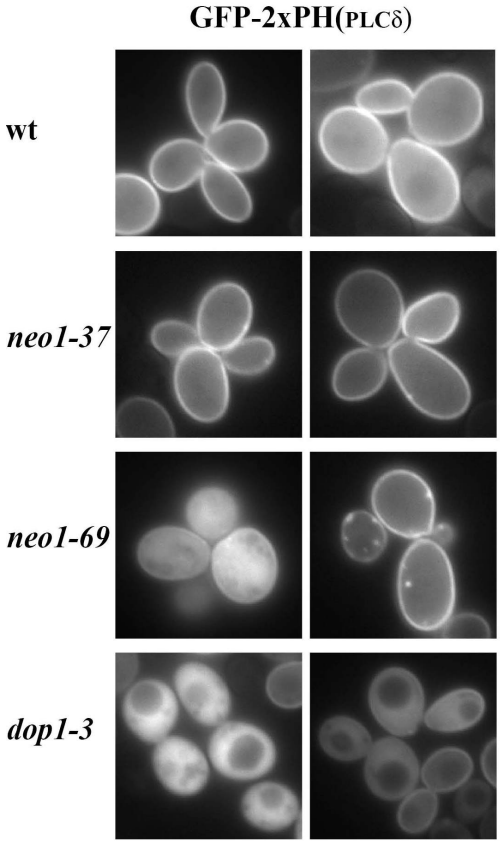

Figure 3.22: Steady-state localization of the PtdIns(4,5)P2-specific FLARE, GFP-2xPH (PLCδ), in the *neo1-37, neo1-69* and *dop1-3* mutants. SB330 (wt), BS915 (*neo1-37*), BS917 (*neo1-69*) and BS1361 (*dop1-3*) expressing GFP-2xPH(PLCδ) were grown in SD media at 25ºC until early logarithmic phase, mounted on a microscope slide with 1.6% agarose. and visualised under the fluorescence microscope using the GFP filter.

3.8.4 GFP-Dop1-3p mutant: localisation and stability of the steady state levels of the protein

Dop1p localises to the TGN and to the endosomal compartment as it was previously demonstrated using several co-localization studies (Efe *et al.* 2005; Gillingham *et al.* 2006; Barbosa *et al.* 2010 and the present study section 3.6.1). Herein, the localisation of Dop1-3p at both permissive and nonpermissive temperatures was studied. The GFP fluorescence of a strain deleted for *DOP1* and harbouring a single copy plasmid expressing GFP-Dop1-3p was compared to the one of an isogenic strain expressing GFP-Dop1p. At permissive temperature, the staining pattern obtained for the wild-type protein was the typical punctuated pattern observed for TGN and endosomal proteins (figure 3.23, A) while for the mutant protein, GFP-Dop1-3p, this was more heterogeneous. In cells expressing GFP-Dop1-3p, 50% of the cell population was devoid of staining, 27% of the cell population accumulated GFP-Dop1-3p in large structures and only 23% of the cell population had a staining which is similar to the

wild-type protein (n=280) (figure 3.23, A). After shift to 37ºC for 2 hours, GFP-Dop1-3p fluorescence was lost in most of the cells (60 %, n=162), the ratio of cells that accumulated GFP-Dop1-3p in larger structures decreased (10 %, n=162) and the ratio of cells with punctuated staining remained stable (30 %, n=162) (figure 3.23, A). In the case of the wild-type protein, the shift of the cells to the non-permissive temperature did not change the staining pattern observed at 25ºC (figure 3.23, A).

Since GFP-dop1-3p accumulates in large structures and a large number of cells do not have fluorescence, it was further analysed whether the GFP-Dop1-3p levels were lost after shift to the non-permissive temperature. Therefore, two isogenic strains expressing either GFP-Dop1p or GFP-dop1-3p from a single copy plasmid under the *DOP1* native promoter were compared for the steady state levels of the GFP-fused protein. As observed in the figure 3.23 (B) GFP-dop1-3p steady state levels diminished after shift to 37ºC while the wild-type protein remains stable, corroborating the previous results obtained by fluorescence in which the staining of GFP-dop1-3p is lost in most of the cell population after shift to 37ºC. Thus, since the cells which accumulate Dop1-3p in large structures at permissive temperature are lost when these are transferred the non-permissive temperature, it is possible that the mutant protein is unfolded and therefore accumulates in large clumps at 25ºC and is further degraded after shift to 37ºC.

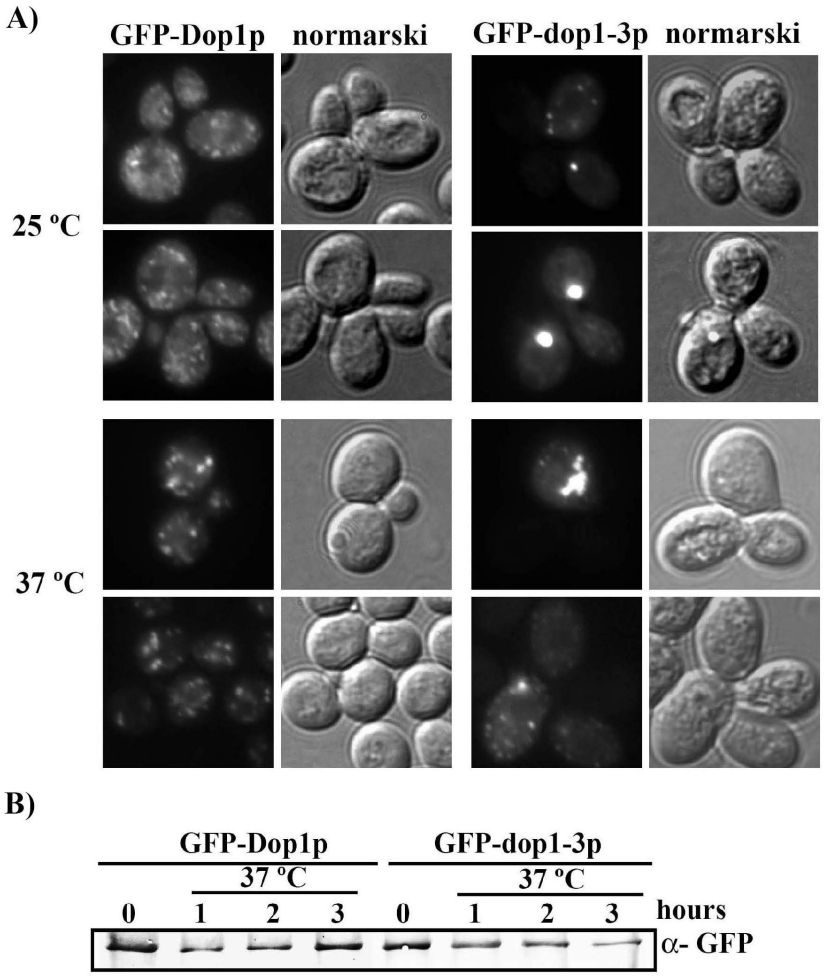

Figure 3.23: Dop1-3p localisation and comparison of the steady state levels of Dop1-3p and Dop1p after shift to 37ºC. A) SB375 (GFP-Dop1p) and SB422 (GFP-Dop1-3p) cells were grown into YPD at 25ºC and either shifted to 37ºC for 2 hours or immediately observed under the fluorescence microscope using the GFP filter. B) SB332 (GFP-Dop1p) and SB335(GFP-Dop1-3p) cells were grown into YPD at 25ºC (time point 0) and then shifted to 37ºC for up to 3 hours. Samples of 1.7 $O.D_{600\ nm}$ of cells were taken at each time point and the same volume of each cell extract was analysed by Western-blotting using the α-GFP antibody (see table 2-3).

3.9 The C-terminal tail of Neo1p has an evolutionary conserved PPXY motif

3.9.1 Sequence alignment reveals the existence of a conserved PPSY motif in the C-terminal tail of Neo1p

The C-terminal tail of Neo1p was previously shown to be essential for the function and correct targeting of the protein to the endosomal system (Wicky *et al.* 2004). The tagging of Neo1p at its C-terminus with a 3-HA epitope was found to render the protein non-functional and to retained it in continuous reticular structures. Furthermore, the truncation of the C-terminal tail of Neo1p, in which the last 21 amino

acids were removed, resulted in a non-functional protein completely retained within the ER (Wicky *et al.* 2004). Thus, the C-terminal tail of Neo1p might have an important role in either the function, targeting or folding of the protein.

To identify some putative conserved domain in the C-terminal tail of Neo1p, an alignment of Neo1p protein sequence with the protein sequence of several of its orthologues was performed. Hence, the complete protein sequences of Neo1p (*Saccharomyces cerevisiae)*, ATP9A (*Homo sapiens)*, ATP9A (*Mus musculus)*, ATP9B (*Homo sapiens)*, ATP9B (*Mus musculus)*, CG31729 isoform A *(Drosophila melanogaster)*, F36H2.1c (*Caenorhabditis elegans)* and NCU03818 (*Neurospora crassa)* were aligned using the CLUSTALW algorithm at EBI http://www.ebi.ac.uk/Tools/clustalw2/index.html. In the figure 3.24 it is illustrated the result of the alignment between these proteins obtained for their C-terminal part.

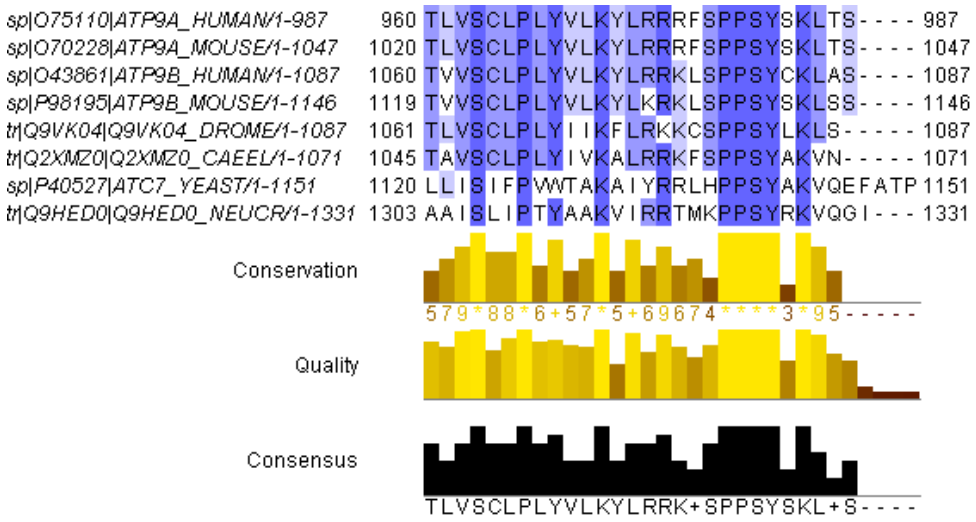

Figure 3.24: Alignment of the C-terminus of Neo1p with the C-termini of its orthologues using the CLUSTALW algorithm. Complete protein sequences of ATP9A_HUMAN, ATP9A_MOUSE, ATP9B_HUMAN, ATP9B_MOUSE, Q9VK04_DROSOPHILA, Q2XMZO_C. ELEGANS, ATC7_YEAST (Neo1p) and Q9HEDO_N. CRASSA were acquired from the Swiss-Prot database and aligned at the EBI website using the CLUSTALW algorithm. The alignment is illustrated using JalView.

Positional prediction of the transmembrane domains of Neo1p, based on the TMHMM algorithm http://www.cbs.dtu.dk/services/TMHMM-2.0/, suggests that its C-terminal tail likely begins with the lysine at the position 1131. Hence, the alignment (figure 3.24) from the position 1131 to the end of the Neo1p sequence unravels a highly conserved motif among all the protein orthologues, PPSY, positioned between the

amino acids 1139 and 1142 of Neo1p. In addition, two highly conserved lysines can be noticed at the position 1131 and 1144.

3.9.2 Neo1p is ubiquitinated

The highly conserved PPSY motif present in the C-terminal tail of Neo1p orthologues resembles the well-characterised short PY motif (L/PPxY) recognised by the WW domains of the E3 ubiquitin ligases from the conserved Nedd4/Rsp5 family (Sudol 1996; Harty *et al.* 2000). The Nedd4/Rsp5 family are HECT-type E3 ubiquitin ligases. They are characterized by the presence of an N-terminal C2 domain, two to four WW domains and a C-terminal catalytic HECT domain. These E3 ubiquitin ligases recognise and bind their substrates through the PPxY motif and transfer an ubiquitin moiety to one or more lysine residues on the substrate (reviewed by Staub and Rotin 2006). The only member of this family of ubiquitin ligases present in *S. cerevisiae* is Rsp5p and it has mainly been involved in ubiquitination of membrane proteins and their subsequent endocytosis (Hein *et al.* 1995 Galan *et al.* 1996) as well as in the ubiquitination of elements from the endocytic machinery like the yeast endophilin/amphiphysin homologue Rvs167 (Stamenova *et al.* 2004). Hence, the presence of the conserved PPSY motif in the C-terminal tail of Neo1p led to hypothesise that Neo1p may be ubiquitinated. As a first approach to address this question, Neo1p was tested for its ubiquitination. Strains lacking *NEO1* and containing either a single copy plasmid encoding Neo1p tagged N-terminally with a 3-HA epitope (BS862) or single copy plasmid containing untagged *NEO1* (BS845) were used to immunoprecipitate HA-Neo1p or to serve as a negative control, respectively. Immunoprecipitation of HA-Neo1p was performed from freshly grown cells using an anti-HA antibody. Briefly, cells were lysed in the presence of NEM (N-ethylmaleimide) and Neo1p was immunoprecipitated in the presence of NEM and 0.01% of NP40 as described in section 2.2.3.3.6. Previous work showed that Sjl2p-HA was ubiquitinated but not is co-partner Sla1p-Myc (Böttcher-Sehlmeyer 2006). Thus, to control the specificity of the method, Sjl2p-HA was isolated similarly in the presence of NEM and 0.2% NP40 from freshly grown cells expressing Sjl2p-HA and Sla1p-Myc (CB207) allowing the co-isolation of Sla1p-Myc. Upon isolation of HA-Neo1p (Figure 3.25; lane 4), Sjl2p-HA and co-isolation of Sla1p-Myc with Sjl2p-HA (Figure 3.25; lane 6), the proteins were tested for the presence of ubiquitin (figure 3.25; lanes 7, 8, 9).

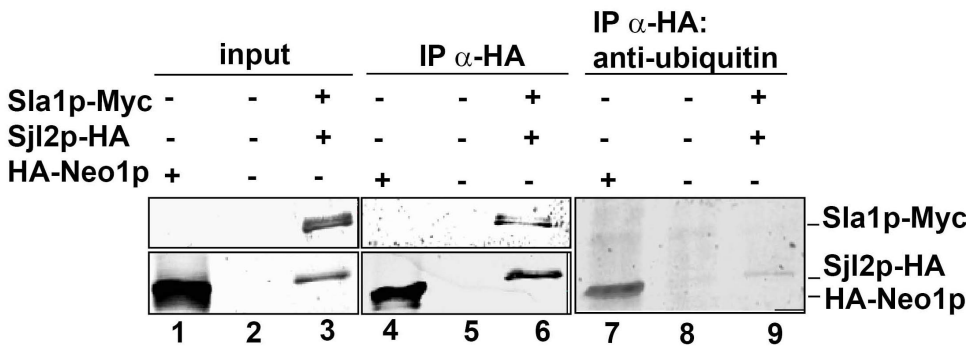

Figure 3.25: HA-Neo1p is ubiquitinated. Cells expressing tagged HA-Neo1p (BS862) (lanes 1, 4, 7) or non-tagged Neo1p (BS845) (lanes 2, 5, 8) were subjected to immunoprecipitation as described in the section 2.2.3.3.6. Cells expressing Sjl2p-3-HA and Sla1p-13-Myc (CB207) (lanes 3, 6, 9) were similarly immunoprecipitated although 2% of NP40 was used to extract the proteins. After immunoprecipitation, about 1% of the cell extracts and 12.5% (to detect the isolate protein) or 50% (to detect ubiquitination) of the immunoprecipitated proteins were analysed by Western-blotting using the specific antibodies (table 2-3): mouse α-Myc (Sla1p-Myc), mouse α-HA (Sjl2p-HA, HA-Neo1p) and mouse α-ubiquitin (for detection of ubiquitination).

The figure 3.25 shows that both HA-Neo1p (lane 7) and Sjl2-3-HA (lane 9) are ubiquitinated whereas Sla1p-13-Myc (lane 9) is not. The ubiquitination signal for HA-Neo1p (lane7) shows a unique well defined band as similarly observed for Sjl2p-HA (lane 9). Thus, these two proteins are neither multi-ubiquitinated nor poly-ubiquitinated since the signals for these types of ubiquitination appear as several bands or as a smear above the molecular weight of the protein. Hence, it is likely that HA-Neo1p has a single lysine ubiquitinated.

3.9.3 Mutation of the tyrosine to alanine in the PPSY domain of Neo1p does not affect its ubiquitination

Subsequently, to study the putative role of the PPXY (PPSY) motif in the ubiquitination of Neo1p, I started to mutate the Y residue within this motif (PPSA). Therefore, to mutate the tyrosine 1142 of Neo1p in pRS315-3-HA-Neo1p, a DNA fragment was generated where the codon coding for the tyrosine 1142 was changed into one coding for alanine, and substituted at the *StuI*/*SalI* position of Neo1p (see section 2.2.2.1.1). The resulting plasmid was transformed into the strain BS845 and the existing pRS316-NEO1 plasmid was shuffled out on 5-FOA plates, leaving the plasmid-encoded *neo1*^{Y1142A} as the single copy of *NEO1* (SB179). This strain was functional as determined by growth at 25ºC and 37ºC. Next, the ubiquitination of Neo1^{Y1142A}p was compared to the ubiquitination of Neo1p. HA-Neo1p and HA-Neo1^{Y1142A}p were

immunoprecipitated as described above from BS862 and SB179 cells, respectively. After immunoprecipitation, the isolated proteins were analysed for ubiquitination. Comparison of the ubiquitin signals obtained for the wild-type HA-Neo1p and the mutated HA-Neo1^{Y1142A}p (figure 3.26; lane 8 and 7, respectively) shows that both proteins are similarly ubiquitinated.

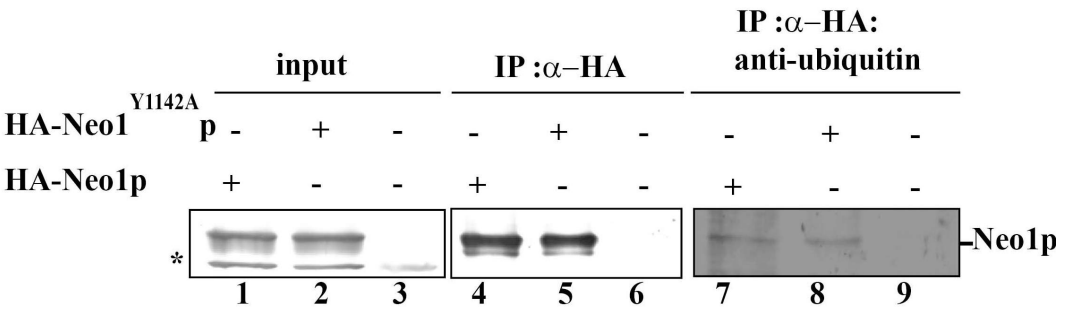

Figure 3.26: Mutation of the tyrosine residue in the conserved PPXY motif of the C-terminal tail of Neo1p does not affect the ubiquitination of the protein. Fifty O.D of cells expressing HA-Neo1^{Y1142A}p (SB179), HA-Neo1p (BS862) or non-tagged Neo1p (BS845) were lysed in the presence of NEM and the proteins immunoprecipitated after extraction with 0.01% NP40. 1% of the clear lysates (lanes 1, 2 and 3) and 8 % of the immunoprecipitated proteins (lanes 4, 5 and 6) were analysed by Western blotting for the mouse α-HA antibody (table 2-3). To analyse ubiquitination (lanes 7, 8, 9) 30% of the immunoprecipitated proteins were analysed by Western blotting with the mouse α-ubiquitin antibody (table 2-3).* indicates a cross reaction from the α-HA antibody.

Since tagging or truncation of the C-terminal tail of Neo1p mislocalised the protein to the E.R compartment (Wicky *et al.* 2004) The localization of HA-Neo1^{Y1142A}p and wt HA-Neo1p was compared after overnight growth at 25ºC and after 2 hours shift at 37ºC to induce the unfolded protein response (UPR). Shift to 37ºC will possibly allow to discriminate between a mislocalisation due to a putative folding defect generated by the mutation and a trafficking defect (figure 3.27). Cells expressing HA-Neo1^{Y1142A}p (SB179) and HA-Neo1p (BS862) were grown overnight at 25ºC and immediately fixed or previously shifted to 37ºC for 2 hours. As observed in the figure 3.27 the staining of HA-Neo1p reveals a punctuated pattern throughout the cytoplasm, typical of a staining for Golgi and endosomal proteins. After shift to 37ºC for 2 hours, the staining of wt HA-Neo1p remained unchanged. Similarlly, HA-Neo1^{Y1142A}p staining reveals the same typical punctuated pattern of Golgi and endosomal proteins. Also, shifting to non-permissive temperature did not influence the staining pattern of this mutant protein, suggesting that this mutation does not have significant effect in the folding of the protein. Unfolded Neo1p should be detected in reticulated structures due to the retention of the mutant protein in the ER as already reported for others Neo1p

mutants (Wicky *et al.* 2004). Together, these results demonstrate that the substitution of the tyrosine residue by an alanine in the PPSY motif does not affect the ubiquitination of HA-Neo1^{Y1142A}p neither affects its targeting to the Golgi/endosomes.

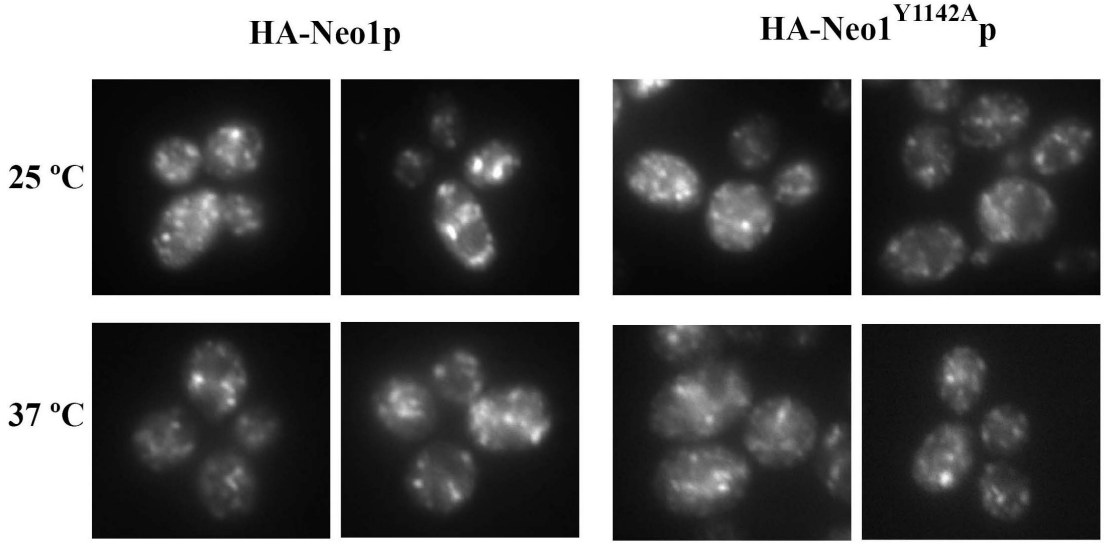

Figure 3.27: The mutation Y1142A introduced in the conserved PPSY motif of Neo1p does not affect the localisation of the protein. Cells expressing either HA-Neo1^{Y1142A}p (SB179) or HA-Neo1p (BS862) were grown until early logarithmic phase at 25ºC (upper panels) or and additionally shifted for 2 hours at 37ºC (lower panels). Cells were fixed and immunostained as described in the section 2.2.4.1.1 using the mouse α-HA (table 2-7) as primary and goat α-mouse-Cy3 (table 2-8) as secondary antibodies. The cells were visualized under the fluorescence microscope using the Cy3 filter.

3.9.4 Point mutations in the conserved PPSY motif of Neo1p enhance the resistance of the cells to high temperatures

As previously mentioned, truncation and tagging of the C-terminal tail of Neo1p is lethal (Wicky *et al.* 2004). Thus it was tested whether addition of mutations within the conserved PPSY motif of the C-terminal tail of Neo1p were causing any growth defect. To generate HA-Neo1p containing two mutations in the PPSY motif, HA-Neo1^{PASA}p, the tyrosine 1142 and the proline 1140 residues from the PPSY motif were each substituted by alanine (see section 2.2.2.1.1). Then, the plasmid HA-Neo1^{PASA}p was also transformed into BS845 and the plasmid pRS316-NEO1 was shuffled out on 5-FOA plates, leaving the plasmid-encoded *neo1^{PASA}* as the single copy of *NEO1* (SB185). Surprisingly, this strain, similarly to the SB179 strain, did not revealed growth defects at either 25ºC or 37ºC. Nevertheless, I have test whether at other temperatures an effect on the growth of these strains could be observed. Thus, BS862 (HA-Neo1p), SB179 (HA-Neo1^{Y1142A}p) and SB185 (HA-Neo1^{PASA}p) were diluted in series, spotted onto YDP

plates and incubated at different temperatures. All the strains grew similarly at 18ºC, 25ºC, 30ºC and 37ºC (figure 3.1 and data not shown). Surprisingly, the strains expressing Neo1p containing mutations in the PPSY motif were tolerating growth at a temperature of 42ºC, while the strain expressing wild-type Neo1p was not. Interestingly, the introduction of a second point mutation in this motif, HA-Neo1^{PASA}p, increased the resistance to high temperature observed when a single point mutation was present.

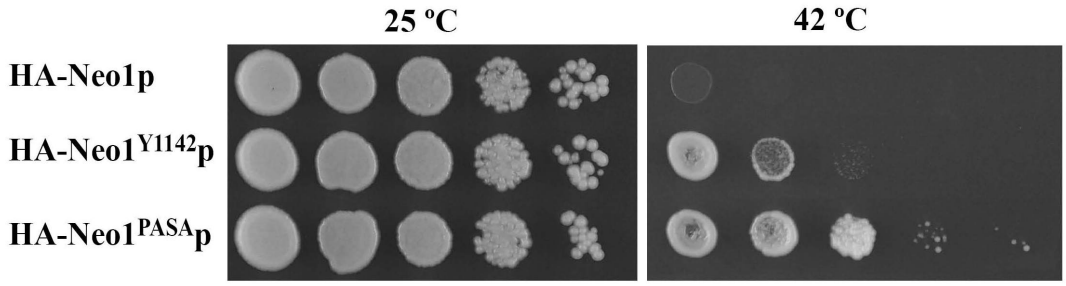

Figure 3.28 Mutations in the PPXY motif of the C-terminal tail of Neo1p renders yeast more resistant to high temperatures. BS862 (HA-Neo1p), SB179 (HA-Neo1^{Y1142A}p) and SB185 (HA-Neo1^{PASA}p) cells were in series in sterile ddH_2O, spotted into YPD media and incubated for 2 to 3 days at the indicated temperatures (see section 2.2.1.2).

Since the strain BS862, which contains a plasmid encoding HA-Neo1p, was sensitive to 42ºC it was tested whether this effect was due to the tag at the N-terminus of the protein by comparing this strain with a strain in which the plasmid encoded *NEO1* does not have a tag (BS845) and a wild-type strain (BS64). Both BS862 and BS845 were not able to grow at 42ºC while the wild-type strain was (data not shown). Thus, I also tested the growth at 40ºC (to not exert such an extreme stress to the cells) of BS862 (HA-Neo1p), SB179 (HA-Neo1^{Y1142A}p) and SB185 (HA-Neo1^{PASA}p) by comparing it with a strain expressing HA-Neo1p from the chromosome (BS1488). As illustrated in the figure 3.29 when the only copy of *NEO1* is chromosomal the cells growth well at 40 ºC (HA-Neo1p - BS1488), while if the only copy of *NEO1* is expressed from a single copy plasmid the cells display a growth defect at 40 ºC (*Δneo1* + pHA-Neo1p - BS862). In accordance with the aforementioned results, when HA-Neo1^{Y1142A}p allele is expressed in a single copy plasmid (*Δneo1* + pHA- Neo1^{Y1142A}p – SB179) the cells show less growth defect than the strain expressing wild-type Neo1p from a plasmid (BS862). In the case of the allele containing the two mutations in the PPSY motif (*Δneo1* + pHA- Neo1^{PASA}p – SB185) the cells grow as well as the strain expressing HA-Neo1p (BS1488) from the chromosome. Thus, the strains containing a plasmid encoding Neo1p are the sensitive ones, and the mutations introduced in the PPSY motif of Neo1p

are able to rescue this sensitivity. While it seems evident that the PPSY motif present in the C-terminal tail of Neo1p is of importance for this protein, it has still to be established its real role.

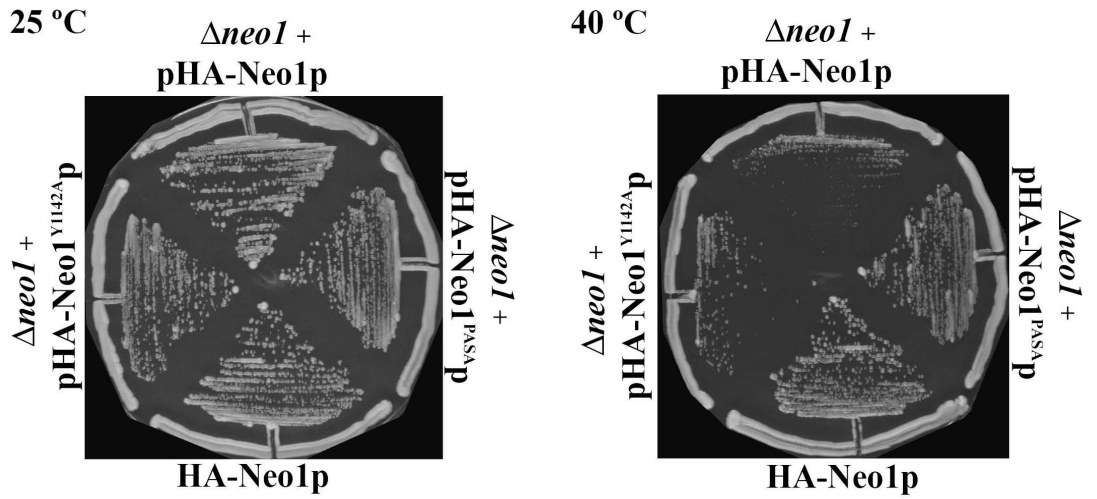

Figure 3.29: Strain expressing plasmid encoded HA-Neo1p has growth defect compared to strain encoding intragenic copy of HA-Neo1p. BS1488 (HA-Neo1p), BS862 (*Δneo1* + pHA-Neo1p), SB179 (*Δneo1* + pHA- Neo1^{Y1142A}p) and SB185 (*Δneo1* + pHA- Neo1^{PASA}p) cells were diluted in series in sterile ddH_2O, spotted into YPD media and incubated for 2 to 3 days at the indicated temperatures (see section 2.2.1.2).

4 Discussion

4.1 Neo1p function is likely independent from the Cdc50 family members

Recently, the Cdc50p family members have emerged as being putative β-subunits for some of the P_4-ATPases (Saito *et al.* 2004; Furuta *et al.* 2007). They were primarily shown to be required for the trafficking of some P_4-ATPases out of the ER and a recent work suggested that they may be involved in the reaction cycle of the P_4-ATPases (Saito *et al.* 2004; Furuta *et al.* 2007; Lenoir *et al.* 2009). Cdc50p members were identified in yeast (Saito *et al.* 2004), humans (Katoh and Katoh 2004), *Leishmania* (Perez-Victoria *et al.* 2006) and in plants (Poulsen *et al.* 2008a). In all these organisms, a higher number of P_4-ATPases is found compared to the Cdc50p isoforms. This imbalanced proportion implies that either one Cdc50p family member may assist several P_4-ATPases or that some P_4-ATPases may function without β-subunit as it is the case for the majority of the P-type ATPases. In *S. cerevisiae*, there are five P_4-ATPases (Drs2p, Neo1p, Dnf1p, Dnf2p and Dnf3p) and three Cdc50p family members (Cdc50p, Lem3p and Crf1p). Cdc50p forms a complex with Drs2p, Crf1p with Dnf3p and Lem3p with Dnf1p and Dnf2p (Saito *et al.* 2004; Furuta *et al.* 2007). Although Neo1p displays a genetic interaction with Cdc50p, so far, none of the Cdc50p family members was found to associate with Neo1p (Saito *et al.* 2004). Given the proposed importance of the β-subunits for the targeting and function of some P_4-ATPases, the putative link between Neo1p and Cdc50p was further investigated here. To determine whether Neo1p and Cdc50p physically interact *in vivo*, two different immunoprecipitation approaches were used. In the first approach, either HA-Neo1p or Cdc50p-Myc was immunoprecipitated from total membranes solubilised with 1% CHAPS while in the second these proteins were isolated from a 100,000 x g supernatant of total cell extracts treated with 0.01% NP40 (figure 3.1). In accordance with the previous results from Saito *et al.* 2004, none of these immunoprecipitation approaches could reveal a physical interaction between Neo1p and Cdc50p (figure 3.1), suggesting that these proteins do not interact *in vivo*. Furthermore, the subcellular TGN/endosomal localisation of HA-Neo1p (Wicky *et al.* 2004) was not affected by the deletion of *CDC50* (figure 3.1) demonstrating that Cdc50p is not required for the correct HA-Neo1p localisation. Thus, the hypothesis of

Cdc50p being a transport chaperone for Neo1p was not validated by these experiments. Additionally, given the previously observed phenotypes for the deletion of a *CDC50* member or *DRS2* member (P_4-ATPase) in which the deletion of a β-subunit phenocopies the deletion of the respective P_4-ATPase (Saito *et al.* 2004), it is unlikely that one of the Cdc50p family members is a β-subunit for Neo1p. *NEO1* is an essential gene and none of the genes coding for the Cdc50p members are essential. On the other hand, the Cdc50p family is an essential family in yeast, so it is possible that each of the Cdc50p members is necessary for chaperoning Neo1p. However, the fact that Neo1p and Cdc50p do not physically interact contradict this hypothesis. Taken together, these data suggest that Neo1p functions independently from the Cdc50p family members.

4.2 Dop1p is a novel component from the Neo1p-Ysl2p-Arl1p network

4.2.1 Dop1p forms a complex with Ysl2p and Neo1p

In the present study the highly conserved protein Dop1 was identified as a component of the endosomal Neo1p-Ysl2p-Arl1p network. Herein, genetic and biochemical data demonstrated that Dop1p is tightly associated to Neo1p and Ysl2p. Since *NEO1* and *DOP1* are essential genes, studies involving these genes were carried out with temperature sensitive alleles. The *neo1-69* and the *dop1-3* mutant alleles display both temperature sensitivity and hypersensitivity to neomycin (Wicky *et al.* 2004; Birgit Singer-Krüger, unpublished results and this work), growth defects that were shown to be suppressed by the overexpression of *DOP1* and *NEO1*, respectively (figure 3.5, figure 3.6, C). Consistently, in the *dop1-3* and *neo1-69* mutants the steady state levels of Neo1p and Dop1p are reduced, respectively (figure 3.4, figure 3.6). An effect that explains the suppression data described above and clearly indicates that these proteins are interdependent. Furthermore, an earlier high throughput screen, in which a complete library of heterozygous diploids deletion mutants was tested for the sensitivity to a broad range of drugs, revealed that the diploids *NEO1/Δneo1* and *DOP1/Δdop1* displayed sensitivities to the same group of drugs (Lum *et al.* 2004). Together, the above mentioned reciprocal genetic interaction, the phenotypes shared by the *neo1* and *dop1* mutants and the specific loss of Dop1p and Neo1p in the *neo1-69* and *dop1-3* mutants, respectively, suggest that Neo1p and Dop1p might be connected. The connection between Neo1p and Dop1p was further strengthened by the observation that

these proteins physically interact *in vivo* as demonstrated after isolation of the Dop1p-TAP protein assemblies (figure 3.2).

Besides the association between Dop1p and Neo1p, an interaction between Dop1p and Ysl2p was also found (Efe *et al.* 2005; Gillingham *et al.* 2006 and this study). In the present work, isolation of Dop1-TAP assemblies co-isolated Ysl2p-HA (figure 3.2) and further analysis of the steady state levels of Ysl2p in the *dop1-3* mutant (figure 3.4) revealed that those are decreased as it was previously observed in the *neo1-69* mutant (Wicky *et al.* 2004). Furthermore, in *Δysl2* cells the levels of Neo1p and Dop1p are clearly reduced when compared to those of the wild-type strain (figure 3.7). *Δysl2* cells display a severe growth defect and temperature sensitivity which can be suppressed by the overexpression of *ARL1*, *NEO1* or *DOP1* (Jochum *et al.* 2002; Wicky *et al.* 2004; Efe *et al.* 2005; this work). Interestingly, overexpression of one of these extragenic suppressors raised the levels of both Dop1p and Neo1p to those observed in the *Δysl2* cells expressing *YSL2* (figure 3.7), a finding that explains the suppression effect generated in *Δysl2*. Together, these results highlight an interdependence of Neo1p, Dop1p and Ysl2p and propose that they are elements of the same complex. In fact, this co-dependency effect has been observed for several complexes. As a first example, deletion or mutation of one of the subunits of the yeast fatty acid synthase, which consists of two subunits, Fas1p and Fas2p, leads to the degradation of the remaining wild-type subunit (Egner *et al.* 1993). Second, in a clathrin light chain deletion mutant (*Δclc1*) the steady-state levels of the clathrin heavy chain (Chc1p) are reduced (Huang *et al.* 1997). Last, the levels of the P_4-ATPase Drs2p are decreased when its β-subunit, Cdc50p, is mutated or not present (Chen *et al.* 2006; Furuta *et al.* 2007). In the case where the levels of HA-Neo1p are decreased in *dop1-3* cells, this effect appears to be largely due to a destabilization of the protein caused by the mutations in its binding partner. As shown by pulse-chase analysis, the half-life time of HA-Neo1p in *dop1-3* cells is reduced to 50% of the one in wild-type cells (figure 3.8). In *dop1-3* cells, the degradation of HA-Neo1p does not take place in the vacuole, since the removal of the vacuolar protease Pep4p did not result in a stabilisation of HA-Neo1p (figure 3.10). Rather, the degradation of HA-Neo1p in *dop1-3* cells appears to be dependent on the proteasome, since addition of the proteasomal inhibitor MG132 led to a delay in its degradation (figure 3.11). Moreover, the levels of synthesis of HA-Neo1p in *dop1-3* cells are also slightly affected (figure 3.8) this may be due to a translational repression

which occurs in cells that undergo stress (Dever 1999). In further attempts to assess the site of degradation of HA-Neo1p in *dop1-3* cells, no clear staining pattern was obtained in the presence of MG132 after a 3 hours shift to 37 ºC. Conditions in which the degradation of HA-Neo1p is delayed and the fluorescent signal for HA-Neo1p is still present (figure 3.11). However, it is most likely that HA-Neo1p is degraded in the ER compartment, since Neo1p was identified as being a substrate of the ERAD machinery (Hitchcock *et al.* 2003). This maybe due to a lower avidity of Dop1-3p for Neo1p that may result in the retention of Neo1p in the ER compartment. Nevertheless, further studies will be required to ascertain the real cause of Neo1p destabilisation in *dop1-3* cells.

4.2.2 Dop1p role within the endosomes

In addition to the key finding that Dop1p, Neo1p and Ysl2p are parts of the same complex, the subcellular localisation of Dop1p was also examined. Previously, Dop1p was reported to be localised to the Golgi compartment (Gillingham *et al.* 2006), whereas Ysl2p and Neo1p were already found to be localised at both the endosomal and the Golgi compartments (Jochum *et al.* 2002; Wicky *et al.* 2004; Efe *et al.* 2005). Thus, since Dop1p, Ysl2p and Neo1p physically interact, this suggested that Dop1p is also present at the endosomes. Indeed, distinct approaches have revealed that in addition to the TGN localisation, Dop1p also localises to the endosomes. First, the scattered structures observed for the GFP-Dop1p localisation in wild-type cells, collapsed together with the class E compartment in *vps27* cells (figure 3.12). Second, GFP-Dop1p colocalised with the endocytic tracer Alexa594-α factor in *Δypt51* cells (figure 3.12), in which a defective delivery to the vacuole leads to cargo accumulation within the endosomes (Singer-Krüger *et al.* 1995). Third, in wild-type cells the GFP-Dop1p fluorescent pattern revealed an extensive degree of co-localisation with the endosomal protein Hse1p-mCherry (Barbosa *et al.* 2010). Last, a high degree of co-localisation was also observed for GFP-Dop1p and the lipophilic dye FM4-64 (Barbosa *et al.* 2010), when the latter was internalised at 15ºC to allow its detection in early endosomes (Vida and Emr 1995). In agreement with the Dop1p localisation to the endosomes are several defects observed for the *dop1* mutant alleles. In an earlier study, the *dop1-2* mutant allele revealed an impaired recycling for the transport markers v-SNARE Snc1p and the modified syntaxin Sso1p, which accumulated into intracellular structures and were

depleted from the plasma membrane (Gillingham *et al.* 2006), thus suggesting that Dop1p is required for the recycling from endosomes. In the present study, as previously demonstrated for both the *ysl2* and *neo1* mutants (Jochum *et al.* 2002; Wicky *et al.* 2004), the *dop1-3* mutant exhibited elevated levels of secreted carboxypeptidase Y (figure 3.20), a defect that indicates impaired sorting from the TGN and endocytic recycling. Additionally, the depletion of the phosphoinositide $PI_{4,5}2P$ from the plasma membrane, a phenotype shared by both *dop1-3* and the *neo1-69* mutant cells (figure 3.22), is also suggestive of sorting defects for the enzymes responsible to maintain the pool of this phosphoinositide at the plasma membrane, such as the phosphoinositide kinases and phosphatases. In agreement with the role of the $PI_{4,5}2P$ in the regulation of actin cytoskeleton (reviewed by Logan and Mandato 2006), defects in the proper organisation of the actin cytoskeleton were observed in the *dop1-3* and *neo1-69* mutant cells (figure 3.21), a phenotype also shared by the *ysl2* mutant (Singer-Krüger and Ferro-Novick 1997). Together, the localisation of Dop1p to the endosomes, the fact that Dop1p is part of the Neo1p-Ysl2p-Arl1p network and the defects observed for the *dop1* mutant alleles strongly hint for a role of Dop1p within the TGN/endosomal system.

A role of Dop1p within the TGN/endosomal system is in agreement with the previous findings regarding its orthologue DopA from *Aspergillus nidulans*. This fungus belongs to the class of filamentous fungi in which vegetative growth occurs almost exclusively by apical extension at hyphal tips, thus representing an extreme example of polarised growth. Mutations in DopA from *Aspergillus nidulans* resulted in an abnormal hyphae formation due to defects in polarised growth (Pascon and Miller 2000). In this organism, the endosomes are highly dynamic, they move bidirectionally across the hypha and they play a critical role in the hyphal tip growth by controlling secretory membrane delivery and compensatory endocytosis (Abenza *et al.* 2009). Furthermore, in the *dopA* mutants, anucleated and binucleated cells were observed during conidial differentiation, suggesting putative failure in mitosis or in nuclear movement. In fact, endosomal recycling is thought to play a central role in cell division and cytokinesis particularly in the remodelling of newly formed plasma membrane (Baluska *et al.* 2006; Boucrot and Kirchhausen 2007). Therefore, one can suggest that defects in the endocytic machinery can lead to a failure in cell division. Although the real function of Dop1p is still unclear, it seems now obvious that this function might take place at the endosomes.

4.2.3 Dop1p domain organization and insights into its function

The *S. cerevisiae* Dop1p is a large protein of about 195 kDa highly conserved from fungi to humans. Comparison of protein sequences between the Dop1p orthologues revealed a highly conserved region within the N-terminus and led to the identification of leucine zipper-like repeats within the C-terminus of these proteins (Pascon and Miller 2000). In the present study, in order to gain some insights in the features of these regions, the *S. cerevisiae* Dop1p was divided into three portions which were expressed as GFP-fusions. The GFP-Nterm fusion which includes the conserved N-terminus, the GFP-internal fusion which includes the internal region of Dop1p with no significant sequence similarity among the ortologues and the GFP-Cterm which contains the conserved C-terminal leucine-zipper like repeats. None of these Dop1p GFP-fused regions was able to restore the viability to *Δdop1* cells (figure 3.15). Nevertheless, they displayed different localisation patterns and different affinities for Neo1p and Ysl2p.

The internal region of Dop1p was here identified as being important for Dop1p localisation to the endosomes. Localisation data showed that in the majority of the cells the fluorescent pattern observed for the GFP-internal fusion was similar to that observed for the full length GFP-Dop1p (figure 3.16). Interestingly, in some cells the GFP-internal fusion was visible in large structures adjacent to the vacuole (figure 3.16) which were further identified as being endosomes (work of B. Singer-Krüger, Barbosa *et al.* 2010). The reason for these possible clustering of endosomes in the presence of the GFP-internal fusion is not yet understood, but suggests that the N- and C-termini of the protein may have an important structural or regulatory effect. Furthermore, immunoprecipitation data showed that the GFP-internal fusion was one of the fused regions of Dop1p that efficiently co-isolated Ysl2p-HA and the one that was most efficient in co-isolating HA-Neo1p (figure 3.19), suggesting a contribution of this region of Dop1p in mediating the binding to Neo1p and Ysl2p.

Collectively, the findings that the internal region of Dop1p is critical for the association of the protein with the endosomes and for the binding to both Neo1p and Ysl2p, suggest that Dop1p might associate with the endosomes by interacting with Neo1p and Ysl2p. The requirement of Ysl2p for the proper localisation of Dop1p was here analysed in a Δysl2 strain. Despite the fact that loss of Ysl2p results in a decrease of the levels of Dop1p, the punctuated staining pattern of the protein remained (figure

3.13). Thus, even though a mislocalisation of the protein to the cytoplasm and subsequent degradation cannot be excluded it seems that Ysl2p is not the major determinant for Dop1p localisation. Moreover, the interaction between Dop1p and Neo1p is independent of Ysl2p (figure 3.3), suggesting that the role of Neo1p in recruiting Dop1p to the TGN/ endosomes might be more significant.

The N-terminus of Dop1p is the region with highest sequence identity among the Dop1p orthologues. Expression of this region fused to GFP (GFP-Nterm) revealed a diffused cytoplasmic staining with some occasional dotted structures (figure 3.16). Additionally, immunoprecipitation studies showed that this region of Dop1p interacts with HA-Neo1p but cannot effectively interact with Ysl2p-HA (figure 3.19). Altogether, this suggests that the weak membrane association of this region is likely happens via Neo1p. Even though an impaired folding of this fusion protein cannot be excluded, the fact that a weak membrane interaction and binding to Neo1p are still taking place suggests that at least some functionality is preserved. Nevertheless, this region may be critical for Dop1p function, since the two described *dop1* alleles (Gillingham *et al.* 2006, this work) carry mutations in this region.

Expression of the GFP-Cterm fusion of Dop1p revealed an unexpected fluorescent pattern characterised mainly by the staining of a single organelle (figure 3.16). Thereafter, using the DNA dye Hoescht 33342 this organelle was identified as being the nucleus (figure 3.17). Whether this localisation is physiologically relevant for Dop1p function is still unknown. However, it may be that Dop1p undergoes nucleocytoplasmic shuttling under special conditions as observed for several endocytic proteins involved in cellular signalling (Pilecka *et al.* 2007) and that the accumulation of its C-terminus in the nucleus maybe due to a missing or inaccessible nuclear export signal. In fact, it was previously suggested that the DopA protein from *Aspergillus nidulans* could act as a transcriptional activator. The *ΔdopA* null cells exhibited an altered expression pattern for some key genes involved in the spatiotemporal control of development in *Aspergillus nidulans*. Moreover, in addition to the leucine zipper-like repeats present at its C-terminus, a feature shared by several proteins that bind DNA, DopA also contains a C-terminal activation domain typical of the CAAT/enhancer binding proteins (Pascon and Miller 2000). Even though this activation domain is not identified in the others orthologues of DopA, it is possible that a low sequence homology renders its detection difficult. Additionally, immunoprecipitation data showed that the GFP-Cterm fusion had a reduced affinity for HA-Neo1p but a substantial affinity for Ysl2p-HA (figure 3.19).

Thus suggesting that this region may be necessary for Dop1p binding to Ysl2p but not for Dop1p binding to Neo1p. The presence of leucine zipper-like repeats at the C-terminus of Dop1p, a structural domain which is commonly involved in the formation of dimeric interactions (Landschulz *et al.* 1988), led to the hypothesis of Dop1p dimerisation. Indeed, two chromosomally tagged version of Dop1p, Dop1p-TAP and GFP-Dop1p, were able to interact *in vivo* when combined into a diploid strain (figure 3.14), and subsequent studies led to the demonstration that the C-terminal domain of Dop1p is able to form dimers or oligomers *in vitro* (work of Dagmar Pratte, Barbosa *et al.* 2010). Thus, suggesting that the C-terminus of Dop1p may contribute for Dop1p dimerisation or oligomerisation. In addition, this region of Dop1p is certainly crucial for the function of the protein since a single point mutation in DopA and the several amino acid changes present Dop1-3p, which most likely alter the leucine zipper-like domain, result in a partial loss of function of these proteins. However, whether the loss of function of these mutants is due to a potential role of this region in the nucleus or to its ability of forming dimers or oligomers awaits further investigations.

In conclusion, these studies suggest a critical involvement of the internal region of Dop1p in the binding to membranes and to Neo1p and Ysl2p while the C-terminal region of Dop1p might be required for Dop1p dimerisation or oligomerisation, probably via the leucine zipper-like repeats present at its C-terminus. Yet, the importance of the ability of Dop1p to self-interact likely by dimerisation or oligomerisation is unknown. However, this ability to form dimers of multimers is a common feature among proteins that generate, stabilise or/and sense membrane curvature. Prominent examples are BAR domain containing proteins and coat components like clathrin. Thus, given that Dop1p is part of the Neo1p-Ysl2p-Arl1p network, this feature could be particularly important. As a possible model, Dop1p dimerisation or oligomerisation could be important to mediate the contacts between the diverse pools of deposited Ysl2p, Arl1p and adaptors in the membrane where Neo1p is located and might translocate phospholipids. This will lead to the formation of an intricate network formed by several pools of these proteins that operate locally to generate membrane curvature. A support for this hypothetical model is the fact that Ysl2p was also found to self-interact and to exist in a high molecular weight complex (Efe *et al.* 2005).

4.3 The conserved C-terminal PPSY motif of Neo1p

The C-terminal tail of Neo1p was previously shown to be required for the functionality and proper localisation of the protein (Wicky *et al.* 2004). In the present study, a protein sequence alignment among the Neo1p orthologues revealed a highly conserved PPSY motif at their C-terminal tail (figure 3.24). This prompted the study of the requirement of this motif for Neo1p functionality and proper localisation to TGN/endosomes. The PPSY motif found in Neo1p resemble the well-characterised short PY motif (L/PPxY) recognised by the WW domains of the E3 ubiquitin ligases from the conserved Nedd4/Rsp5 family (Sudol 1996; Harty *et al.* 2000). This coincidence led to the hypothesis that Neo1p could be ubiquitinated by Rsp5p, the only member of this family in yeast. Indeed, Neo1p was found to be ubiquitinated (figure 3.25). However, the mutation of the Neo1p PPxY motif into "PPxA" failed to reveal a significant change in the ubiquitination state of this protein (figure 3.26). The localisation of the protein to the Golgi and endosomal compartments was also unaffected by this mutation (figure 3.27). Nevertheless, these observations do not exclude the involvement of this motif as a binding motif for Rsp5p since it is possible that a unique point mutation is not enough to abolish the interaction between Rsp5 and Neo1p. In fact, a similar result was obtained for the protein Rvs167p which is monoubiquitinated by Rsp5p. Mutation of the two prolines from the PPxY motif of Rvs167p still resulted in the monoubiquitination of the protein albeit in a lesser extent (Stamenova *et al.* 2004). Hence, the implication of the PPSY motif in Neo1p ubiquitination cannot be excluded, but awaits further investigations.

Additionally, since deletion of *NEO1* results in lethality as well as truncation or tagging of the C-terminus of the protein (Wicky *et al.* 2004), strains containing a plasmid encoding HA-Neo1p with one (PPxA) or two (PAxA) point mutations in the PPSY motif were tested for their ability to grow at different temperatures. None of these strains revealed a growth defect at the tested temperatures when compared to the strain encoding the wild-type HA-Neo1p. Surprisingly, they even grew better at 42 ºC than the strain encoding the wild-type protein (figure 3.28). A more detailed analysis revealed that when HA-Neo1p was expressed from a single copy plasmid the cells were less resistant to high temperatures than when HA-Neo1p was expressed from the chromosome (figure 3.29). Under the circumstances in which HA-Neo1p is expressed from a single copy plasmid, the addition of point mutations in the PPSY motif of Neo1p renders the strain more resistant to high temperatures (figure 3.29). Thus, due to the fact

that when HA-Neo1p is expressed from a plasmid, more HA-Neo1p is present in the cells than when the protein is expressed from the chromosome (data not shown), it is probable that an excess of HA-Neo1p is detrimental for the cells at a high temperature. This could be a consequence of a large amount of HA-Neo1p that needs to be degraded due to an unfolding protein response signal. However, in this scenario it is unlikely that mutations in the PPSY motif of Neo1p reverse this effect. Rather, the addition of point mutations might result in a loss of the proper folding of the protein and consequently in a higher rate of degradation. Thus, it seems more likely that the conserved PPSY motif of Neo1p has a more specific role still to be uncovered.

The aforementioned putative connection of this motif with ubiquitination through Rsp5 binding may be the best hypothesis at the moment. Thus, as a kind of suggestion for future work, it will be interesting to test if the complete mutation of the PPSY motif will result in a decrease of the ubiquitination of Neo1p. Additionally, the link to Rsp5p should be tested by using mutant alleles for the several WW domains of this protein and co-immunoprecipitation. If this hypothesis is proven true, the putative role of Neo1p ubiquitination could be analysed. This role may most likely be related either to ubiquitin-dependent internalisation of the protein, sorting from the Golgi to endosomes or sorting to internal vesicles of the MVB, since these are the most common roles of Rsp5p ubiquitination in intracellular trafficking (Staub and Rotin 2006; Belgareh-Touze *et al.* 2008).

References

Abazeed, M. E. and R. S. Fuller (2008). "Yeast Golgi-localized, gamma-Ear-containing, ADP-ribosylation factor-binding proteins are but adaptor protein-1 is not required for cell-free transport of membrane proteins from the trans-Golgi network to the prevacuolar compartment." *Mol Biol Cell* **19**(11): 4826-4836.

Abenza, J. F., A. Pantazopoulou, et al. (2009). "Long-distance movement of Aspergillus nidulans early endosomes on microtubule tracks." *Traffic* **10**(1): 57-75.

Alder-Baerens, N., Q. Lisman, et al. (2006). "Loss of P4 ATPases Drs2p and Dnf3p disrupts aminophospholipid transport and asymmetry in yeast post-Golgi secretory vesicles." *Mol Biol Cell* **17**(4): 1632-1642.

Amor, J. C., D. H. Harrison, et al. (1994). "Structure of the human ADP-ribosylation factor 1 complexed with GDP." *Nature* **372**(6507): 704-708.

Antonny, B., P. Gounon, et al. (2003). "Self-assembly of minimal COPII cages." *EMBO Rep* **4**(4): 419-424.

Arbuzova, A., K. Martushova, et al. (2000). "Fluorescently labeled neomycin as a probe of phosphatidylinositol-4, 5-bisphosphate in membranes." *Biochim Biophys Acta* **1464**(1): 35-48.

Axelsen, K. B. and M. G. Palmgren (1998). "Evolution of substrate specificities in the P-type ATPase superfamily." *J Mol Evol* **46**(1): 84-101.

Balasubramanian, K. and A. J. Schroit (2003). "Aminophospholipid asymmetry: A matter of life and death." *Annu Rev Physiol* **65**: 701-734.

Baluska, F., D. Menzel, et al. (2006). "Cytokinesis in plant and animal cells: endosomes 'shut the door'." *Dev Biol* **294**(1): 1-10.

Barbosa, S., D. Pratte, et al. (2010). "Oligomeric Dop1p is part of the endosomal Neo1p-Ysl2p-Arl1p membrane remodeling complex." *Traffic*.

Barlowe, C., L. Orci, et al. (1994). "COPII: a membrane coat formed by Sec proteins that drive vesicle budding from the endoplasmic reticulum." *Cell* **77**(6): 895-907.

Becherer, K. A., S. E. Rieder, et al. (1996). "Novel syntaxin homologue, Pep12p, required for the sorting of lumenal hydrolases to the lysosome-like vacuole in yeast." *Mol Biol Cell* **7**(4): 579-594.

Behnia, R. and S. Munro (2005). "Organelle identity and the signposts for membrane traffic." *Nature* **438**(7068): 597-604.

Belgareh-Touze, N., S. Leon, et al. (2008). "Versatile role of the yeast ubiquitin ligase Rsp5p in intracellular trafficking." *Biochem Soc Trans* **36**(Pt 5): 791-796.

Bell, R. M., L. M. Ballas, et al. (1981). "Lipid topogenesis." *J Lipid Res* **22**(3): 391-403.

Bishop, W. R. and R. M. Bell (1985). "Assembly of the endoplasmic reticulum phospholipid bilayer: the phosphatidylcholine transporter." *Cell* **42**(1): 51-60.

Black, M. W. and H. R. Pelham (2000). "A selective transport route from Golgi to late endosomes that requires the yeast GGA proteins." *J Cell Biol* **151**(3): 587-600.

Boehm, M. and J. S. Bonifacino (2001). "Adaptins: the final recount." *Mol Biol Cell* **12**(10): 2907-2920.

Boehm, M. and J. S. Bonifacino (2002). "Genetic analyses of adaptin function from yeast to mammals." *Gene* **286**(2): 175-186.

Bonifacino, J. S. and J. Lippincott-Schwartz (2003). "Coat proteins: shaping membrane transport." *Nat Rev Mol Cell Biol* **4**(5): 409-414.

Böttcher-Sehlmeyer, C. (2006). Subcellular localization and molecular interactions of phosphoinositide 5'-phosphatases of the yeast synaptojanin-like protein family. Institut für Biochemie. Stuttgart, University Stuttgart. **PhD**.

Boucrot, E. and T. Kirchhausen (2007). "Endosomal recycling controls plasma membrane area during mitosis." *Proc Natl Acad Sci U S A* **104**(19): 7939-7944.

Burda, P., S. M. Padilla, et al. (2002). "Retromer function in endosome-to-Golgi retrograde transport is regulated by the yeast Vps34 PtdIns 3-kinase." *J Cell Sci* **115**(Pt 20): 3889-3900.

Buton, X., G. Morrot, et al. (1996). "Ultrafast glycerophospholipid-selective transbilayer motion mediated by a protein in the endoplasmic reticulum membrane." *J Biol Chem* **271**(12): 6651-6657.

Carroll, S. Y., P. C. Stirling, et al. (2009). "A yeast killer toxin screen provides insights into a/b toxin entry, trafficking, and killing mechanisms." *Dev Cell* **17**(4): 552-560.

Catty, P., A. de Kerchove d'Exaerde, et al. (1997). "The complete inventory of the yeast Saccharomyces cerevisiae P-type transport ATPases." *FEBS Lett* **409**(3): 325-332.

Chantalat, S., S. K. Park, et al. (2004). "The Arf activator Gea2p and the P-type ATPase Drs2p interact at the Golgi in Saccharomyces cerevisiae." *J Cell Sci* **117**(Pt 5): 711-722.

Chen, C. Y., M. F. Ingram, et al. (1999). "Role for Drs2p, a P-type ATPase and potential aminophospholipid translocase, in yeast late Golgi function." *J Cell Biol* **147**(6): 1223-1236.

Chen, L. and N. G. Davis (2000). "Recycling of the yeast a-factor receptor." *J Cell Biol* **151**(3): 731-738.

Chen, S., J. Wang, et al. (2006). "Roles for the Drs2p-Cdc50p complex in protein transport and phosphatidylserine asymmetry of the yeast plasma membrane." *Traffic* **7**(11): 1503-1517.

Chen, S. H., S. Chen, et al. (2005). "Ypt31/32 GTPases and their novel F-box effector protein Rcy1 regulate protein recycling." *Mol Biol Cell* **16**(1): 178-192.

Chernomordik, L. V. and M. M. Kozlov (2008). "Mechanics of membrane fusion." *Nat Struct Mol Biol* **15**(7): 675-683.

Chvatchko, Y., I. Howald, et al. (1986). "Two yeast mutants defective in endocytosis are defective in pheromone response." *Cell* **46**(3): 355-364.

Cooper, A. A. and T. H. Stevens (1996). "Vps10p cycles between the late-Golgi and prevacuolar compartments in its function as the sorting receptor for multiple yeast vacuolar hydrolases." *J Cell Biol* **133**(3): 529-541.

Costaguta, G., C. J. Stefan, et al. (2001). "Yeast Gga coat proteins function with clathrin in Golgi to endosome transport." *Mol Biol Cell* **12**(6): 1885-1896.

Cowles, C. R., W. B. Snyder, et al. (1997a). "Novel Golgi to vacuole delivery pathway in yeast: identification of a sorting determinant and required transport component." *EMBO J* **16**(10): 2769-2782.

Cowles, C. R., W. B. Snyder, et al. (1997b). "Novel Golgi to vacuole delivery pathway in yeast: identification of a sorting determinant and required transport component." *EMBO J* **16**(10): 2769-2782.

d'Enfert, C., L. J. Wuestehube, et al. (1991). "Sec12p-dependent membrane binding of the small GTP-binding protein Sar1p promotes formation of transport vesicles from the ER." *J Cell Biol* **114**(4): 663-670.

D'Souza-Schorey, C. and P. Chavrier (2006). "ARF proteins: roles in membrane traffic and beyond." *Nat Rev Mol Cell Biol* **7**(5): 347-358.

Daleke, D. L. (2007). "Phospholipid flippases." *J Biol Chem* **282**(2): 821-825.

Daleke, D. L. and W. H. Huestis (1985). "Incorporation and translocation of aminophospholipids in human erythrocytes." *Biochemistry* **24**(20): 5406-5416.

Darland-Ransom, M., X. Wang, et al. (2008). "Role of C. elegans TAT-1 protein in maintaining plasma membrane phosphatidylserine asymmetry." *Science* **320**(5875): 528-531.

Darsow, T., C. G. Burd, et al. (1998). "Acidic di-leucine motif essential for AP-3-dependent sorting and restriction of the functional specificity of the Vam3p vacuolar t-SNARE." *J Cell Biol* **142**(4): 913-922.

De Matteis, M. A. and A. Godi (2004). "PI-loting membrane traffic." *Nat Cell Biol* **6**(6): 487-492.

Dell'Angelica, E. C., R. Puertollano, et al. (2000). "GGAs: a family of ADP ribosylation factor-binding proteins related to adaptors and associated with the Golgi complex." *J Cell Biol* **149**(1): 81-94.

Dever, T. E. (1999). "Translation initiation: adept at adapting." *Trends Biochem Sci* **24**(10): 398-403.

Donaldson, J. G. and C. L. Jackson (2000). "Regulators and effectors of the ARF GTPases." *Curr Opin Cell Biol* **12**(4): 475-482.

Doray, B., P. Ghosh, et al. (2002). "Cooperation of GGAs and AP-1 in packaging MPRs at the trans-Golgi network." *Science* **297**(5587): 1700-1703.

Durr, K. L., N. N. Tavraz, et al. (2009). "Functional significance of E2 state stabilization by specific alpha/beta-subunit interactions of Na,K- and H,K-ATPase." *J Biol Chem* **284**(6): 3842-3854.

Efe, J. A., F. Plattner, et al. (2005). "Yeast Mon2p is a highly conserved protein that functions in the cytoplasm-to-vacuole transport pathway and is required for Golgi homeostasis." *J Cell Sci* **118**(Pt 20): 4751-4764.

Egner, R., M. Thumm, et al. (1993). "Tracing intracellular proteolytic pathways. Proteolysis of fatty acid synthase and other cytoplasmic proteins in the yeast Saccharomyces cerevisiae." *J Biol Chem* **268**(36): 27269-27276.

Emoto, K. and M. Umeda (2000). "An essential role for a membrane lipid in cytokinesis. Regulation of contractile ring disassembly by redistribution of phosphatidylethanolamine." *J Cell Biol* **149**(6): 1215-1224.

Fadok, V. A., D. L. Bratton, et al. (2000). "A receptor for phosphatidylserine-specific clearance of apoptotic cells." *Nature* **405**(6782): 85-90.

Fadok, V. A., D. R. Voelker, et al. (1992). "Exposure of phosphatidylserine on the surface of apoptotic lymphocytes triggers specific recognition and removal by macrophages." *J Immunol* **148**(7): 2207-2216.

Farge, E. and P. F. Devaux (1992). "Shape changes of giant liposomes induced by an asymmetric transmembrane distribution of phospholipids." *Biophys J* **61**(2): 347-357.

Farge, E., D. M. Ojcius, et al. (1999). "Enhancement of endocytosis due to aminophospholipid transport across the plasma membrane of living cells." *Am J Physiol* **276**(3 Pt 1): C725-733.

Farsad, K. and P. De Camilli (2003). "Mechanisms of membrane deformation." *Curr Opin Cell Biol* **15**(4): 372-381.

Farsad, K., N. Ringstad, et al. (2001). "Generation of high curvature membranes mediated by direct endophilin bilayer interactions." *J Cell Biol* **155**(2): 193-200.

Ford, M. G., I. G. Mills, et al. (2002). "Curvature of clathrin-coated pits driven by epsin." *Nature* **419**(6905): 361-366.

Furuta, N., K. Fujimura-Kamada, et al. (2007). "Endocytic recycling in yeast is regulated by putative phospholipid translocases and the Ypt31p/32p-Rcy1p pathway." *Mol Biol Cell* **18**(1): 295-312.

Galan, J. M., V. Moreau, et al. (1996). "Ubiquitination mediated by the Npi1p/Rsp5p ubiquitin-protein ligase is required for endocytosis of the yeast uracil permease." *J Biol Chem* **271**(18): 10946-10952.

Gall, W. E., N. C. Geething, et al. (2002). "Drs2p-dependent formation of exocytic clathrin-coated vesicles in vivo." *Curr Biol* **12**(18): 1623-1627.

Gallop, J. L., C. C. Jao, et al. (2006). "Mechanism of endophilin N-BAR domain-mediated membrane curvature." *EMBO J* **25**(12): 2898-2910.

Gao, M. and C. A. Kaiser (2006). "A conserved GTPase-containing complex is required for intracellular sorting of the general amino-acid permease in yeast." *Nat Cell Biol* **8**(7): 657-667.

Gauss, R., M. Trautwein, et al. (2005). "New modules for the repeated internal and N-terminal epitope tagging of genes in Saccharomyces cerevisiae." *Yeast* **22**(1): 1-12.

Geering, K. (2001). "The functional role of beta subunits in oligomeric P-type ATPases." *J Bioenerg Biomembr* **33**(5): 425-438.

Geering, K. (2008). "Functional roles of Na,K-ATPase subunits." *Curr Opin Nephrol Hypertens* **17**(5): 526-532.

Gillingham, A. K. and S. Munro (2007). "The small G proteins of the Arf family and their regulators." *Annu Rev Cell Dev Biol* **23**: 579-611.

Gillingham, A. K., J. R. Whyte, et al. (2006). "Mon2, a relative of large Arf exchange factors, recruits Dop1 to the Golgi apparatus." *J Biol Chem* **281**(4): 2273-2280.

Goldberg, J. (1998). "Structural basis for activation of ARF GTPase: mechanisms of guanine nucleotide exchange and GTP-myristoyl switching." *Cell* **95**(2): 237-248.

Gomes, E., M. K. Jakobsen, et al. (2000). "Chilling tolerance in Arabidopsis involves ALA1, a member of a new family of putative aminophospholipid translocases." *Plant Cell* **12**(12): 2441-2454.

Graham, T. R. (2004). "Flippases and vesicle-mediated protein transport." *Trends Cell Biol* **14**(12): 670-677.

Griffiths, G. and K. Simons (1986). "The trans Golgi network: sorting at the exit site of the Golgi complex." *Science* **234**(4775): 438-443.

Halleck, M. S., J. J. Lawler, et al. (1999). "Differential expression of putative transbilayer amphipath transporters." *Physiol Genomics* **1**(3): 139-150.

Hanahan, D. (1983). "Studies on transformation of Escherichia coli with plasmids." *J Mol Biol* **166**(4): 557-580.

Harlan, J. E., P. J. Hajduk, et al. (1994). "Pleckstrin homology domains bind to phosphatidylinositol-4,5-bisphosphate." *Nature* **371**(6493): 168-170.

Harty, R. N., M. E. Brown, et al. (2000). "A PPxY motif within the VP40 protein of Ebola virus interacts physically and functionally with a ubiquitin ligase: implications for filovirus budding." *Proc Natl Acad Sci U S A* **97**(25): 13871-13876.

Heilker, R., M. Spiess, et al. (1999). "Recognition of sorting signals by clathrin adaptors." *Bioessays* **21**(7): 558-567.

Hein, C., J. Y. Springael, et al. (1995). "NPl1, an essential yeast gene involved in induced degradation of Gap1 and Fur4 permeases, encodes the Rsp5 ubiquitin-protein ligase." *Mol Microbiol* **18**(1): 77-87.

Helfrich, W. (1973). "Elastic properties of lipid bilayers: theory and possible experiments." *Z Naturforsch C* **28**(11): 693-703.

Henne, W. M., H. M. Kent, et al. (2007). "Structure and analysis of FCHo2 F-BAR domain: a dimerizing and membrane recruitment module that effects membrane curvature." *Structure* **15**(7): 839-852.

Hirst, J., W. W. Lui, et al. (2000). "A family of proteins with gamma-adaptin and VHS domains that facilitate trafficking between the trans-Golgi network and the vacuole/lysosome." *J Cell Biol* **149**(1): 67-80.

Hitchcock, A. L., K. Auld, et al. (2003). "A subset of membrane-associated proteins is ubiquitinated in response to mutations in the endoplasmic reticulum degradation machinery." *Proc Natl Acad Sci U S A* **100**(22): 12735-12740.

Holthuis, J. C., B. J. Nichols, et al. (1998). "The syntaxin Tlg1p mediates trafficking of chitin synthase III to polarized growth sites in yeast." *Mol Biol Cell* **9**(12): 3383-3397.

Holthuis, J. C., T. Pomorski, et al. (2001). "The organizing potential of sphingolipids in intracellular membrane transport." *Physiol Rev* **81**(4): 1689-1723.

Hua, Z., P. Fatheddin, et al. (2002). "An essential subfamily of Drs2p-related P-type ATPases is required for protein trafficking between Golgi complex and endosomal/vacuolar system." *Mol Biol Cell* **13**(9): 3162-3177.

Hua, Z. and T. R. Graham (2003). "Requirement for neo1p in retrograde transport from the Golgi complex to the endoplasmic reticulum." *Mol Biol Cell* **14**(12): 4971-4983.

Huang, K. M., L. Gullberg, et al. (1997). "Novel functions of clathrin light chains: clathrin heavy chain trimerization is defective in light chain-deficient yeast." *J Cell Sci* **110 (Pt 7)**: 899-910.

Inoue, H., H. Nojima, et al. (1990). "High efficiency transformation of Escherichia coli with plasmids." *Gene* **96**(1): 23-28.

Ito, H., Y. Fukuda, et al. (1983). "Transformation of intact yeast cells treated with alkali cations." *J Bacteriol* **153**(1): 163-168.

Itoh, T., S. Koshiba, et al. (2001). "Role of the ENTH domain in phosphatidylinositol-4,5-bisphosphate binding and endocytosis." *Science* **291**(5506): 1047-1051.

Jackson, C. L. and J. E. Casanova (2000). "Turning on ARF: the Sec7 family of guanine-nucleotide-exchange factors." *Trends Cell Biol* **10**(2): 60-67.

Jenness, D. D., A. C. Burkholder, et al. (1986). "Binding of alpha-factor pheromone to Saccharomyces cerevisiae a cells: dissociation constant and number of binding sites." *Mol Cell Biol* **6**(1): 318-320.

Jochum, A., D. Jackson, et al. (2002). "Yeast Ysl2p, homologous to Sec7 domain guanine nucleotide exchange factors, functions in endocytosis and maintenance of vacuole integrity and interacts with the Arf-Like small GTPase Arl1p." *Mol Cell Biol* **22**(13): 4914-4928.

Kahn, R. A., J. Cherfils, et al. (2006). "Nomenclature for the human Arf family of GTP-binding proteins: ARF, ARL, and SAR proteins." *J Cell Biol* **172**(5): 645-650.

Kato, U., K. Emoto, et al. (2002). "A novel membrane protein, Ros3p, is required for phospholipid translocation across the plasma membrane in Saccharomyces cerevisiae." *J Biol Chem* **277**(40): 37855-37862.

Katoh, Y. and M. Katoh (2004). "Identification and characterization of CDC50A, CDC50B and CDC50C genes in silico." *Oncol Rep* **12**(4): 939-943.

Kinnunen, P. K. and J. M. Holopainen (2000). "Mechanisms of initiation of membrane fusion: role of lipids." *Biosci Rep* **20**(6): 465-482.

Kirchhausen, T. (1999). "Adaptors for clathrin-mediated traffic." *Annu Rev Cell Dev Biol* **15**: 705-732.

Kirchhausen, T. (2000). "Clathrin." *Annu Rev Biochem* **69**: 699-727.

Kirchhausen, T., J. S. Bonifacino, et al. (1997). "Linking cargo to vesicle formation: receptor tail interactions with coat proteins." *Curr Opin Cell Biol* **9**(4): 488-495.

Kornberg, R. D. and H. M. McConnell (1971). "Inside-outside transitions of phospholipids in vesicle membranes." *Biochemistry* **10**(7): 1111-1120.

Laemmli, U. K. (1970). "Cleavage of structural proteins during the assembly of the head of bacteriophage T4." *Nature* **227**(5259): 680-685.

Landschulz, W. H., P. F. Johnson, et al. (1988). "The leucine zipper: a hypothetical structure common to a new class of DNA binding proteins." *Science* **240**(4860): 1759-1764.

Lee, M. C., L. Orci, et al. (2005). "Sar1p N-terminal helix initiates membrane curvature and completes the fission of a COPII vesicle." *Cell* **122**(4): 605-617.

Lemmon, M. A., K. M. Ferguson, et al. (1995). "Specific and high-affinity binding of inositol phosphates to an isolated pleckstrin homology domain." *Proc Natl Acad Sci U S A* **92**(23): 10472-10476.

Lenoir, G., P. Williamson, et al. (2009). "Cdc50p plays a vital role in the ATPase reaction cycle of the putative aminophospholipid transporter drs2p." *J Biol Chem* **284**(27): 17956-17967.

Letourneur, F., E. C. Gaynor, et al. (1994). "Coatomer is essential for retrieval of dilysine-tagged proteins to the endoplasmic reticulum." *Cell* **79**(7): 1199-1207.

Lewis, M. J., B. J. Nichols, et al. (2000). "Specific retrieval of the exocytic SNARE Snc1p from early yeast endosomes." *Mol Biol Cell* **11**(1): 23-38.

Liu, K., Z. Hua, et al. (2007). "Yeast P4-ATPases Drs2p and Dnf1p are essential cargos of the NPFXD/Sla1p endocytic pathway." *Mol Biol Cell* **18**(2): 487-500.

Liu, K., K. Surendhran, et al. (2008). "P4-ATPase requirement for AP-1/clathrin function in protein transport from the trans-Golgi network and early endosomes." *Mol Biol Cell* **19**(8): 3526-3535.

Logan, M. R. and C. A. Mandato (2006). "Regulation of the actin cytoskeleton by PIP2 in cytokinesis." *Biol Cell* **98**(6): 377-388.

Longtine, M. S., A. McKenzie, 3rd, et al. (1998). "Additional modules for versatile and economical PCR-based gene deletion and modification in Saccharomyces cerevisiae." *Yeast* **14**(10): 953-961.

Lopez-Marques, R. L., L. R. Poulsen, et al. (2010). "Intracellular targeting signals and lipid specificity determinants of the ALA/ALIS P4-ATPase complex reside in the catalytic ALA alpha-subunit." *Mol Biol Cell* **21**(5): 791-801.

Luini, A., A. Ragnini-Wilson, et al. (2005). "Large pleiomorphic traffic intermediates in the secretory pathway." *Curr Opin Cell Biol* **17**(4): 353-361.

Lum, P. Y., C. D. Armour, et al. (2004). "Discovering modes of action for therapeutic compounds using a genome-wide screen of yeast heterozygotes." *Cell* **116**(1): 121-137.

Lundmark, R., G. J. Doherty, et al. (2008). "Arf family GTP loading is activated by, and generates, positive membrane curvature." *Biochem J* **414**(2): 189-194.

Luo, W. and A. Chang (2000). "An endosome-to-plasma membrane pathway involved in trafficking of a mutant plasma membrane ATPase in yeast." *Mol Biol Cell* **11**(2): 579-592.

Maniatis, T., E. F. Fritsch, et al. (1989). Molecular cloning : a laboratory manual, New York : Cold Spring Harbor Laboratory Press.

Manno, S., Y. Takakuwa, et al. (2002). "Identification of a functional role for lipid asymmetry in biological membranes: Phosphatidylserine-skeletal protein interactions modulate membrane stability." *Proc Natl Acad Sci U S A* **99**(4): 1943-1948.

Marcusson, E. G., B. F. Horazdovsky, et al. (1994). "The sorting receptor for yeast vacuolar carboxypeptidase Y is encoded by the VPS10 gene." *Cell* **77**(4): 579-586.

Masuda, M., S. Takeda, et al. (2006). "Endophilin BAR domain drives membrane curvature by two newly identified structure-based mechanisms." *EMBO J* **25**(12): 2889-2897.

McMahon, H. T. and J. L. Gallop (2005). "Membrane curvature and mechanisms of dynamic cell membrane remodelling." *Nature* **438**(7068): 590-596.

Merrifield, C. J., D. Perrais, et al. (2005). "Coupling between clathrin-coated-pit invagination, cortactin recruitment, and membrane scission observed in live cells." *Cell* **121**(4): 593-606.

Moriyama, Y. and N. Nelson (1988). "Purification and properties of a vanadate- and N-ethylmaleimide-sensitive ATPase from chromaffin granule membranes." *J Biol Chem* **263**(17): 8521-8527.

Mullins, C. and J. S. Bonifacino (2001). "Structural requirements for function of yeast GGAs in vacuolar protein sorting, alpha-factor maturation, and interactions with clathrin." *Mol Cell Biol* **21**(23): 7981-7994.

Musacchio, A., T. Gibson, et al. (1993). "The PH domain: a common piece in the structural patchwork of signalling proteins." *Trends Biochem Sci* **18**(9): 343-348.

Natarajan, P., J. Wang, et al. (2004). "Drs2p-coupled aminophospholipid translocase activity in yeast Golgi membranes and relationship to in vivo function." *Proc Natl Acad Sci U S A* **101**(29): 10614-10619.

Nossal, R. (2001). "Energetics of clathrin basket assembly." *Traffic* **2**(2): 138-147.

Op den Kamp, J. A. (1979). "Lipid asymmetry in membranes." *Annu Rev Biochem* **48**: 47-71.

Owen, D. J., B. M. Collins, et al. (2004). "Adaptors for clathrin coats: structure and function." *Annu Rev Cell Dev Biol* **20**: 153-191.

Pascon, R. C. and B. L. Miller (2000). "Morphogenesis in Aspergillus nidulans requires Dopey (DopA), a member of a novel family of leucine zipper-like proteins conserved from yeast to humans." *Mol Microbiol* **36**(6): 1250-1264.

Pasqualato, S., L. Renault, et al. (2002). "Arf, Arl, Arp and Sar proteins: a family of GTP-binding proteins with a structural device for 'front-back' communication." *EMBO Rep* **3**(11): 1035-1041.

Paulusma, C. C., D. E. Folmer, et al. (2008). "ATP8B1 requires an accessory protein for endoplasmic reticulum exit and plasma membrane lipid flippase activity." *Hepatology* **47**(1): 268-278.

Paulusma, C. C. and R. P. Oude Elferink (2005). "The type 4 subfamily of P-type ATPases, putative aminophospholipid translocases with a role in human disease." *Biochim Biophys Acta* **1741**(1-2): 11-24.

Pearse, B. M. (1975). "Coated vesicles from pig brain: purification and biochemical characterization." *J Mol Biol* **97**(1): 93-98.

Pelham, H. R. (2002). "Insights from yeast endosomes." *Curr Opin Cell Biol* **14**(4): 454-462.

Pelham, H. R. (2004). "Membrane traffic: GGAs sort ubiquitin." *Curr Biol* **14**(9): R357-359.

Perez-Victoria, F. J., M. P. Sanchez-Canete, et al. (2006). "Phospholipid translocation and miltefosine potency require both L. donovani miltefosine transporter and the new protein LdRos3 in Leishmania parasites." *J Biol Chem* **281**(33): 23766-23775.

Peter, B. J., H. M. Kent, et al. (2004). "BAR domains as sensors of membrane curvature: the amphiphysin BAR structure." *Science* **303**(5657): 495-499.

Pilecka, I., M. Banach-Orlowska, et al. (2007). "Nuclear functions of endocytic proteins." *Eur J Cell Biol* **86**(9): 533-547.

Piper, R. C., N. J. Bryant, et al. (1997). "The membrane protein alkaline phosphatase is delivered to the vacuole by a route that is distinct from the VPS-dependent pathway." *J Cell Biol* **138**(3): 531-545.

Piper, R. C., A. A. Cooper, et al. (1995). "VPS27 controls vacuolar and endocytic traffic through a prevacuolar compartment in Saccharomyces cerevisiae." *J Cell Biol* **131**(3): 603-617.

Polishchuk, R. S., E. V. Polishchuk, et al. (2000). "Correlative light-electron microscopy reveals the tubular-saccular ultrastructure of carriers operating between Golgi apparatus and plasma membrane." *J Cell Biol* **148**(1): 45-58.

Pomorski, T., J. C. Holthuis, et al. (2004). "Tracking down lipid flippases and their biological functions." *J Cell Sci* **117**(Pt 6): 805-813.

Pomorski, T., R. Lombardi, et al. (2003). "Drs2p-related P-type ATPases Dnf1p and Dnf2p are required for phospholipid translocation across the yeast plasma membrane and serve a role in endocytosis." *Mol Biol Cell* **14**(3): 1240-1254.

Poulsen, L. R., R. L. Lopez-Marques, et al. (2008a). "The Arabidopsis P4-ATPase ALA3 localizes to the golgi and requires a beta-subunit to function in lipid translocation and secretory vesicle formation." *Plant Cell* **20**(3): 658-676.

Poulsen, L. R., R. L. Lopez-Marques, et al. (2008b). "Flippases: still more questions than answers." *Cell Mol Life Sci* **65**(20): 3119-3125.

Puts, C. F. and J. C. Holthuis (2009). "Mechanism and significance of P4 ATPase-catalyzed lipid transport: lessons from a Na+/K+-pump." *Biochim Biophys Acta* **1791**(7): 603-611.

Raths, S., J. Rohrer, et al. (1993). "end3 and end4: two mutants defective in receptor-mediated and fluid-phase endocytosis in Saccharomyces cerevisiae." *J Cell Biol* **120**(1): 55-65.

Richnau, N., A. Fransson, et al. (2004). "RICH-1 has a BIN/Amphiphysin/Rvsp domain responsible for binding to membrane lipids and tubulation of liposomes." *Biochem Biophys Res Commun* **320**(3): 1034-1042.

Riezman, H. (1985). "Endocytosis in yeast: several of the yeast secretory mutants are defective in endocytosis." *Cell* **40**(4): 1001-1009.

Rigaut, G., A. Shevchenko, et al. (1999). "A generic protein purification method for protein complex characterization and proteome exploration." *Nat Biotechnol* **17**(10): 1030-1032.

Robinson, M. S. and J. S. Bonifacino (2001). "Adaptor-related proteins." *Curr Opin Cell Biol* **13**(4): 444-453.

Rodriguez-Boulan, E. and A. Musch (2005). "Protein sorting in the Golgi complex: shifting paradigms." *Biochim Biophys Acta* **1744**(3): 455-464.

Roth, M. G. (2004). "Phosphoinositides in constitutive membrane traffic." *Physiol Rev* **84**(3): 699-730.

Rothman, J. E. and F. T. Wieland (1996). "Protein sorting by transport vesicles." *Science* **272**(5259): 227-234.

Ruaud, A. F., L. Nilsson, et al. (2009). "The C. elegans P4-ATPase TAT-1 regulates lysosome biogenesis and endocytosis." *Traffic* **10**(1): 88-100.

Saarikangas, J., H. Zhao, et al. (2009). "Molecular mechanisms of membrane deformation by I-BAR domain proteins." *Curr Biol* **19**(2): 95-107.

Saito, K., K. Fujimura-Kamada, et al. (2004). "Cdc50p, a protein required for polarized growth, associates with the Drs2p P-type ATPase implicated in phospholipid translocation in Saccharomyces cerevisiae." *Mol Biol Cell* **15**(7): 3418-3432.

Sandvig, K. and B. van Deurs (2002). "Transport of protein toxins into cells: pathways used by ricin, cholera toxin and Shiga toxin." *FEBS Lett* **529**(1): 49-53.

Savill, J., V. Fadok, et al. (1993). "Phagocyte recognition of cells undergoing apoptosis." *Immunol Today* **14**(3): 131-136.

Schekman, R. and L. Orci (1996). "Coat proteins and vesicle budding." *Science* **271**(5255): 1526-1533.

Seaman, M. N. (2008). "Endosome protein sorting: motifs and machinery." *Cell Mol Life Sci* **65**(18): 2842-2858.

Sechi, A. S. and J. Wehland (2000). "The actin cytoskeleton and plasma membrane connection: PtdIns(4,5)P(2) influences cytoskeletal protein activity at the plasma membrane." *J Cell Sci* **113 Pt 21**: 3685-3695.

Seigneuret, M. and P. F. Devaux (1984). "ATP-dependent asymmetric distribution of spin-labeled phospholipids in the erythrocyte membrane: relation to shape changes." *Proc Natl Acad Sci U S A* **81**(12): 3751-3755.

Shaw, J. D., K. B. Cummings, et al. (2001). "Yeast as a model system for studying endocytosis." *Exp Cell Res* **271**(1): 1-9.

Sheetz, M. P. and S. J. Singer (1974). "Biological membranes as bilayer couples. A molecular mechanism of drug-erythrocyte interactions." *Proc Natl Acad Sci U S A* **71**(11): 4457-4461.

Shibata, Y., J. Hu, et al. (2009). "Mechanisms shaping the membranes of cellular organelles." *Annu Rev Cell Dev Biol* **25**: 329-354.

Singer-Krüger, B. and S. Ferro-Novick (1997). "Use of a synthetic lethal screen to identify yeast mutants impaired in endocytosis, vacuolar protein sorting and the organization of the cytoskeleton." *Eur J Cell Biol* **74**(4): 365-375.

Singer-Krüger, B., M. Lasic, et al. (2008). "Yeast and human Ysl2p/hMon2 interact with Gga adaptors and mediate their subcellular distribution." *EMBO J* **27**(10): 1423-1435.

Singer-Krüger, B., H. Stenmark, et al. (1994). "Role of three rab5-like GTPases, Ypt51p, Ypt52p, and Ypt53p, in the endocytic and vacuolar protein sorting pathways of yeast." *J Cell Biol* **125**(2): 283-298.

Singer-Krüger, B., H. Stenmark, et al. (1995). "Yeast Ypt51p and mammalian Rab5: counterparts with similar function in the early endocytic pathway." *J Cell Sci* **108 (Pt 11)**: 3509-3521.

Slepnev, V. I. and P. De Camilli (2000). "Accessory factors in clathrin-dependent synaptic vesicle endocytosis." *Nat Rev Neurosci* **1**(3): 161-172.

Sollner, T., S. W. Whiteheart, et al. (1993). "SNAP receptors implicated in vesicle targeting and fusion." *Nature* **362**(6418): 318-324.

Solum, N. O. (1999). "Procoagulant expression in platelets and defects leading to clinical disorders." *Arterioscler Thromb Vasc Biol* **19**(12): 2841-2846.

Stahelin, R. V., F. Long, et al. (2002). "Phosphatidylinositol 3-phosphate induces the membrane penetration of the FYVE domains of Vps27p and Hrs." *J Biol Chem* **277**(29): 26379-26388.

Stamenova, S. D., R. Dunn, et al. (2004). "The Rsp5 ubiquitin ligase binds to and ubiquitinates members of the yeast CIN85-endophilin complex, Sla1-Rvs167." *J Biol Chem* **279**(16): 16017-16025.

Staub, O. and D. Rotin (2006). "Role of ubiquitylation in cellular membrane transport." *Physiol Rev* **86**(2): 669-707.

Stefan, C. J., A. Audhya, et al. (2002). "The yeast synaptojanin-like proteins control the cellular distribution of phosphatidylinositol (4,5)-bisphosphate." *Mol Biol Cell* **13**(2): 542-557.

Stenmark, H. (2009). "Rab GTPases as coordinators of vesicle traffic." *Nat Rev Mol Cell Biol* **10**(8): 513-525.

Stenmark, H., R. Aasland, et al. (2002). "The phosphatidylinositol 3-phosphate-binding FYVE finger." *FEBS Lett* **513**(1): 77-84.

Stepp, J. D., K. Huang, et al. (1997). "The yeast adaptor protein complex, AP-3, is essential for the efficient delivery of alkaline phosphatase by the alternate pathway to the vacuole." *J Cell Biol* **139**(7): 1761-1774.

Stepp, J. D., A. Pellicena-Palle, et al. (1995). "A late Golgi sorting function for Saccharomyces cerevisiae Apm1p, but not for Apm2p, a second yeast clathrin AP medium chain-related protein." *Mol Biol Cell* **6**(1): 41-58.

Stowell, M. H., B. Marks, et al. (1999). "Nucleotide-dependent conformational changes in dynamin: evidence for a mechanochemical molecular spring." *Nat Cell Biol* **1**(1): 27-32.

Sudol, M. (1996). "Structure and function of the WW domain." *Prog Biophys Mol Biol* **65**(1-2): 113-132.

Swerdlow, P. S., D. Finley, et al. (1986). "Enhancement of immunoblot sensitivity by heating of hydrated filters." *Anal Biochem* **156**(1): 147-153.

Tang, X., M. S. Halleck, et al. (1996). "A subfamily of P-type ATPases with aminophospholipid transporting activity." *Science* **272**(5267): 1495-1497.

Toshima, J. Y., J. Toshima, et al. (2006). "Spatial dynamics of receptor-mediated endocytic trafficking in budding yeast revealed by using fluorescent alpha-factor derivatives." *Proc Natl Acad Sci U S A* **103**(15): 5793-5798.

Valdivia, R. H., D. Baggott, et al. (2002). "The yeast clathrin adaptor protein complex 1 is required for the efficient retention of a subset of late Golgi membrane proteins." *Dev Cell* **2**(3): 283-294.

van Meer, G., D. R. Voelker, et al. (2008). "Membrane lipids: where they are and how they behave." *Nat Rev Mol Cell Biol* **9**(2): 112-124.

Vida, T. A. and S. D. Emr (1995). "A new vital stain for visualizing vacuolar membrane dynamics and endocytosis in yeast." *J Cell Biol* **128**(5): 779-792.

Voeltz, G. K. and W. A. Prinz (2007). "Sheets, ribbons and tubules - how organelles get their shape." *Nat Rev Mol Cell Biol* **8**(3): 258-264.

Wang, Y. J., J. Wang, et al. (2003). "Phosphatidylinositol 4 phosphate regulates targeting of clathrin adaptor AP-1 complexes to the Golgi." *Cell* **114**(3): 299-310.

Waters, M. G., T. Serafini, et al. (1991). "'Coatomer': a cytosolic protein complex containing subunits of non-clathrin-coated Golgi transport vesicles." *Nature* **349**(6306): 248-251.

Weissenhorn, W. (2005). "Crystal structure of the endophilin-A1 BAR domain." *J Mol Biol* **351**(3): 653-661.

Wendland, B., K. E. Steece, et al. (1999). "Yeast epsins contain an essential N-terminal ENTH domain, bind clathrin and are required for endocytosis." *EMBO J* **18**(16): 4383-4393.

Whyte, J. R. and S. Munro (2002). "Vesicle tethering complexes in membrane traffic." *J Cell Sci* **115**(Pt 13): 2627-2637.

Wicky, S., H. Schwarz, et al. (2004). "Molecular interactions of yeast Neo1p, an essential member of the Drs2 family of aminophospholipid translocases, and its role in membrane trafficking within the endomembrane system." *Mol Cell Biol* **24**(17): 7402-7418.

Wiederkehr, A., S. Avaro, et al. (2000). "The F-box protein Rcy1p is involved in endocytic membrane traffic and recycling out of an early endosome in Saccharomyces cerevisiae." *J Cell Biol* **149**(2): 397-410.

Wilbur, J. D., P. K. Hwang, et al. (2005). "New faces of the familiar clathrin lattice." *Traffic* **6**(4): 346-350.

Xu, P., J. Okkeri, et al. (2009). "Identification of a novel mouse P4-ATPase family member highly expressed during spermatogenesis." *J Cell Sci* **122**(Pt 16): 2866-2876.

Yarar, D., C. M. Waterman-Storer, et al. (2005). "A dynamic actin cytoskeleton functions at multiple stages of clathrin-mediated endocytosis." *Mol Biol Cell* **16**(2): 964-975.

Yeung, B. G. and G. S. Payne (2001). "Clathrin interactions with C-terminal regions of the yeast AP-1 beta and gamma subunits are important for AP-1 association with clathrin coats." *Traffic* **2**(8): 565-576.

Yeung, B. G., H. L. Phan, et al. (1999). "Adaptor complex-independent clathrin function in yeast." *Mol Biol Cell* **10**(11): 3643-3659.

Yoda, K. and Y. Noda (2001). "Vesicular transport and the Golgi apparatus in yeast." *J Biosci Bioeng* **91**(1): 1-11.

Yu, J. W. and M. A. Lemmon (2001). "All phox homology (PX) domains from Saccharomyces cerevisiae specifically recognize phosphatidylinositol 3-phosphate." *J Biol Chem* **276**(47): 44179-44184.

Zachowski, A. (1993). "Phospholipids in animal eukaryotic membranes: transverse asymmetry and movement." *Biochem J* **294 (Pt 1)**: 1-14.

Zachowski, A., E. Favre, et al. (1986). "Outside-inside translocation of aminophospholipids in the human erythrocyte membrane is mediated by a specific enzyme." *Biochemistry* **25**(9): 2585-2590.

Zhdankina, O., N. L. Strand, et al. (2001). "Yeast GGA proteins interact with GTP-bound Arf and facilitate transport through the Golgi." *Yeast* **18**(1): 1-18.

Zhou, X. and T. R. Graham (2009). "Reconstitution of phospholipid translocase activity with purified Drs2p, a type-IV P-type ATPase from budding yeast." *Proc Natl Acad Sci U S A* **106**(39): 16586-16591.

Ziman, M., J. S. Chuang, et al. (1996). "Chs1p and Chs3p, two proteins involved in chitin synthesis, populate a compartment of the Saccharomyces cerevisiae endocytic pathway." *Mol Biol Cell* **7**(12): 1909-1919.

Zimmerberg, J. and M. M. Kozlov (2006). "How proteins produce cellular membrane curvature." *Nat Rev Mol Cell Biol* **7**(1): 9-19.

Acknowledgements

This thesis, while an individual work, benefited from the interaction with several people. My thanks go to all of them.

I first want to express my gratitude to my supervisor, Priv.-Doz Dr. Birgit Singer-Krüger who gave me the opportunity to work on this exciting project. Without her scientific advices and support in the past years, I would not have been able to finish this study. I'm particularly thankful for the freedom she granted me which allowed my creativity and my sense of criticism to develop. I learned a lot in the past years.

Next, I want to convey my sincere thanks to Prof. Dr. Dieter Wolf who gave me the possibility to accomplish my PhD project at the Institute for Biochemistry. In particular, I'm grateful for his precious support and care.

I'm also grateful to my colleges from the south lab with whom I had the chance to work: Maja Lasić, Claudia Böttcher, Anna-Maria Bürger, Dagmar Pratte, Jessica Heringer, Viola Günther, Yi Wang, Svenja Kaden, Meng Wei, Katharina Eydt and Dominick Rais. Thanks to all for the enjoyable work atmosphere. I'm especially grateful to Maja Lasić and Claudia Böttcher who have arranged my moving to Stuttgart and for their support with my integration in the lab and social life in Stuttgart.

I also wish to thank (without any kind of order) Lise, Elena, Alex, Bernhard, Frederik, Antja, Ingo and Mario for the great times in the lab.

I wish to thank Ms. Elizabeth Tosta for her administrative help and friendly words. To Dragicza I thank for all the help in the lab and patience with my German.

Above all on a more personal basis but also professional, my gratitude goes to Olivier, for his continuous support, patience and comprehension which were of extreme importance in this period of my life.

On personal basis I have no words to express my gratitude to my family, which always supported me. Especially, to my mother which every day asked me: "How many pages you wrote today?" and "How much more you have still to write?". To my father who just says: "You went for 3 years and you are already there for almost 5 years". To them I also want to apology for my absence in the last years.

Curriculum Vitae

PERSONAL INFORMATION

NAME	Sónia Cristina de Oliveira Barbosa
NATIONALITY	Portuguese
SEX	Female
DATE OF BIRTH	29-03-1976
PLACE OF BIRTH	Paris, France

Contact data:
Present address: 60, Strafford Gate, EN6 1PL, GroβBritannien
e-mail: sonia.barbosa@ibc.uni-stuttgart.de

EDUCATION

2005-today	PhD project at the Institute for Biochemistry, University of Stuttgart, Stuttgart, Germany
2001-2002	Post-Graduate Program in Biochemical Engineering at the Department of Biochemistry and of Chemical Engineering Faculty of Sciences and Technology, University of Coímbra, Coímbra, Portugal
1995-2000	Master degree in Biochemistry **"**Licenciatura em Bioquímica" Departament of Biochemistry, Faculty of Sciences and Technology, University of Coímbra, Coímbra, Portugal

RESEARCH EXPERIENCE

2005-2010 **PhD student at the Institute of Biochemistry, University of Stuttgart, Stuttgart, Germany**
Title
Under the supervision of Dr. Birgit Singer-Krüger

2003–2005 **Research fellow at the Biology Department/ Centre, School of Sciences, Minho University, Braga, Portugal**
"Construction of *Saccharomyces cerevisiae* strains with the capacity to remove malic-acid under genetic control". Under the supervision of Prof. Margarida Casal

2002–2003 **Research fellow at the Biology Department/ Centre, School of Sciences, Minho University, Braga, Portugal**
"Molecular and Genetic Analysis of Monocarboxylic Acid Transporters in Yeast". Under the supervision of Prof. Margarida Casal

1999-2000 **Diploma thesis at the CNC University of Coímbra, Portugal:** "Clonning expression and Characterisation of the recombinant Cardosin A" Under the supervision of Prof. Dr. Euclides Pires and Dr. Carlos Faro

THEACHING EXPERIENCE

2005-2010 Teaching assistant for undergraduated students, Biochemistry laboratory courses, University of Stuttgart, Germany

2002-2005 Teaching assistant for undergraduated students, Genetic Engineering laboratory courses, Biology Department, Minho University, Braga, Portugal

PUBLICATIONS

Barbosa, S., Pratte, D., Schwarz, H., Pipkorn, R., and Singer-Krüger, B. (2010) **"**Oligomeric Dop1p is part of the endosomal Neo1p-Ysl2p-Arl1p membrane remodeling complex" Traffic; (DOI: 10.1111/j.1600-0854.2010.01079.x)

Paiva, S., Devaux, F., **Barbosa, S.**, Jacq, C., Casal, M. (2004) Ady2p is essential for the acetate permease activity in the yeast *Saccharomyces cerevisiae* Yeast; **21**: 201-210.

ORAL PRESENTATIONS

Sónia Barbosa "Links between Dop1p and the aminophospholipid translocase Neo1p" Regular Meeting of the RTN Network "Flippases" in Budapest 7th to 9th February 2008

Sónia Barbosa "The role of Neo1p in membrane trafficking" Regular Meeting of the RTN Network "Flippases" in Granada 22nd to 25th March 2007

Sónia Barbosa "The role of Neo1p in *Saccharomyces cerevisiae*" Mid-Term Meeting of the RTN Network "Flippases" in Copenhagen 24nd to 26th August 2006

Sónia Barbosa "Deciphering the function of Neo1p a P-type ATPase in *Saccharomyces cerevisiae*" Regular Meeting of the RTN Network "Flippases" in Berlin 24th to 27th November 2005

Sónia Barbosa "The transcription of the monocarboxylic acid transporters *JEN1* and *ADY2* is downregulated by the gene *DHH1* in *Saccharomyces cerevisiae*" XII Jornadas de Biologia de Leveduras "Prof. Nicolau van Uden" Aveiro, Portugal, 13-15 May, 2004

POSTER PRESENTATIONS

Barbosa, S. and Singer-Krüger, B. "Dop1p is an essential component of the Neo1p-Ysl2p-Arl1p network" Flippases 2008 "How lipids cross a membrane" – Centro Stefano Franscini, Monte Verita, Ascona, Switzerland, 2nd -7th November 2008

Barbosa, S., Paiva, S. and Casal, M. "The transcription of the monocarboxylic acid transporters *JEN1* and *ADY2* is downregulated by the gene *DHH1* in *Saccharomyces cerevisiae"* Gene transcription in yeast – Euresco conferences – May, 2004 San Felieu de Guixols, Spain

Barbosa S., Paiva S. and Casal M. "The transcription of the monocarboxylic acid transporters *JEN1* and *ADY2* is regulated by the gene *DHH1* in *Saccharomyces cerevisiae"* Yeast Genetics and Molecular Biology Meeting Seattle, USA July 2004

ATTENDED COURSES

"*Leishmania parasites* as a cellular model for the studies of flippases" RTN Network "flippases" Instituto de Parasitología y Biomedicina "Lopez-Neyra" Consejo Superior de Investigaciones Científicas 26th – 28th March 2007 Granada, Spain.

"Characterization of P-type pumps purified from heterologous expression systems" RTN Network "flippases" The Royal Veterinary and Agricultural University (KVL) Copenhagen 28th -29th August 2006 Copenhagen, Denmark.

"Measuring Transbilayer Lipid Movement and Membrane Fusion" RTN Network "flippases" Humboldt-University Berlin 28th -29th November 2005 Berlin, Germany.

Post-graduate training programme: "Plasma Membrane Transporters - Physiology, Genetics and Phylogeny" Biology Centre of Minho University, Portugal, 2nd to 13th June 2003 **(**10 full days total: 30 hours of seminars and 40 hours lab work).

Advanced training in Microbiology and Microbial Molecular genetic,
Biology Centre of Minho University, Portugal, 8th to 12th July 2002 (20 hours of seminars and 20 hours lab work).